TECHNISCHE UNIVERSITÄT MÜNCHEN

Lehrbereich Anorganische Chemie, Lehrstuhl für Bauchemie

Synthesis and Working Mechanism of Humic Acid Graft Copolymer Fluid Loss Additives Suitable for Cementing High Pressure / High Temperature Oil and Gas Wells

Oyewole Taye Salami

Vollständiger Abdruck der von der Fakultät für Chemie der Technischen Universität München zur Erlangung des akademischen Grades eines

Doktors der Naturwissenschaften (Dr. rer. nat.)

genehmigten Dissertation.

Vorsitzender: Univ.-Prof. Dr. Michael Schuster

Prüfer der Dissertation: 1. Univ.-Prof. Dr. Johann P. Plank

2. Univ.-Prof. Dr. Cordt Zollfrank

Die Dissertation wurde am 20.01.2014 bei der Technischen Universität München eingereicht und durch die Fakultät für Chemie am 13.02.2014 angenommen.

WE ALL HAVE DREAMS. BUT IN ORDER TO MAKE DREAMS COME INTO REALITY, IT TAKES AN AWFUL LOT OF DETERMINATION, DEDICATION, SELF-DISCIPLINE, AND EFFORT

Jesse Owens, 1913-1980

"DETERMINATION AND PERSEVERANCE CAN OPEN A LOCKED DOOR WHEN ONE BELIEVES IN THE INCREDIBLE POWER OF THE MIND WITH THE RIGHT APPROACH TO ACCOMPLISH A SET TARGET"

Salami Taye, 2014

ACKNOWLEDGEMENT

I am highly fortunate to have ***Prof. Dr. Johann Plank*** as my academic supervisor, who "initiated" me into the field of construction chemistry with specialization on drilling and cementing. The "propagation" has yielded results and the in-depth "polymerized" knowledge has been formed. With completion of this dissertation, my deepest and sincere thanks go to him for the transformation that has occurs and the knowledge inoculated in me over the past years. I will like to thank him immensely for the assistance rendered and the trust shown in my work. Also, his patience, guidance, encouragement and invaluable advice towards the completion of my dissertation and his words of wisdom will continue to motivate me throughout my career.

I will also like to extend a heart-felt "thank you" to the president, the board member and workers of TUM graduate school in general for providing a pleasant, comfortable environment for our memorable "kick-off seminar" in *Herrsching*. I thank them for the support and generous assistance with funds to attend conferences and an intensive seminar on "Leading teams in projects" which prepare me for the challenges ahead.

An enabling environment is a catalyst for generation of good ideas. On this note, I like to thank my lab colleagues: Constantin Tiemeyer, Dr. Daniel Bülichen, Timon Echt, Thomas Hurnaus and Manuel Ilg for such a lively atmosphere we created for ourselves. I wish everyone much success and happiness in the nearest future.

I will also like to thank the pioneer members of the oilfield group: Dr. Andreas Brandl, Dr. Nils Recalde Lummer and Dr. Fatima Dugonjic–Bilic for setting down a good legacy of diligence in the group.

I am also highly pleased to thank other member of the team of Bauchemie TU Munchen: Dr. Oksana Storcheva, Dr. Ahmad Habbaba, Dr. M. Zhang-Presse for their help and advice; Tom Pavlitschek, Dr. Markus Gretz, Friedrich von Hoessle, Dr. Hang Bian, Stefan Bauer-egger, Dr. Elina Dubina, Michael Glanzer-Heinrich Dr. Markus Gretz, Dr. Mirko Gruber, Yu Jin, Dr. Helena Keller, Somruedee Klaithong, Dr. Tobias Kornprobst, Alex Lange, Lei Lei,

Matthias Lesti, Markus Meier, Maike Müller, Dr. Vera Nilles, Dr. Bee Geok Serina Ng, Julia Pickelmann, Johanna de Reese, Dr. Birgit Wieneke, Bin Yang, Fan Yang, Nan Zou, Dr. Nadia Zouaoui, Johannes Paas, Markus Schönlein, for sticking together like a family and also thank everyone for the assistance rendered during my program.

Furthermore, I want to warmly show appreciation for the contribution of Richard Beiderbeck and Dagmar Lettrich, for the technical assistance rendered and Tim Dannemann our departmental secretary and Ms. Daniela Michler, our former secretary for kind gesture, swift response in administrative and bureaucratic issues with passion and eagerness.

Lastly, I strongly thank my parents for their aspiration for me to achieve this goal. I also thank them for my moral upbringing and their unflagging encouragement; my twin brother for his invaluable assistance and advice; my wife for being my pillar of support, her perseverance, steadfastness and her devotion makes me to focus and accomplish this program; my younger brothers and sisters; my children, all my friends and well-wishers in general.

ABSTRACT

Drilling and well completion fluids of oil and gas wells require the use of water retention agents commonly known as fluid loss additives (FLAs). They prevent the uncontrolled loss of water from the drilling mud or/cement slurry into the rock formation. This function is achieved through the formation of a tight filter cake, even under conditions of high temperature, pressure and salinity. For such application, two humic acid graft copolymer fluid loss additives, one with viscosifying and one with dispersing property, were synthesized by grafting chains of 2-acrylamido-2-methylpropane sulfonic acid (AMPS®)-co-N,N–dimethyl acrylamide (NNDMA)-co-acrylic acid (AA) onto humic acid as backbone using aqueous free radical polymerization. The feeding molar ratios of AMPS®, NNDMA and AA were 1:1.46:0.07 for the viscosifying graft copolymer and 1:0.63:0.07 for the dispersing copolymer. In all polymers, the wt. ratio between humic acid and graft chains was 20:80. Thermogravimetric analysis revealed that the graft copolymers possess a much higher temperature stability than the humic acid backbone alone. Also, their effectiveness as FLA in API Class G oil well cement slurries was studied at temperature up to 200 ^{o}C using stirred and static filtration cells containing 35 % by weight of cement (bwoc) of silica fume. Both polymers were able to provide API fluid loss values of less than 50 mL at a bottom hole circulating temperature of 200 ^{o}C. The dispersing graft copolymer reduces the rheology of the cement slurries while the viscosifying one slightly increases rheology. Both polymers exhibited good compatibility with AMPS® or tartaric acid-based retarders.

The working mechanism of both copolymers was found to rely on adsorption onto the surfaces of hydrating cement and silica which leads to constriction of the filter cake pores, as was evidenced by adsorption and zeta potential measurements. Since oil or gas often occur below salt formations, the influence of electrolytes on the performance of the graft

copolymers was probed and compared with that of a conventional AMPS®/NNDMA copolymer and a lignite-based graft copolymer. The cementing systems tested were prepared from fresh water, 20 % NaCl solution and sea water as mixing water and the effects of individual ions on the effectiveness of the FLAs were identified. The graft copolymers were found to perform well in fresh water as well as in 20 % NaCl, in spite of its very high concentration of electrolytes (200 g/L). While in sea water, performance of the graft copolymers was severely impeded. This effect is owed to the presence of Mg^{2+} in sea which under highly alkaline pH condition of cement slurry precipitates as $Mg(OH)_2$. The voluminous $Mg(OH)_2$ precipitate entraps a significant amount of the graft copolymer and thus reduces the effective concentration which is available for fluid loss control. Other electrolytes such as e.g. SO_4^{2-}, Cl^-, CO_3^{2-}, HCO_3^-, K^+, Na^+ or Ca^{2+} do not perturb their effectiveness. To overcome the negative effect of Mg^{2+} in sea water, a mitigating strategy is proposed whereby the graft copolymer is added to cement in a delayed mode. The study also provides insights into the physicochemical interactions which present the basis for functionality of oil well cement additives.

TABLE OF CONTENTS

TERMS AND DEFINITIONS

Adsorption	A process in which atoms or molecules move from a bulk phase (that is solid, liquid, or gas) onto a solid or liquid phase
Aggregates	The formation of groups or clusters of particles in fluids
American Petroleum Institute (API)	An oil industry organization that is the leading standard-setting body for oilfield equipment and products
Annulus	In a borehole, the space between the drill pipe and the borehole, between tubing and casing, or between casing and formation
Appraisal well	A well drilled as part of an appraisal drilling program which is carried out to examine the physical extent, reserves and likely production rate of a field
Blow-out	An uncontrolled flow of gas, oil, or other well fluids occurring sometimes catastrophically to the surface when formation pressure exceeds the pressure exerted to it by the column of drilling mud
Blow-out preventers (BOPs)	Are high pressure wellhead valves, designed to shut off the uncontrolled flow of hydrocarbons
Borehole	This is the hole made by drilling or boring with a drill bit.
Casing	A borehole lining (pipe) placed in an oil or gas well as drilling progresses to prevent the wall of the hole from caving in; used to seal off formation fluids during drilling and to provide a conduit for extracting petroleum during production
Casing string	The steel tubing that lines a well after it has been drilled. It is formed from sections of steel tube screwed together
Christmas tree	The assembly of fittings, pressure gauges and valves on the top of the casing which control the production rate of oil and gas after the well has been drilled and completed

Completion	The installation of permanent wellhead equipment for the production of oil and gas
Condensate	Hydrocarbons in the gaseous state under reservoir conditions which become liquid when temperature or pressure is reduced
Coring	Taking rock samples from a well by means of a special tool called "core barrel"
Crude Oil	Liquid petroleum as it comes out of the ground, as opposed to refined oil manufactured out of it
Cuttings	Rock chips cut from the formation by the drill bit, and brought to the surface with the mud. Used by geologists to obtain formation data
Derrick	The tower-like structure that houses most of the drilling controls
Diagenesis	A mineralogical and chemical change that takes place under the influence of subsurface temperature, pressure and electrochemical environment to a sediment after deposition which includes: compaction, cementation, leaching and replacement, excluding weathering and metamorphism
Drilling rig	A drilling unit that is not permanently fixed to the seabed, e.g. a drillship, a semi-submersible or a jack-up unit. Also means the derrick and its associated machinery
Dry hole	A well which was proven to be non-productive with no economic value
Enhanced oil recovery	A process whereby oil is recovered other than by natural or applied pressure from a reservoir
Exploration drilling	Drilling carried out to determine whether hydrocarbons are present in a particular area or structure
Exploration phase	The phase of operation which covers the search for oil or gas by carrying out detailed geological and geophysical surveys; where

	promising followed up by exploratory drilling
Evaporites	Chemical sediment or sedimentary rocks that are formed by precipitation from evaporating waters; gypsum, salt, nitrates and borates are examples of evaporite minerals
Field	A geographical area under which an oil or gas reservoir lies
Filter cake	Compacted solid or semisolid material remaining after liquid/solid separation
Fishing	Retrieving objects from the borehole, such as a broken drill string, or tools
Fluid loss	Refers to the volume of filtrate lost to a permeable substrate due to the process of filtration
Fluid loss agent	A group of additives specifically designed to lower the volume of filtrate that passes through a filter medium
Formation	A body of strata of predominantly one type or a combination of types
Formation pressure	The pressure at the bottom of a well when it is shut in at the wellhead
Formation water	Salt water present in formations
Fracturing	A method of breaking down a formation by pumping fluid at very high pressures, with the objective to increase production rate from this reservoir
Gas Channeling	Penetration of gas through solids, especially during the transition of the plastic cement slurry to a solid
Gas injection	The process whereby gas is pumped back into a reservoir for conservation purposes or to maintain the reservoir pressure
Kick	A "kick" occurs when the formation pressure exceeds the pressure exerted by the mud column; this allows water, oil, gas or other

	formation fluids to enter the well bore
Killing a well	Filling the borehole with drilling mud of suitable density to stop flow of oil, gas and any other formation fluids
Lithology	The study and description of rocks, including their mineral composition and texture; it is also used in reference to the compositional and textural characteristics of a rock
Mud	A mixture of a base substance and additives used to lubricate the drill bit and to counteract the pressure of the formation
Natural gas	Gas, occurring naturally and often found in association with crude petroleum
Oil in place	An estimated measure of the total amount of oil contained in a reservoir and, as such, a higher figure than the estimated recoverable reserves of oil
Oil shale	Fined-grained, dark-colored sedimentary rock (shale) of extremely low permeability and porosity which is composed mainly of consolidated clay or mud
Oil sand	Surface near-sands which are rich in petroleum
Payzone	Rock from which oil or gas are extracted
Perforating gun	A device fitted with bullets, lowered into a specific depth in a well and fired to create holes in casing, cement and formation
Petroleum	A generic name for hydrocarbons, including crude oil, natural gas liquids, natural gas and their products
Petrology	Utilizes the classical fields of minerology, petrography, optical minerology and chemical analysis to describe the composition and texture of rocks
Petrophysical data	Valid data created from several rock specimens to develop the best standard from which to make the calculations of the petrophysical

	parameters for lithography, porosity, water saturation and permeability at the reservoir level
Platform	An offshore structure that is fixed to the seabed
Porosity	The percentage of void in a porous rock compared, to the total volume
Primary recovery	Recovery of oil or gas from a reservoir purely by using the natural pressure in the reservoir to induce the oil or gas
Reservoir	The underground formation where oil and gas has accumulated; it consists of a porous rock to hold the oil or gas, and a cap rock that prevents its escape
Rheology	The term relates to the viscosity (or fluidity) of e.g. the cement slurry when subjected to mixing and pumping into the borehole
Riser (drilling)	A pipe between a seabed BOP and a floating drilling rig
Riser (production)	The section of pipework that joins a seabed wellhead to the Christmas tree
Sedimentology	Encompasses the study of modern sediment such as sand, mud (silt), clay and the processes that result in their deposition during geological history which is applied to petroleum exploration and exploitation
Slurry	A mixture of suspended solids (e.g. cement) and liquid (water)
Thickening time	Essentially a setting time under conditions of controlled temperature and pressure ramps, designed to simulate the conditions for a given well depth
Viscosity	A property of fluids & slurries that indicates their resistance to flow; a plastic viscosity is defined as the ratio of shear stress to shear rate
Workover	Remedial work within a well, the well and relating to attempts to increase the rate of flow

1. INTRODUCTION

Extraction of oil and gas from underground reservoir rocks is a complex operation which requires in-depth technical knowledge and proven technology; affirmed by the quotation below:

"In the decades ahead, the world will need to expand energy supplies in a way that is safe, secure, affordable and environmentally responsible. The scale of the challenge is enormous and requires an integrated set of solutions and the pursuit of all economic options" Rex W. Tillerson [1].

It is thus very clear that today's oil and gas wells cover a wider range of depths and temperature conditions than at any other time in the history of oil and gas exploration. Now, crude oil is explored in even deeper and non-conventional reservoirs like tight sand, oil shale and deepwater which often encounter high temperature and pressure.

These wells vary from freezing temperatures to above 500 °F (260 °C), true vertical depths (TVDs) of up to 8,000 m (33,000 ft) and pressures above 20,000 psi, with hostile reservoir fluids and sometimes high salinity or in water depths of more than 10,000 ft [2-5].

For oil and gas to be affordable and its processing to be safe, the focus should be on how to pursue excellence in drilling & completion and at the same time on high temperature and salt tolerant additives in order to reduce uncertainties, provide structural and chemical integrity and deal with bore hole challenges such as sour gas.

All these require considerable development of new operational practices and sophisticated technologies due to the challenges to equipment and technologies in comparison to low conventional, temperature wells [6-9].

To achieve ultimate success, well completion depends greatly on the cementing process which requires not only the selection of competent and durable materials, but also a complete understanding of placement techniques which will reduce the risk of cement failure [10,11]. These is because the wells drilled need to be sealed, cemented to eventually provide support for casing in the borehole, restrict fluid migration, prevent water migration, stabilize the

borehole, bond, support and protect the casing from drilling shock and corrosion from porous and/or saline formations. These conditions either drain water from the cement or push over-pressured formation fluids into the cement.

These functions and requirements make cementing of the wells an extremely important operation performed in well construction. In addition to the prevention of fluid migration, a fluid loss additive in the cement composition also helps to prevent gas migration (exclusion of free water) between formation and borehole with the aim that the cementitious material should withstand the various stresses occurring during the life of the well and at the same time eliminates mud contamination [12] which could hinder cement strength development, or causes gas channels within the cement sheath.

These effects can lead to major problems like cross flow, pressurized annulus or catastrophic situations (blowout out and infrastructure damage) which was the case in the Mancodo well disaster [13,14].

To achieve the aforementioned zonal isolation (seal of cement to casing and cement to formation), a general knowledge of fluid chemistry, drilling fluid types, is a must for good cement slurry design, tailored towards individual borehole conditions [15,16].

Hence, in this thesis first a general overview of oil and gas technology and materials needed is presented. Also, the testing which is conducted on cement slurries to unveil necessary information prior to placement of the slurry in a well relative to performance prediction and slurry behavior is discussed. Moreover, different factors affecting cement slurry design that are to be taken into account during the formulation process utilizing specialized equipment (see **Figure 1**) and test procedures in accordance with API Specifications simulating down-hole cementing conditions are described.

Furthermore, properties such as rheology of the cement slurry, thickening time (pumping time and safety factor), density of the slurry, compressive strength development and fluid loss rate during placement, all critical parameters for successful slurry design were engineered utilizing self-synthesized humic acid graft copolymer fluid loss additives, a conventional sulfonated FLA (AMPS®-co-NNDMA), a lignite-based graft copolymer and high temperature stable retarders.

Synthesis, characterization and assessment of a humic acid graft copolymer as HP/HT fluid loss additive and its interaction with other admixtures used in oil well cement was investigated. Its behavior in cement and working mechanism is explicitly revealed.

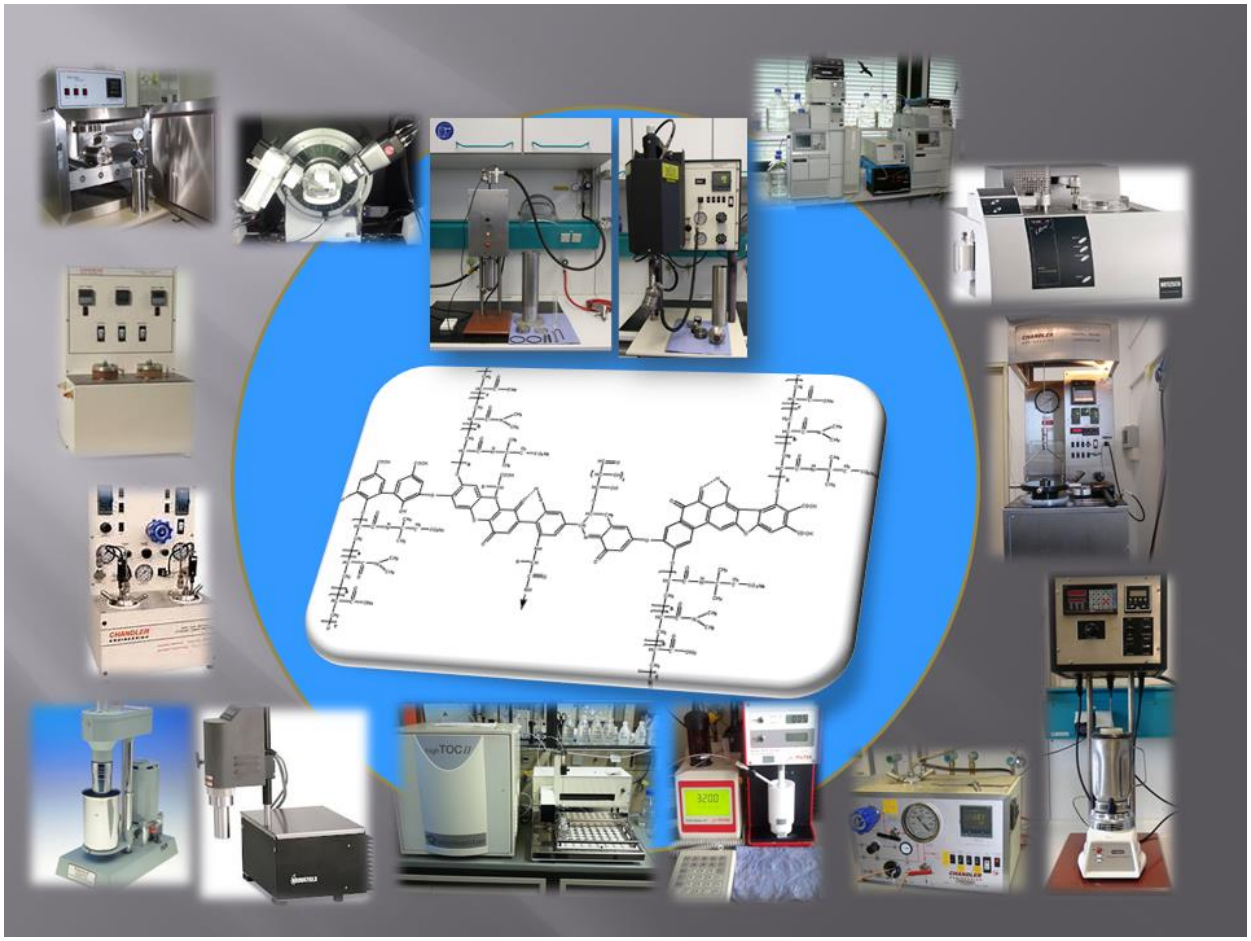

Figure 1: General overview of equipment for oil well cement testing and the structure of the humic acid graft copolymer used in the study

2. THEORETICAL BACKGROUND

2.1 Oilfield chemicals

Oilfield chemicals are various functionalised and speciality additives used in the petroleum industry. They have limitless versatility to specific function which facilitates the exploration and processing of oil and gas for both upstream and downstream activities. A significant

proportion of these additives are either added to the drilling fluid or the cement slurry. A proper understanding of the ideal chemical additives suitable for specific cases is inevitable for oil and gas exploration.

Polymers form the bulky part of these oilfield chemicals which comprise of varieties of natural and synthetic origin. A typical example of polymeric material of natural origin is the group of biopolymers. The biopolymers are polysaccharides that comprise of cellulose derivatives: carboxy methylcellulose (CMC), hydroxy ethyl cellulose (HEC), hydroxy propyl cellulose (HPC), carboxy methyl hydroxy ethyl cellulose (CMHEC), ethyl hydroxy ethyl cellulose, hydrophobically modified hydroxy ethyl cellulose (HMHEC) and guar derivatives: guar, hydroxy ethyl guar (HEG), hydroxy propyl guar (HPG), carboxy methyl guar (CMG), carboxy methyl hydroxyl propyl guar (CMHPG); starch and xanthan gum. Out of all these polysaccharide derivatives, only CMC, HEC, CMHEC, guar gum, HPG and xanthan gum which are non-ionic or slightly negatively charged are commonly used either as thickener, gelling agent, stabilizer, friction reducer or fluid loss agent in drilling fluids, cementing, completion fluids, acidizing and fracturing.

There is still conflicting information about the working mechanism of polysaccharide derivatives in general. It is certain that all polysaccharides have high water sorption capability and in water tend to form hydrocolloidal microgels, polymer associates or networks (e.g. MHEC and HEC) [17, 18]. By modifying the surface of these biopolymers via molar substitution of functional groups like carboxyl, hydroxyl propyl onto the backbone of these polysaccharide chains, surface modification is achieved which can either reduce or improve the tendency of the polymers to form associates and at the same time to provide adsorptive behavior, for example with carboxyl functional groups or non-adsorptive with propyl or other hydrophobic functional groups [19-21].

All these biopolymers have different temperature limitations which thus reduce their application at elevated temperatures (> 150 °C).

Xanthan gum is known to be a rigid polymer which is not shear degradable and to possess high salt tolerance, even in the presence of divalent ions. Also, HEC is another non-ionic polymer that is tolerant to salt under mild salt concentration. But HEC has poor metal crosslinking property and this restricts its application in shale fracking. Thus, non-ionic HPG is the most commonly used, where non-adsorptive property and high viscosity crosslinked polymers are desirable.

Adsorptive polymers are desirable for instance in cement slurries, drilling muds and completion fluids while non-adsorptive polymers are suitable for fracturing fluids in order to avoid adsorption of such polymers to formation rock which will cause concentration depletion of the polymer from the aqueous phase and reduction of viscosity.

Due to the temperature limitations of these biopolymers, synthetic polymers are now used because deep hot reservoir (> 150 °C) exploration is on the increase. High temperature formations require high temperature stable polymers whereas shallow, low temperature reservoirs can use polysaccharide admixtures.

Examples of synthetic polymers used are low molecular weight polyacrylates as clay deflocculant and at high molecular weight as fluid loss additive. The polyacrylates are best utilized in fresh water at low salinity because even low concentrations of Ca^{2+} ions precipitate polyacrylates. Thus, polyacrylate performs poorly in cement slurries and found limited application. Other polymers include polyacrylamides which can generate excessive viscosity and create immense problems when mixing most especially in cement slurry with formation of polymer-cement lumps. Another polymer used for a similar purpose is partially hydrolyzed polyacrylamide (PHPA). This polymer has shear thinning property and is sensitive to high salinity [22].

To overcome this setback for both polyacrylates and polyacrylamide, copolymers or terpolymers for example with 2-acrylamido-2-methyl propane sulfonic acid (AMPS®; sulfonate group) and addition of monomer with a more hydrophobic group such as N,N-dimethyl acrylamide are prevalent. These copolymers or terpolymers produces a polymer that is compatible with brines with the effect emanating from AMPS® monomer while addition of monomer with a more hydrophobic group such as N,N- dimethyl acrylamide introduces a more shear resistant effect into the copolymer (AMPS®-co-NNDMA) structural build up. These copolymers and terpolymers have high temperature stability ≥ 150 °C and were found to adsorb on cement hydrates [23].

In order to suppress the adsorbing properties of the synthetic polymers for fracturing fluid application, where non-adsorptive behavior is desirable, more hydrophobic groups are incorporated into the polymer chains. This polymer engineering approach makes the polymers to become non-adsorptive and to form molecular associates like the biopolymers [24-26].

Today, hundreds of chemical additives exist due to the present challenges encountered in various branches of the oil and gas industry such as in exploration where they are used as retarder [27], fluid loss additive [28-34] and dispersant [35,36]. Also, in oil and gas production, drag reducing agents and lubricants [37,38] which comprises of high molecular weight polymers and sometimes fatty acid esters, help to decrease turbulence in pipes allowing for oil to be pumped through at lower pressures thereby saving energy and cost. Others are used in water shutoff [39,40]. Whereas, in downstream activities such as refining of oil and gas, they are used as emulsifiers, wetting agents, surfactants, scale inhibitors, desulfurization, denitrogenation and other crude oil refining processes [41-43].

2.1. Humic acid

Humus is ubiquitous and constitutes a large portion of the total organic carbon pool in terrestrial and aquatic environments. It plays a very important role in the global carbon cycle and in the mobility and fate of plant nutrients and likewise as environmental contaminant [44, 45]. Humus which is an organic matter is believed to constitute an anaerobically decomposed product of leaves and other detritus formed in soil as a deposit over time (see **Figure 2**). It is known to occur as peat bags in the form of lignite and brown coal deposits and many other types, such as Leonardite, a humic acid bearing ore [46].

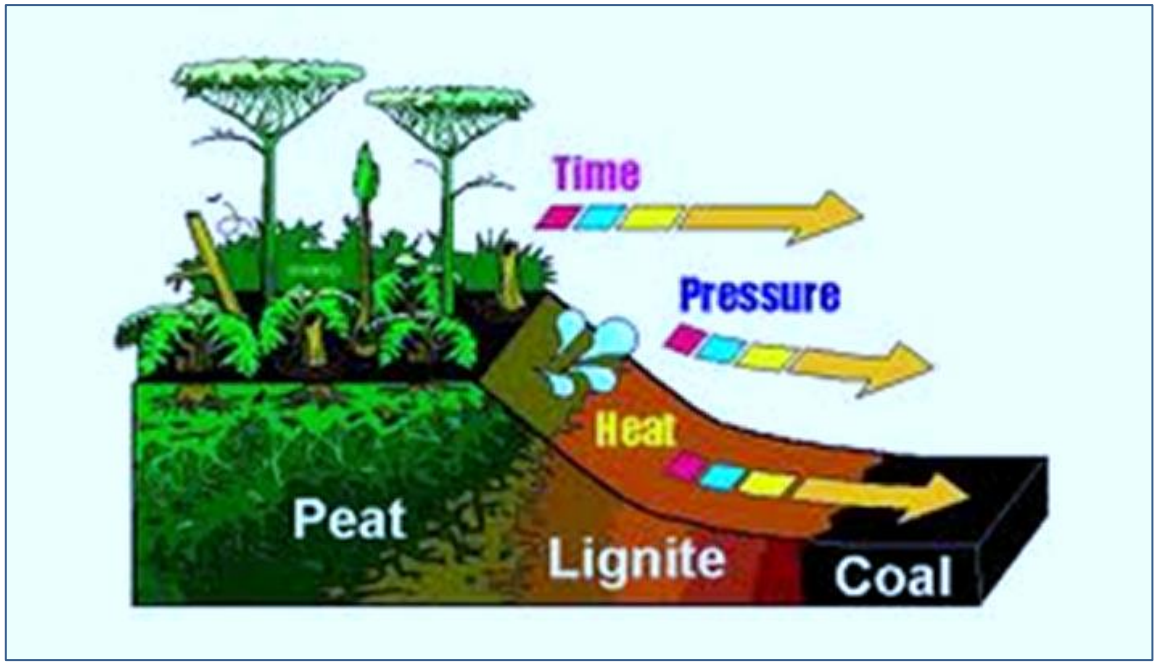

Figure 2: Formation of fossil fuels over millions of years [from teachengineering.org]

Humus is known to contain specifically humic acid, fulvic acid and humins. The fraction of humus that is insoluble in water under acidic conditions (pH < 2) and which is highly soluble under alkaline conditions (high pH) are generally accepted to be humic acids. They are polydisperse with variable chemical features comprised of a mixture of weak aliphatic and aromatic acids. Whereas, fulvic acids are a mixture of weak aliphatic and aromatic organic acids, that are soluble in water at all pH conditions (acidic and alkaline medium). They have many carboxyl (-COOH) and -COH, less phenolic and aromatic functional groups compared to humic acid from the same source and are thus more reactive than humic acid [47,48].

Nevertheless, the recovery of the humic acids from their ore involves a process of mild oxidation and subsequent alkali extraction [49-51]: Several processes are known for producing a solid oxidized ore containing humic acid. One of such process involves mixing the ore with an aqueous medium to produce slurry having a pH in the range of 4 to 9, adjusted with alkali hydroxide solution. The emanating slurry is then reacted with a gaseous oxidant selected from oxygen, air or a mixture of both under conditions of temperature and pressure, and left in the reactor for a time sufficient to cause the oxidation of the ore. This process thereby leads to the production of oxidized ore containing humic and fulvic acid which are separated from the aqueous medium [48,51].

Despite the fact that humic substances have a great range of application, its chemical composition is not well understood due to their large chemical heterogeneity and geographical variability, with conflicting proposition from different researchers [52]. Owed to this problem, several analytical approaches have been used for its characterization and, more importantly, for its molecular weight determination [53-58]. They show that humic acid encompasses a very wide molecular range (30,000 - 200,000 g/mol) while fulvic acid's molar mass $\leq$ 10,000 g/mol, with no clear cut defined standard method for its molecular weight determination. The proposed chemical structures of humic acid and fulvic acid are presented in **Figure 3** [45,59]. Humic acid possesses a 1:1 hydrogen-to-oxygen molar ratio and a significant content of aromatic groups, compared to fulvic acid which exhibits a low hydrogen-to-oxygen ratio. Such ratio is an indication of fewer acidic functional groups.

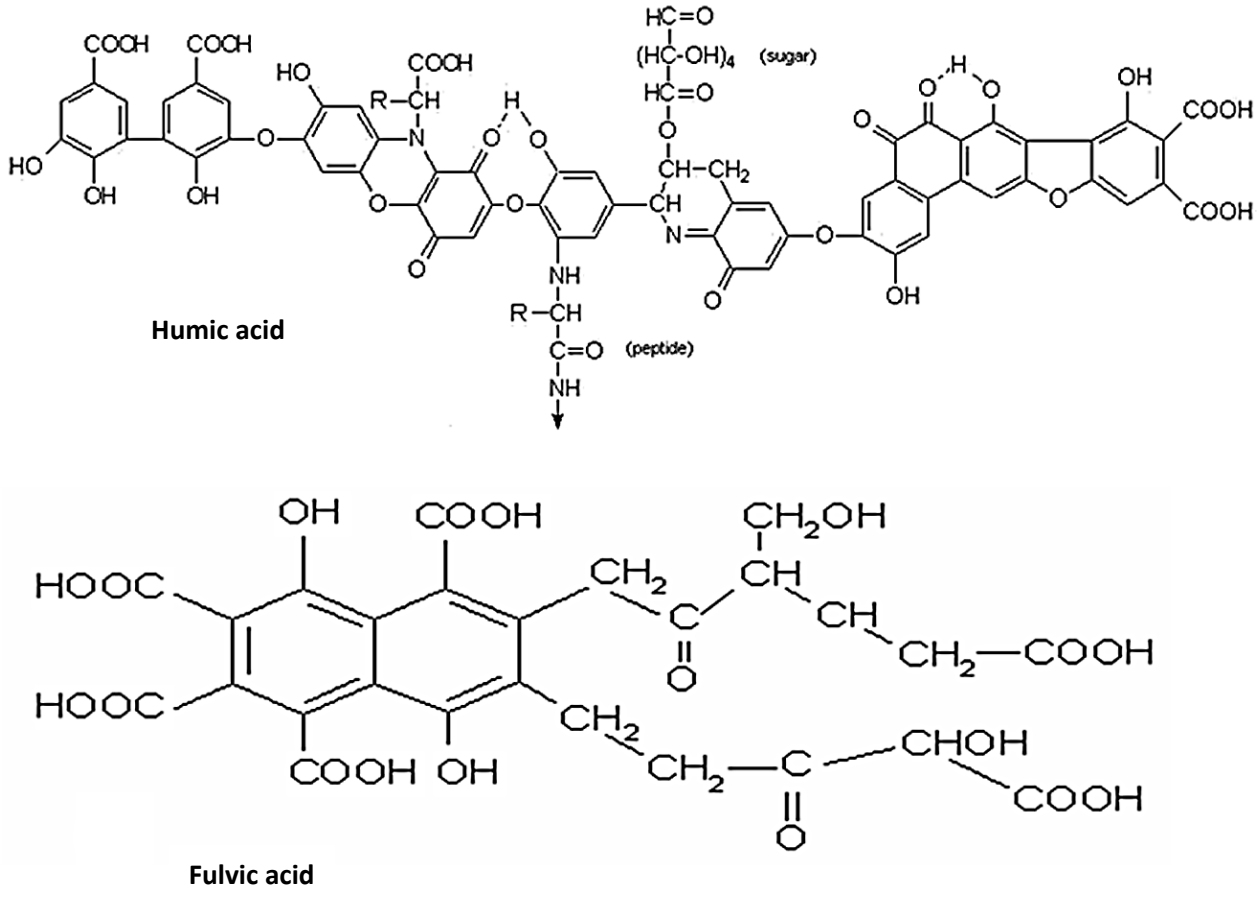

Figure 3: Model structures of humic acid by *Stevenson* [45] and of fulvic acid by *Buffle* [59].

It is thus apparent that humic substances consist of a heterogeneous mixture of compounds which are primarily free and bound phenolic OH groups, quinone structures, sugar moieties, nitrogen and oxygen as bridge units and carboxylic (COOH) groups distributed on aromatic rings [45]. Several humic acid molecules are believed to be bonded together by weak Van der Waals forces and hydrogen bonding. The heterogeneous mixture of these compounds was confirmed by the most recent work of *Thorn* et al. [60].

In terms of application, humic acid plasticizers are known in the oil industry and are used as flocculants and thinner for drilling fluids [61]. Even when lignite which is primarily composed of fulvic acid, humic acid and humins is used as a thinner for high temperature applications [62-64], there is always an underlying assumption that the humic acid constituent may be the factor responsible for its thinning capability since leonardite contains 72 % humic acid and lignite with ~ 52 % [65].

Furthermore, humic acid, lignite and lignin are considered as natural abundant polymeric material and low cost feedstock for oilfield polymers. They now have found wide application either by physically blending with synthetic or biopolymers or modest chemical modifications like grafting of different vinyl monomers onto their surface. These are common approaches to enhance and manipulate their macromolecular structures in order to further improve their performance. By this method, suitable polymeric materials with immense potential for oil and gas applications can be obtained.

2.2. Derivatization

Polysaccharides (e.g. cellulose and starch), leornadite (source of lignite and humic acid), and lignin obtained from wood are the most abundant naturally occurring organic materials that have limited application without physical or chemical derivation or modification. Their performance can be improved by several means, either by blending with different polymers or by synthetically linking different polymer chains onto their structures by covalent bonding known as grafting.

Grafting is a technique or method used to covalently bond lateral chains of one polymer onto the polymer chain of another categorized as the backbone for its surface modification via a polymerization process and it is thus irreversible [66].

2.3. Grafting

Grafting performed via free radical polymerization presents the cheapest and preferred method of polymerization suitable to obtain a cost effective graft copolymer. This polymerization method proceeds through the formation of active free-radicals, known as the initiation. The generated radicals elongate or propagate the chains and successively combine with monomers to give a long active radical chain which is thus terminated by recombination or addition of small amounts of foreign substances like oxygen, bisulphite or hydroquinone which suppress the polymerization process due to quenching of free radicals.

The grafting process can be subdivided mainly into two: grafting-onto and grafting-from techniques. The processes of grafting-onto [67] and grafting-from [68] are different ways to alter the chemical reactivity of the surface. In the so-called grafting-onto mechanism, a

polymer chain is first independently propagated in solution and then grafted onto a surface (the backbone) in solution. The pre-polymerized chains have a thermodynamically favored conformation in solution. This favored conformation acts as a barrier (limiting factor) to the number of polymer chains that can reach the surface of the polymer backbone and adhere. The phenomenon makes their grafting density to be self-limiting and thus the grafting-onto mechanism is characterized with low grafting density. Whereas in the more expensive grafting-from mechanism, a polymer chain is initiated and propagated on the backbone. The grafting-from technique overcomes this phenomenon and allows for higher grafting densities.

The mechanism of free radical polymerization used for grafting is centered on different methods of initiation. The traditional method of redox reaction is the most common conventional approach to generate free radicals using different redox reagents in which radicals can be obtained and relayed to the polymer backbone (for grafting-from) or to monomers (typical for grafting-onto) so that the grafting reaction occurs at relatively lower temperatures within 0 - 60 °C.

Certain compounds like AIBN (azo-isobutyronitrile) and per sulfate are capable of undergoing homolytic fission on heating which produces free radicals and transferring them onto the monomer to be initiated. The ease of radical generation of persulfate at lower temperatures makes it the most commonly employed initiator. Likewise, transition metal ions like Fe in their lower oxidation states are easily oxidized in aqueous medium to their highest valence, mostly in the presence of hydrogen peroxide (Fenton's reagent) or persulfate which also leads to the formation of free radicals (see eqn. 1 & 2).

$$Fe^{2+} + H_2O_2 \rightarrow Fe^{3+} + OH^- + OH^{\bullet} \qquad \text{eqn. 1}$$

$$Fe^{2+} + S_2O_8^{2-} \rightarrow Fe^{3+} + SO_4^{2-} + SO_4^{-\cdot} \qquad \text{eqn. 2}$$

According to *Misra,* ferrous ammonium sulfate and potassium persulfate redox initiator (FAS-KPS) was used for grafting ethyl acrylate onto cellulose backbone [69]. It was observed that the primary sulfate radical generated reacted with water used for solving the monomers and formed secondary hydroxyl radicals which were responsible for initiating the active center on the cellulose polymeric backbone during grafting (see eqn. 3). The FAS-KPS

redox system was also compared with Fenton's reagent and it was found that Fenton's reagent reactivity is several times better than that of the FAS-KPS redox system.

$$SO_4^{-\cdot} + H_2O \rightarrow HSO_4^- + OH^{\cdot} \qquad \text{eqn. 3}$$

Khalil et al. [70] reported the graft polymerization of acrylamide onto maize starch using only potassium persulfate (KPS). Parameters like concentration of initiator and nature of monomers, polymerization time and temperature and liquor ratio were investigated. The optimum condition obtained for efficient grafting reaction was: temperature (60 °C); liquor to solid ratio of 5 and initiator concentration of 0.3 mol /L. Also, out of the monomers tested for the grafting, acrylamide exhibits the highest grafting proficiency, followed by acrylonitrile and methacrylic acid while acrylic acid was found to be the least.

Hosseinzadeh [71] reported the use of KPS to induce grafting polymerization of acrylamide onto another polysaccharide, kappa-carrageenan. The grafting mechanism was found to occur by hydrogen abstraction from the hydroxyl group of the polysaccharide to form alkoxyl radicals on the substrate (kappa-carrageenan). This study shows that persulfate initiator is capable of initiating an active center on polymeric polysaccharide backbone for propagation of the grafting reaction.

In another example, *Chen* et al. [72,73] reported the grafting of acrylamide and acrylic acid onto lignosulfonate using Fenton's reagent (Fe^{2+}/H_2O_2 redox system) in water as the solvent. It was found that the calcium salt of lignosulfonate presented a better basis than sodium or ammonium lignosulfonate.

Recently, *Witono* et al. reported about the graft copolymerization of cassava starch with acrylic acid using Fenton's redox system in water. It was found that out of eight variables examined, only temperature, starch concentration and ratio of starch to monomer had a pronounced influence on the response parameters which were grafting efficiency and fraction of the desired product. The optimal conditions reported for good grafting efficiency were moderate reaction temperature (40 $^{\circ}$C) and a starch concentration of 10 %. A low starch to monomer ratio was found to decrease grafting efficiency [74].

The most reported redox initiator system for grafting of macromolecules is based on cerium compounds, most especially on cerium ammonium nitrate (CAN).

Cerium possesses two oxidation states, Ce^{3+} and Ce^{4+}. The stability of Ce^{4+} is attributed to the empty 4f shell in its electron configuration ([Xe], 4f°. In acidic medium, it is known to be an oxidant and a strong electron acceptor.

$$Ce^{4+} + e^{-} \leftrightarrow Ce^{3+} \qquad \text{eqn. 4}$$

The redox potential of both Ce^{4+}/ Ce^{3+} ions depends mostly on the nature of the acid used and its concentration. The redox potentials for the acids as follows increases in the order of HCl < H_2SO_4 < HNO_3 < $HClO_4$ (1M HCl, 1.28V; 1M H_2SO_4, 1.44V; 1M HNO_3, 1.61V; 1M $HClO_4$, 1.70 V and 8M $HClO_4$, 1.87V) [75]. The oxidation power of of Ce^{4+} is exploited in grafting reactions, most especially for grafting vinyl monomers onto polysaccharides [76-84] or lignin [85-87]. The mechanism of grafting monomers onto lignin was proposed to occur via hydrogen abstraction from the phenolic functional group present in lignin [86]. This proposition was thoroughly discussed and confirmed by *Philips* et al.[88]. This is because hydrogen abstraction reaction has the lowest favorable dissociation energy from the other entire moiety present in lignin.

Similarly, *Shadeghi* et al. [89] studied the mechanism of graft copolymerization of methacrylamide monomer onto carboxymethyl cellulose using cerium ammonium nitrate. The mechanism of reaction was proposed to occur with the aids of thermally dissociated Ce^{3+}-Ce^{4+} complex which disconnects the C-C bond from the CMC backbone. This step forms the corresponding macro initiator that initiates the grafting of methacrylamide onto the CMC backbone leading to the graft copolymer, as illustrated in **Figure 4**.

All these approaches to graft synthetic monomers onto biopolymers, coal and wood derivatives are an important measure to obtain tailored functional polymers for the growing scientific interest and endless demand from industries for high performance polymers with unique physical and chemical properties.

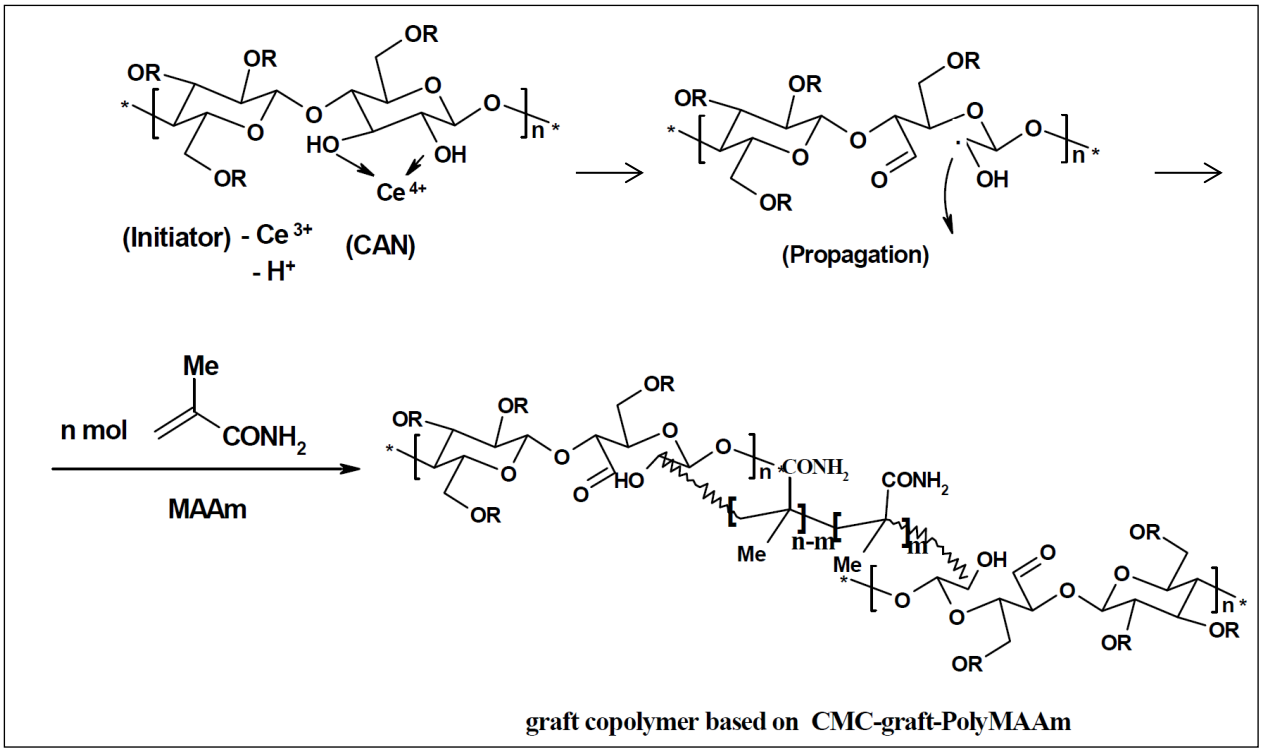

Figure 4: Schematic representation of the proposed mechanism for Ce-induced grafting of methacrylamide onto CMC [89]

2.4. Portland Cement

Portland cement is a typical example of a hydraulic binder that reacts with water to form a viscous paste, undergo setting, harden and gain strength to form a rock-like mass known as concrete. These processes occur through chemical reactions called hydration which is accompanied by evolution of heat [90,91].

Nowadays, production are carried out mainly in continuously operating rotary kilns with a capacity of up to 10,000 tons per day in some Asian plant (see **Figure 5**).

Figure 5: Modern cement rotary kiln production line with a daily output of 5,000 tons [obtained from Jiangsu Pengfei Group Co., Ltd]

The cements are made by quarrying calcareous and argillaceous material that are generally a mixture of limestone (a principal raw material for clinker production) and clay mixed together in the required proportions. These are finely milled and blended together to form a uniform composition achieved either by wet or dry blending. The mixture is then heated to a temperature at which partial fusion occurs. Iron and alumina are occasionally added if not present in sufficient proportions in the clay to ensure uniformity and high quality of the clinker.

The clinkerization process involves four major reaction steps: (a) dissociation of limestone; (b) solid-state reactions; (c) liquid phase sintering and (d) reorganization of clinker microstructure through cooling. The clinkerization generally occurs in a rotary kiln at temperatures ranging from 600 - 1500 ° C [92].

The resultant product is called clinker which is subsequently cooled, pulverized, and blended with a small amount of gypsum to yield cement powder. The gypsum added is used for controlling the setting time of finished cement to prevent a phenomenon known as flash set. These clinkers: alite - tricalcium silicate ($3CaO{\cdot}SiO_2$), belite - dicalcium silicate ($2CaO{\cdot}SiO_2$), tricalcium aluminate ($3CaO{\cdot}Al_2O_3$), and tetracalcium aluminoferrite known as Brownmillerite ($4CaO{\cdot}Al_2O_3{\cdot}Fe_2O_3$) [93] are essentially crystalline phases in close intergrowth which typically contained foreign ions.

Several methods are employed to determine the phase composition of cement because the performance characteristics of cements are influenced by their phase composition. These methods include microscopy, chemical analysis and X-ray diffraction. Also, the oxide content of clinker is often used to determine the phase composition via the *Bogue* calculation [94] as stated in ASTM C150-07 [95]. **Figure 6** outlines a typical brief summary of set of procedures involved in qualitative and quantitative XRD analysis of cement and clinker phases.

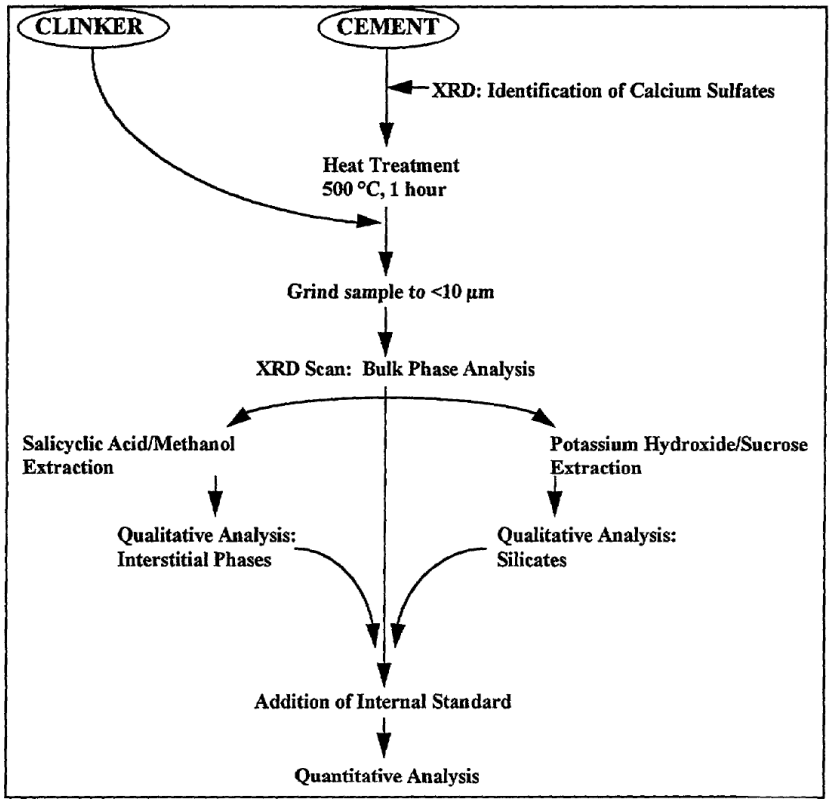

Figure 6: Scheme of XRD characterization of clinker and cement [95]

The clinker phases have well defined X-ray diffraction peaks in ICDD database: Alite (13-272, 49-442 and 33-301); Belite (33-302 and 73-2091); tricalcium aluminate (orthorhombic: 32-150, 33-251; cubic: 38-1429 and 1-070); tetracalcium aluminoferrite (33-311). In addition, cement clinker contains some free calcium oxide and minor quantities of periclase (MgO). **Figure 7** shows typical manifestations of the main clinker phases in a clinker grain, as can be observed under a polarizing microscope with Alite (C_3S) appearing in the form of large, hexagonal, yellow crystals; Belite (C_2S) is however visible as rounded, brown, crossed-lamellar crystals; Brownmillerite (C_4AF) is the enamel matrix of C_3S and C_2S while C_3A occurs in the form of very small, orthorhombic, gray-colored crystals; MgO (periclase) is small, hexagonal, pink colored phases while CaO is roundish and turquoise, with characteristic reptile tail drawing.

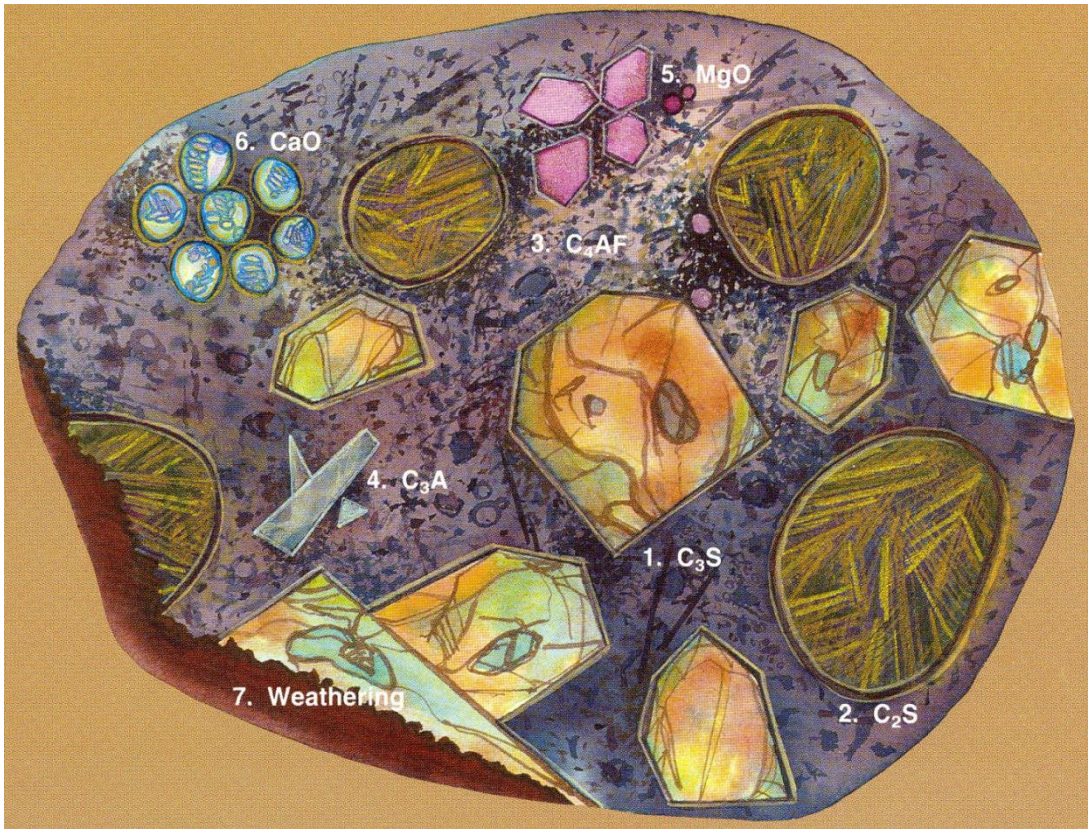

Figure 7: Schematic representation of the components of a Portland cement clinker (edge length 30 microns); etching was carried out with 1, 2-cyclohexane-N,N,N',N'-tetraacetic acid disodium salt (CDTA) [97].

2.5.1 Oil well cement

API grade oil well cements are Portland cements produced with low aluminate (C_3A) content and capable of responding towards additives in order to prevent rapid setting under conditions of elevated temperatures and pressures.

Among several agencies responsible for cement quality regulation, the most commonly employed in the oil industry are the ASTM standards which are applicable to cements used for construction and building, and the API standards for cements used in the oil industry. The ASTM specifications provide for five types of Portland cement: type **I**: Ordinary Portland cement used for all purposes under normal condition; type **II**: Blended cement with moderate sulfate resistance that has resistance to alkali attack and characterized by low C_3A content (< 8 %), used for mass concrete; type **III**: Blast furnace slag cement with high early strength (C_3A < 15 %) used for precast concrete and in cold weather; type **IV**: Low heat Pozzolanic cement used for massive structures like bridges and type **V**: high sulfate resistant composite cement (C_3A < 5 %) with maximum alkali resistance. Whereas, API specifies eight types (see **Table 1**) designated as Classes **A** through **H** [98]. Class A (similar to ASTM type I), Class B (similar to ASTM type II and class C (similar to ASTM type **III** and high sulfate resistance type) are used for surface activities within a depth of 6,000 ft and where early strength is required, with resistance to sulfate environment. Classes **D**, **E** and **F** suitable for high temperatures and pressures are rarely used. Since oil wells are subject to a wide range of temperatures, pressures and hostile conditions where addition of additives like accelerators, retarders, fluid loss additives, weighting agents, dispersants, lost circulation materials, extenders, salts, silica flour and special agent like antifoams are needed to facilitate working in such environment, the less reactive Class **G** and **H** cements found wide application in the exploration for oil and gas. This is because they satisfy the requirements for materials that are capable of forming low-viscosity slurries which remain pumpable to a considerate depth. They also have good response to additives which allows them to be tailored to harden rapidly once in place, with acceptable strength development. The cement in place must immediately develop and maintain enough mechanical strength and thermal stability, most especially on injection wells [99], and low enough permeability in order to prevent invasion of liquids or gases over the life span of the well.

At temperatures above 110 °C, cement is known to undergo strength retrogression due to the formation of α-C_2SH (calcium silicate hydrate) and several other metastable phases [100] characterized by high Ca/Si ratio > 1.0 (see **Figure 8**). This process modifies the physical, chemical and mechanical properties of Portland cement. Addition of 30 - 40 wt. % of silica flour to Class G/H cement replaces the old class J cement used for the same purpose. This composite cement (class G/H and silica flour) produces hydration phase of Ca/Si ≤ 1.0 which is thus more suitable for HP/HT oil wells in order to achieve a cement sheath with low permeability and high mechanical strength.

Table 1: API Cement Classes, their composition, well depth and temperature range

API Class	**Average content of clinker phase (M. - %)**				**Well depth (ft)**	**Temperature range (° C)**
	C_3S	**C_2S**	**C_3A**	**C_4AF**		
A	53	24	8+	8	0 – 6,000	27 – 77
B	47	32	5-	12	0 – 6,000	27 – 77
C	58	16	8	8	0 – 6,000	27 – 77
D	26	54	2	12	6,000 – 12,000	77 – 127
E	26	54	2	12	6,000 – 14,000	77 – 143
F	26	54	2	12	10,000 –16,000	115 – 160
G	50	30	5	12	0 – 8,000	27 – 93
H	50	30	5	12	0 – 8,000	27– 93

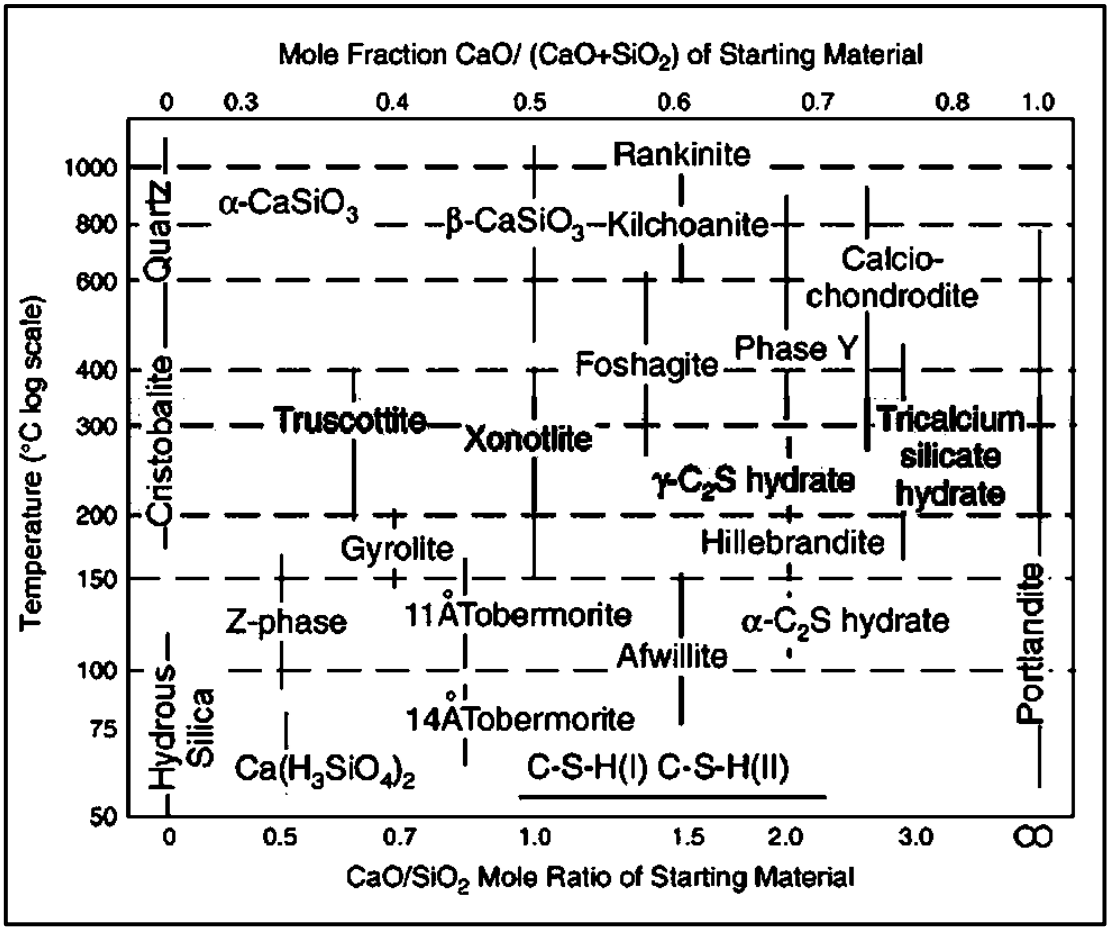

Figure 8: $CaO\text{-}SiO_2\text{-}H_2O$ phases formed at 50 to 1000 °C; from *Meller* et al. [101]

2.5.2 Cement hydration

Cement hydration is the process which involves the transformation of anhydrous cement into a slurry by reaction with water, to form an amorphous paste through a chemical reaction and which gains strength by transformation into a rock-like mass known as concrete [93].

This process follows a dissolution/precipitation mechanism via solution as described by Barret [102, 103]. Upon contact of cement with water, calcium ions in the surface layer of the anhydrous cement phase pass rapidly into solution. Initially, the Ca^{2+}/SiO_2 molar ratio is very high (3:1) indicating in congruent dissolution of tricalcium silicate [104]. This relatively high initial silicate concentration observed only seconds after mixing is only transitory and decreases very quickly to extremely low values, i.e. to about 10 µmol/L. Contrary to that, the

concentration of calcium hydroxide continues to increase, exceeding the value of 20 mmol/L which would be expected from the solubility product of $Ca(OH)_2$.

At elevated temperatures, the hydration of ß-dicalcium silicate is found to accelerate in relation to that of C_3S, which could be related to the higher solubility of silicate and lower solubility of Ca^{2+} under this condition. This was ascertained by *Durgun* et al. [105]. He explained that the fast hydration of C_3S at low temperatures in comparison to C_2S is mainly related to the reactive sites around C_3S which involves ionic oxygen atoms that are absent in C_2S. The dissolution rate of both C_3S and C_2S was recently confirmed to depend on the concentration of $Ca(OH)_2$ in the pore solution which acts as the limiting factor for early silicate hydration [106].

The calcium hydroxide formed at the beginning of hydration is tagged to be the alkali reservoir of cement paste and accounts for the high pH of cement pore solution. Potassium and sodium are also present in small amount as sulfates, e.g. K_2SO_4, double alkali sulfates like syngenite ($K_2SO_4 \cdot Ca_2SO_4$) and langbeinite ($K_2SO_4 \cdot 2Ca_2SO_4$). The alkali ions readily enter into cement pore solution and accelerate early hydration reactions. Also, C_3S and C_3A which can contain a limited amount of (0.75 %) contribute as well to the alkali content of the cement pore solution [93]. Thus, C_3S and C_2S which constitute about 80 % of the weight fraction of the cement (see **Table 1**) fully participate in the dissolution process. Another reactive phase is C_3A which forms ettringite crystals in the presence of dissolved sulfate during the induction and dormant periods within 0 - 15 min and 1- 2 h respectively of mixing the cement with water (see **Figure 9)**.

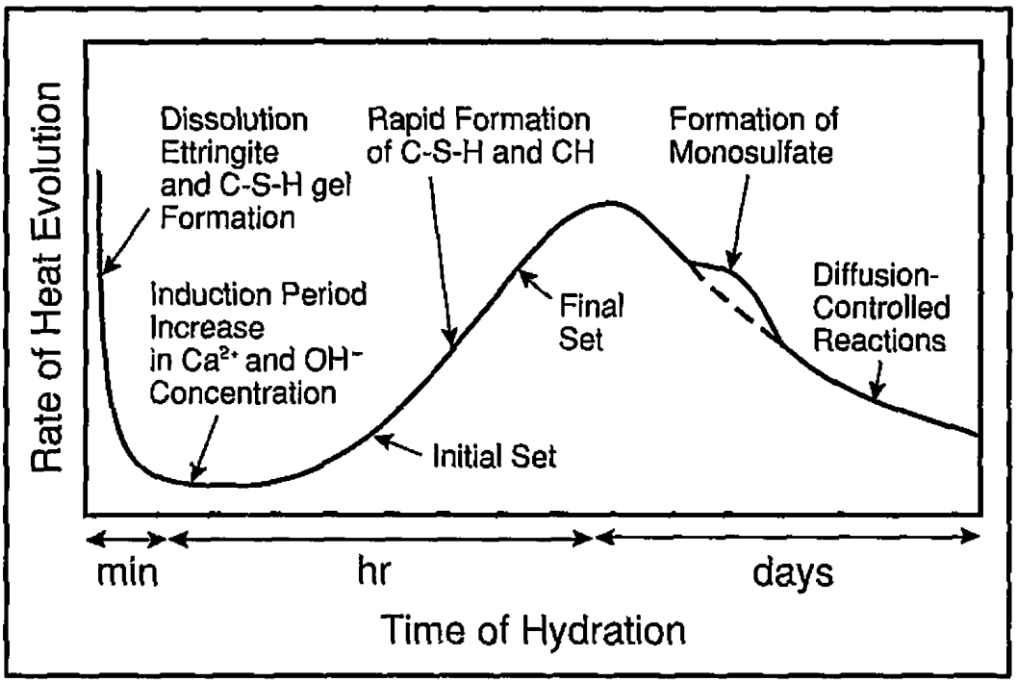

Figure 9: Schematic representation of Portland cement hydration [107]

It is very important to review the hydration products formed within these two earliest periods because it produces cement phases for additive interaction rather than the other periods: (acceleration period, 2-5 h; deceleration period, 5-18 h; and final period, 1-180 days) which are at least well known due to the formation of well-defined crystalline phases over time.

The early hydration phase of cement is a very complex process due to the formation of several hydration products like ettringite, portlandite and poorly crystalline C-S-H phases [108-113]. This becomes even more complex and complicated at elevated temperatures due to array of chemical reactions taking place simultaneously at a much faster rate.

For instance, when water is added to cement, parts of the clinker sulfates and gypsum are readily dissolved to produce an alkaline, sulfate rich solution during the induction period. In this period, the most reactive phase C_3A reacts with water to form an aluminate rich gel that subsequently reacts with the sulfate rich solution emanated from gypsum ($CaSO_4$. $2H_2O$) to form ettringite ($Ca_6Al_2(SO_4)_3(OH)_{12} \cdot 32\ H_2O$), a rodlike crystalline, phase (see **Figure 10**). Its formation is described in the chemical reaction of equation 5 [112].

$$C_3A + 3\ CaSO_4 \cdot 2\ H_2O + 26\ H_2O \rightarrow C_3A \cdot 3\ CaSO_4 \cdot 32\ H_2O \quad \text{eqn. 5}$$

This process is possible mostly at high sulfate concentrations (≥ 2.35 g/L) and a temperature below 115 °C. This is because ettringite that is believed to be the host for additive adsorption is known to degrade at temperatures of ~ 80 °C to 115 ^{o}C [114 -118].

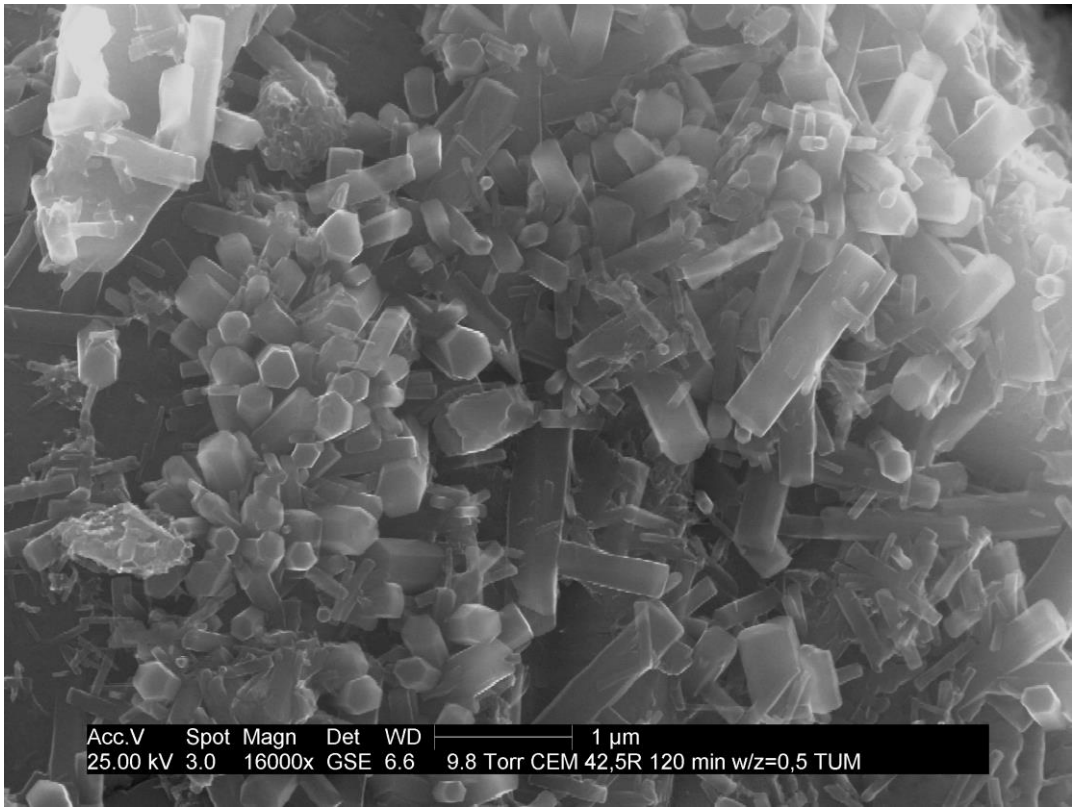

Figure 10: Ettringite formation from C_3A hydration with ESEM in the presence of gypsum after 2 h (dormant period) of hydration (ESEM micrograph)

Afterwards, when the sulfate concentration decreases to below 2.35 g/L which occurs at elevated temperature (above 115 °C) due to the increased rate of hydration (increased sulfate consumption), monosulfoaluminate, a crystalline, platy phase (in **Figure 11**) is formed, either by reaction of ettringite with C_3A or with remaining gypsum, as is shown in equation 6.

$$C_3A + CaSO_4 \cdot 2\,H_2O + 10\,H_2O \rightarrow C_3A \cdot CaSO_4 \cdot 12\,H_2O \qquad \text{eqn. 6}$$

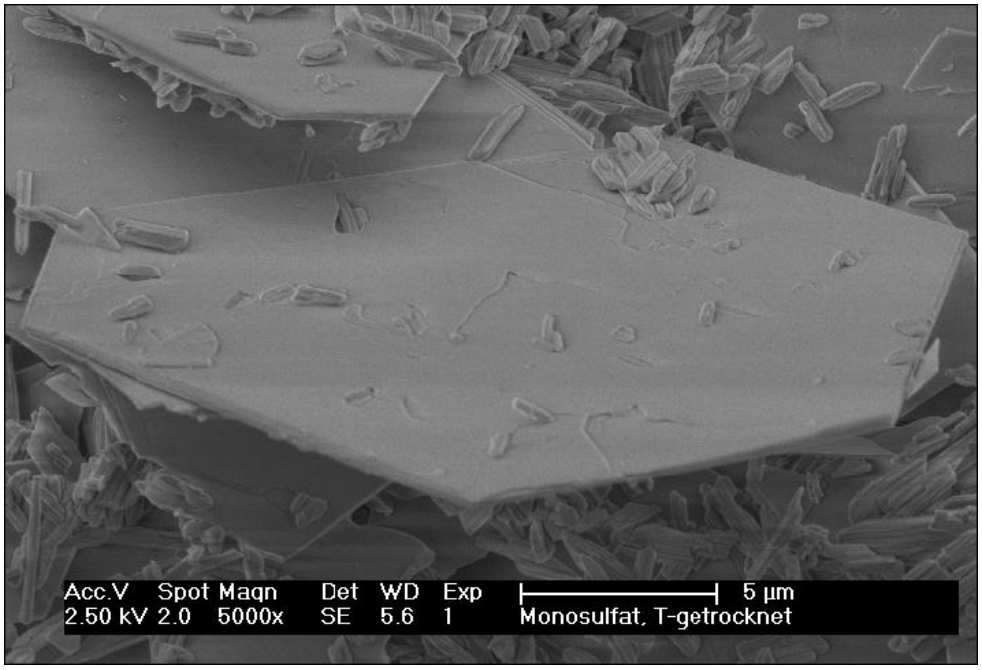

Figure 11: Hydration of C_3A in the presence of gypsum showing a monosulfate crystal (ESEM micrograph)

Out of all these cement hydration products, the hydration phase most investigated in recent times is the calcium silicate hydrates [119-124]. This is because the hydration reaction of the silicates (C_3S and C_2S) involves a more complicated process, most especially during the induction or pre-induction period where a poorly crystalline C-S-H gel known as intermediate C-S-H is believed to be formed along with a calcium hydroxide (portlandite), a crystalline cubic phase [125-127]. The C-S-H formation was also recently observed by *Muller* et al., where increased densification of C-S-H was found from cement hydration over a period of time. This corresponds to the growth of low density C-S-H with few layers containing gel pores to a higher density product devoid of gel pores using NMR spectroscopy [128]. Investigation of these hydration products becomes very important because of the necessity to understand admixture-cement interface interaction and likewise its consequences for the anchoring possibilities of polyelectrolytes (cationic and anionic) on the main hydration products: sulfoaluminate hydration products (ettringite, monosulfate etc.) and calcium silicate hydrates (C-S-H).

A complete understanding of all the processes and hydration phases of cement and the factors responsible for cement workability (setting time) will generally serve as a strong basis for understanding the mechanism of different polymer additives interaction with binders.

2.5.3 Influence of additives on cement hydration

Polymers (oilfield additives) are indispensable for fluids adjustment before placement, most especially cement additives in order to adjust the properties of the fluid according to specific needs of the job.

There are hundreds of these additives which are distinguished by the properties of the cement slurry which they influence, such as accelerator, retarder, dispersants and fluid loss additive, with distinct and specific working mechanism.

For example, tartaric acid, a low temperature (about 95 °C) cement retarder is known to form an insoluble calcium tartarate precipitate in the presence of calcium from cement pore solution. Its mechanism of cement hydration retardation occurs by precipitating on C_3A via calcium complexation [27,114]. Whereas, another retarder, nitrotris (methylene) triphosphonate was found to accelerate ettringite formation by enhancing calcium ion dissolution, forming a calcium rich layer on C_3A in the presence of gypsum. It was also found to inhibit C-S-H formation by calcium complexation forming calcium phosphonate precipitate layers on hydrating cement [129].

Recently, sucrose, a known effective cement hydration inhibitor was ascertain to selectively adsorb on hydrating silicate surfaces by using advanced solid – state NMR spectroscopy techniques [130]. Sucrose retards C_3S hydration directly by nucleation poisoning and surface adsorption due to solubilization of silicate species [131]. Hence, based on the mode of actions of these retarders, the cement slurry remains plastic/fluid for a long time as needed in cementing operations.

It thus becomes most probable that additives interact non-selectively with both sulfoaluminate and silicate hydrate phases. Hence, non-selective adsorption of polymers on hydrating cement particles and intermediate calcium silicate hydrate, a substantial component of hydrating cement with surface composition and charge varying from being either positive or negative, depending on the presence of ions incorporated [122, 132-134], which influences cohesion [193,194] between the C-S-H substrate and the water content [136,137], is most likely to occur. This is also supported by the high pH (~ 13) of cement pore solution that

favours formation of $Ca(OH)^+$ ions on hydrating cement particles which are most likely to be prominent at elevated temperature above 140 °C, suitable for anionic polyelectrolyte adsorption. This findings was recently collaborated by *Mishra* et al. [138] who found that C_3S reacts with grinding agents (organic ethanol amines) used during the production of cement. The mechanism of adsorption of the organic molecules was found to be based on superficial coordination of calcium ions, electrostatic interaction and hydrogen bonding on the surfaces.

Moreover, the surface area of amorphous C-S-H phase is higher than that of the crystalline phase [139], which makes it a suitable host for polymer interaction. This shows a high probability of this mineralization process for anchoring anionic polyelectrolytes on crystalline calcium silicate phases, hydrating silicate and anhydrous silicate particles, most especially at temperatures above 140 °C where increased hydration of silicates occurs.

Still, possible high temperature stable calcium aluminate sulfates like monosulfate or calcium aluminium oxide hydrate [140], a product similar to ettringite, cannot be completely excluded at elevated temperature. This review thus opens up fundamental questions such as:

What happens to admixtures which initially anchor on ettringite when this phase decomposes at elevated temperatures?

At high temperatures, which cement phase allows adsorption of admixtures to function well?

2.6 Oil and Gas Technology

The oil and gas industry is subdivided into two major parts which comprise of the upstream and downstream sector. The upstream sector refers to the search for potential underground or subsea oil and gas fields; drilling of exploratory wells; testing of the productivity of the wells; recover and bringing the crude oil and/or raw natural gas to the surface and its production.

While the downstream sector is a term commonly used to refer to the refining of crude oil and the selling and distribution of natural gas and products derived from crude oil. The products include liquefied petroleum gas (LPG), gasoline or petrol, jet fuel, diesel oil, other fuel oils, asphalt and petroleum coke. This sector includes oil refineries, petrochemical plants, petroleum product distribution, retail outlets and natural gas distribution.

The oil and gas technology is thus centered on these two main sectors. Oil well cementing presents one of the steps of well bore construction which starts from drilling into a target reservoir, to well evaluation (well logging), well completion and testing, cementing/perforation, acidizing and fracturing and to the final stage which is oil production. All these activities from drilling to the point of preparing the well for production is termed upstream segment.

The exploration commences from the primary objective of identifying a sedimentary basin with good hydrocarbon potential. Once a potential oil and gas reservoir is found, either onshore (i.e., on land) or offshore (i.e., in the ocean), drilling commence with drilling of an appraisal well to test the specific prospect of the area (for more details see [141]).

Extraction of oil and gas from the well bore requires sophisticated technology. The task ahead for both conventional and unconventional formations (HP/HT wells, deep water, tight gas, heavy oil, coal-bed methane (CBM), gas hydrate, shale oil and gas) is enormous (see **Figure 12**).

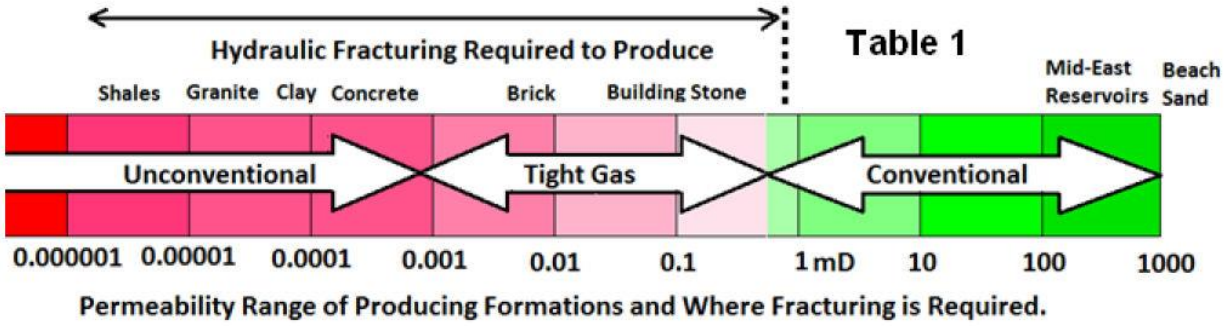

Figure 12: Permeability range of conventional, tight gas and unconventional formations [from 142**]**

This includes elaborate knowledge about deeper reservoirs in deep water areas, knowledge of petroleum systems and reservoir distribution, reservoir temperatures or pressures, reservoir-rock composition and properties, fluid composition and characteristics, reservoir management and optimization, wellbore integrity and intervention by providing safer and efficient methods for drilling, well logging and evaluation, coring and fracturing in order to reduce uncertainties and risks for the benefit of the society.

2.6.1 Hydrocarbon Reservoirs

Oil and gas reservoirs are accumulations of fluids and gases over geological time in an independent trap known as the sedimentary basin originated from the compaction and/or consolidation of sediments. They contain hydrocarbons stored in porous or fissured strata of the earth's outer crust under high temperature, pressure and saline environment with specific geometric configuration and boundary conditions, storage and flow properties [143, 144].

The position of these reservoirs depends on the chemistry of the reservoir, most especially the rock-fluid interaction and reservoir mineralogy. This is because the composition, content, occurrence, and distribution characteristic of clay minerals in the reservoir determines the storage capacity, productivity and the sensitivity of the reservoir.

The reservoirs need to contain four types of geological features which include: oil and gas source rock, reservoir rocks, a seal and a trap (see **Figure 13**).

Clay minerals are known to be an important composition of source and reservoir rocks that can generate and store oil and gas respectively. They also have influence on the physical and chemical properties of conventional sandstone, carbonate and unconventional shale.

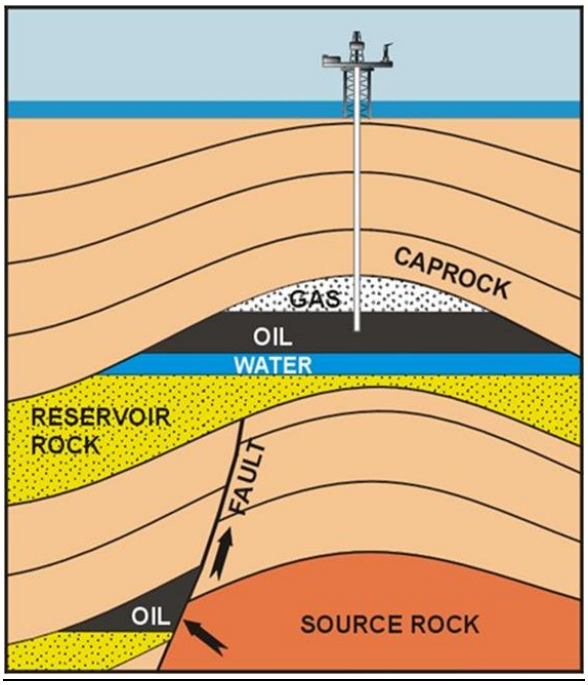

Figure 13: Scheme of an oil and gas reservoir [145]

Reservoir rocks: Reservoir rocks are rocks that are capable of holding oil and gas and releasing its content during production. They are normally characterized as either oil-wet or water-wet (wettability property), and by their fracture distribution and rock types. These are distinguished based on their permeability, porosity in terms of the effective storage space and specific surface area. The rocks are dominantly sandstones termed siliciclastic reservoirs which are basically quartz (SiO_2), with little feldspar, rock fragments (debris) and fine clay minerals (basically mudstones) for binding the quartz grains together.

Sandstone is a chemically fairly stable mineral and is not easily altered by changes in pressure, temperature or acidity of pore fluids. Hence, sandstone usually has uniform porosity (> 5- 25 %) [146].

Generally, porosity and permeability normally decrease with increasing depths. But anomaly high porosity and permeability in deep buried sandstone reservoirs are common. This is higher than typical sandstone subpopulations where a porosity loss by both mechanical and by chemical compaction is retarded by high pore pressure ≥ 16.9 MPa/km due to: (1) grain coats and grain rims, (2) early emplacement of hydrocarbons and (3) development of fluid overpressure [147].

Pure quartz is known to be strongly hydrophilic based on its silanol surface groups. But the mineralogy of the sandstone reservoir determines the distribution of crude oil within the sandstone pores as their storage is largely determined by the nature and the distribution of clay minerals. These factors make sandstone reservoirs scarcely being oil wet.

The other type of reservoir rock is limestone [148]. This carbonaceous reservoir rock is essentially composed of more than 50 % calcium carbonate such as calcite ($CaCO_3$) and sometimes contains dolomite ($CaMgCO_3$) due to calcium being substituted by magnesium during the diagenesis. Also, it contains low amounts of bioclasts (skeletal fragments of marine or land organisms), quartz and feldspars. These reservoir rocks are characteristically porous, permeable and offer a porous formation for the accumulation and free flow of oil and gas. This is because it contains a complex interconnected network of microscopic pores created by dissolved carbonates. The picture of a core sample in **Figure 14** is an example of a carbonate reservoir filled with white saddle dolomite.

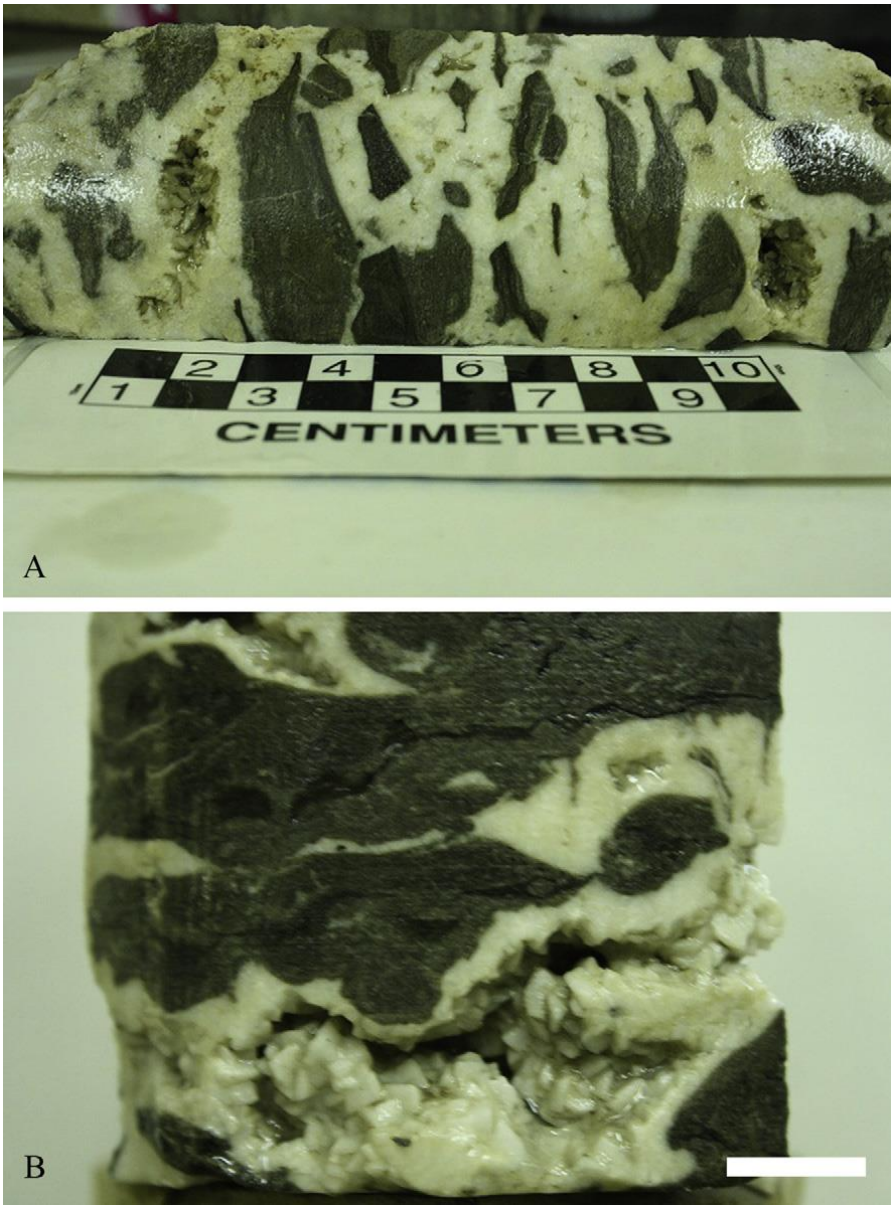

Figure 14: Core photographs of Trenton Group (Sherman Fall Formation) carbonates, southwestern Ontario. (A) Chaotic breccia, interparticle space filled with white saddle dolomite, (B) Mosaic breccia, interparticle porosity partially occluded by white saddle dolomite; obtained from [149].

A seal: is also known as cap rock [150]. These rock types do not allow fluid or gas migration and are generally very fined-grained rocks with very low permeability and ductile when compacted. The most common of these caps suitable for gas injection wells, e.g. for underground CO_2 storage, are argillaceous (mudstones, clays and shales) and evaporites (salt

and anhydrite) [151]. These cap rocks are normally tagged as being good or bad for underground storage (e.g. carbon capture and storage), based on their permeability to gases.

A trap: is the end result of the entire geological process, which is known to occur by physical arrangement between the reservoir rock fluids and the seal. There are mainly two types: structural, stratigraphic and sometimes a mixture of both together [148, 152]. The former have been formed when the reservoir rock and the overlaying seal have been deformed either by folding or faulting. This makes the oil and gas to migrate upward through the reservoir and accumulate in the highest part of the structure with a gas cap because of its low density (structural trap); whereas the latter (stratigraphic trap) are formed when the reservoir rock is deposited as a discontinuous layer.

There are many oil reserves located throughout the world, as shown in **Table 2**. According to the EIA report 2011, the total oil reserves worldwide are 1,471.2 billion barrels as of January 1, 2011 [153].

Table 2: World oil reserves by country as of January 1, 2011 (billion barrels) [153]

Country	**Oil reserves**	**Percentage of world total**
Saudi Arabia	260.1	17.68
Venezuela	211.2	14.35
Canada	175.2	11.91
Iran	137.0	9 .31
Iraq	115.0	7.82
Kuwait	101.5	6.90
United Arab Emirates	97.8	6.65
Russia	60.0	4.08
Libya	46.4	3.16
Nigeria	37.2	2.53
Kazakhstan	30.0	2.04
Qatar	25.4	1.73
United States	20.7	1.41
China	20.4	1.38
Brazil	12.9	0.87
Algeria	12.2	0.83
Mexico	10.4	0.71
Angola	9.5	0.65
Azerbaijan	7.0	0.48
Ecuador	6.5	0.44
Rest of the world	74.9	5.09
World total	**1,471.2**	**100.0**

2.6.2 Interface Formation- Fluids

Naturally occurring rocks are generally permeated with fluids which comprise of water, oil, gas or their combinations in varied proportion. The quality and quantity of the fluids within the reservoir and their transmissibility is of utmost importance in drilling and well completion. These reservoir fluids fall into three broad categories; (i) aqueous solutions with dissolved salts (connate water), (ii) liquid hydrocarbons, and (iii) gases (hydrocarbons and non-hydrocarbons).When hydrocarbons are produced, connate water is brought to the surface as an oil/water mixture and this water produced with oil is called produced water. The major constituent of this produced water is oil and grease, while the salt content (expressed as salinity, conductivity, or TDS) is a primary concern in onshore operations. In addition, the produced water also contains many organic and inorganic compounds which vary from one location to another and even over time in the same well [154].

Due to the presence of these diverse fluids confined together in a place, a sensitivity analysis (water, salt, alkali, acid and stress) is often used to ascertain their state in the reservoir. It is used to develop the best method for water shutoff on producing wells.

It is well known that most shallow formations contain some expandable clays like smectites which are mostly reactive to water and cause formation swelling. This effect can resist the flow through the rock pores, a typical problem in petroleum production [155] which mostly occurs when the injection water is incompatible with the formation water. This normally causes costly damage to the reservoir permeability as a result of a chemical shock.

The knowledge of the reservoir wettability (water-wet, oil-wet or gas wet) plays a significant role in the coexistence of oil, gas and water in the reservoir rock which is the result of complex interactions between the crude oil, the connate water and the rock surfaces. The composition fundamentally depends upon their origin, history, and present thermodynamic conditions (a limiting factor for the fluid mobility) which determines fluids characteristics like interfacial tension, density, viscosity, pour point etc.

For instance, fluid interaction with each other and to the reservoir rock can be determined by measuring the interfacial tension (IFT) and contact angle which is often altered by emulsifiers or surfactants in order to recover oil more efficiently [156-159].

The greater the time of contact between the oil and water, the lower is the interfacial tension which is an indication of improved wettability of the rocks. In case of bacterial infestation, a

clear interface between the oil and water may completely be absent due to secretion of surfactant, biofilms and other byproducts during microbial activity. This property is employed in microbial enhanced oil recovery (MEOR) [160, 161].

Since hydrocarbons have limited solubility in water, hydrocarbon degrading bacteria can modify the interface to attain contact with both fluids. For this purpose, bio-surfactants are injected which are a heterogeneous group of surface-active molecules with hydrophilic and hydrophobic moiety [162].

An examination of reservoir fluids under various pressures, volumes, and temperatures (PVT) is important to understand reservoir fluid chemistry which defines the relative volumes of each fluid in a reservoir. For active characterization of formations, the most important parameters that are normally considered includes: formation water properties like pH and total salinity; crude oil properties like density, viscosity and pour point for flow property of fluids; types of natural gas present (CO_2 and H_2S and other associated gases), bottom hole formation temperature and pressure in order to design and implement adequate hydrostatic mud pressure.

2.6.3 Drilling Process

The principle of drilling an oil or gas wellbore involves drilling through the overlaying layers of the earth's crust, mostly with a rotatory hydraulic technique to a specific geological formation. This activity involves high-tech machinery and the engineering required to drill properly can be highly complex.

Numerous factors are always considered for designing downhole tools and the fluids to be used for such operations, such as: formation types (soft, medium soft, hard or medium hard formation) and stability of wellbore (hole enlargement, formation with no cohesive strength, fluid interaction with formation, etc.) [163-165]; down hole pressure and temperature [166-168]; down hole tools for data transmission [169], environmental and disposal issue [170] and limitation of drilling fluids with respect to their stability [171-173] and hole cleaning [174].

Generally, a rotatory drill bit is coupled to the drill string which serves as the fluid conduit to the drill bit. At the same time imparted rotary motion to the drill bit, provides and allows weight (force) to be set on the drill bit by the drilling collar mounted directly on the bit. The drill collar then provides strength needed to run in compression for crushing the rocks when rotated while applying axial force to the bit. A drilling fluid called “drilling mud” is pumped down the borehole through the interior of the drilling tool assembly (drill string), and outward through appropriate orifices, called nozzles or jets disposed in the body of the drill bit while drilling. The cuttings created by the drill bit that must be removed are carried by the drilling mud pumped through the bit are forced through the annulus (space between the drill pipe and the outer casing) as drilling proceeds which aids the transportation of the rock cuttings and debris up to the surface.

The drilling rig for deep onshore or offshore, extended reach wells, horizontal wells, multi branched-wells is set up in a more difficult environment with risk of positioning failure compared to conventional low temperature low pressure wells. For instance, an offshore rig comprises of a rotary table, derrick, drill line and prime movers. But, more sophisticated downhole equipment with complex bottomhole assemblies (BHA) is required for wells like deepwater and HP/HT.

For deep waters, it is common practice to conduct drilling operations from drilling ships, floating vessels or platforms depending on their capabilities, limitations (water depths), and of course cost (see **Figure 15**).

To conduct operation on those platforms, unlike in a land operation, deepwater drilling requires a long riser pipe to encapsulate drilling equipment which allows workers above the surface of the water to drill deep from the surface down to a subsea wellhead on the ocean floor (see **Figure 16**). The riser pipe serves to guide the drilling string and to provide a return conduit for circulating drilling fluids.

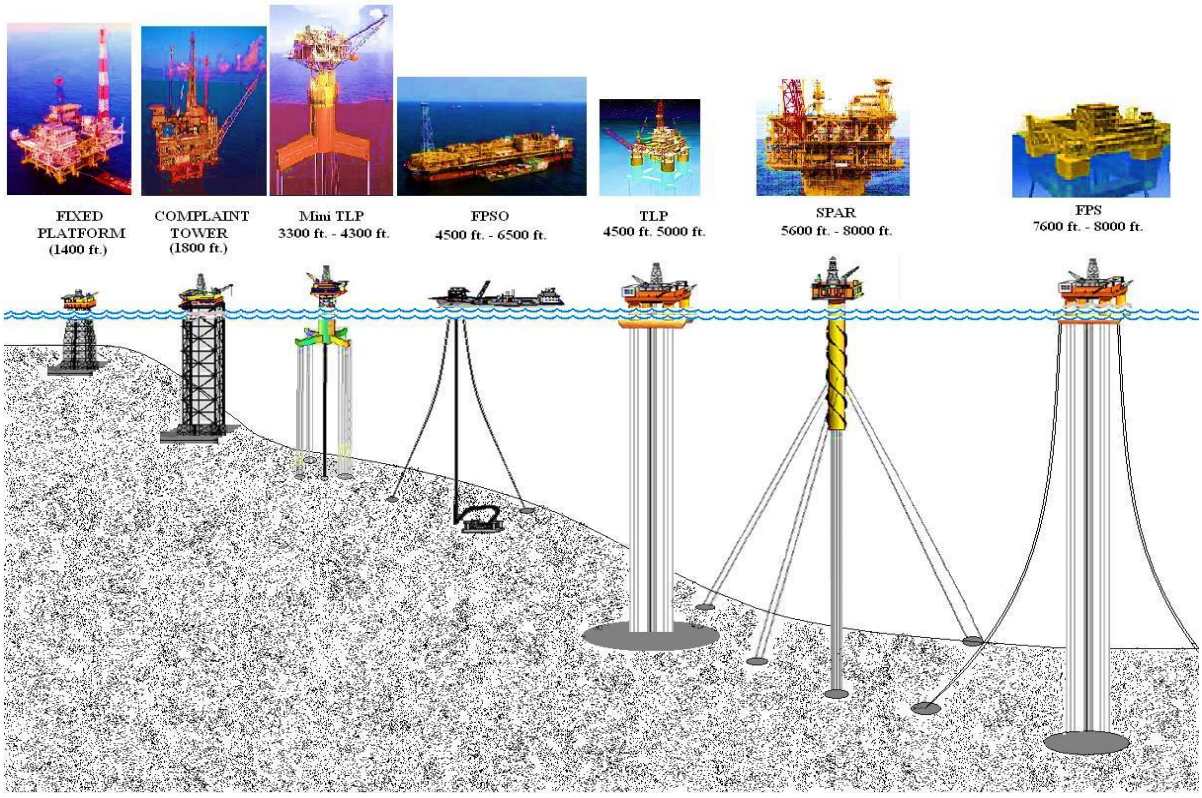

Figure 15: Types of offshore drilling rigs [175]

Figure 16: Riser for deepwater drilling [175]

Recently, dual gradient drilling (DGD) technology that was introduced over 50 years ago for deepwater exploration has now reached a stage of implementation and became hot with respect to intellectual property rights. Thus, several hundred patents were filed [176-179].

DGD technology (dual-gradient drilling) promises to overcome the limitations imposed on the formation which occurs by sending drilling mud through thousands of feet of drill pipe and riser. This new technique is set to dramatically change conventional drilling process, such that the rig effectively sits on the seafloor, rather than at its actual physical location thousands of feet above on the sea surface. A schematic representation of this technology is shown in **Figure 17**.

In DGD, the mud column extends only from the bottom of the hole to the mud line with the use of subsea pumps to reduce the hydrostatic head from the mud line to the surface. This gives benefits which include reducing the number of casing strings, enabling the use of larger completion strings for increased flow capacity, improved drilling efficiency and decreased mechanical risk.

The Maurer approach seeks to achieve the same benefit by pumping lightweight solid additives (LWSAs) from the drillship into the riser at mud line which consists of hollow glass spheres and polymeric beads (polypropylene). It has undergone extensive testing. However, an investigation of alternative material is still under investigation. This technology seems to be the future for offshore drilling as highlighted in the 2013 workshop organized by the International Association of Drilling Contractors (IADC) on dual gradient drilling [180].

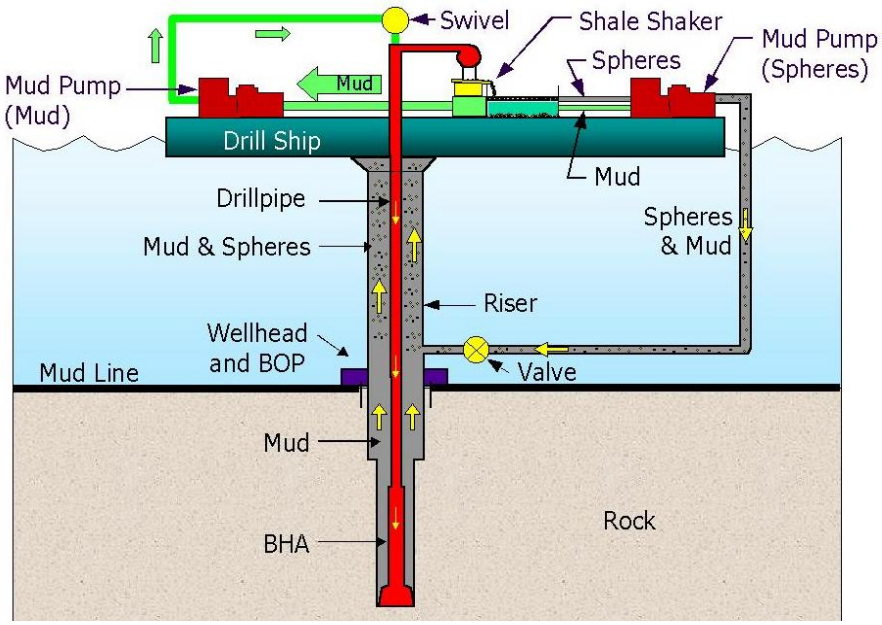

Figure 17: Schematic of a Dual-Gradient Drilling operation (source: Maurer Technology [181])

2.6.4 Drilling Fluids

Drilling fluids are mixtures of natural and synthetic chemical compounds that provide the following functions: filtration and rheology control (thinning/dispersing effect), densification/weight, viscosity, pH control or alkalinity, lubricity, lost circulation control, flocculation and shale stabilization. They also assist in the acquisition of information about the formation being drilled, e.g. through drill cuttings, electric logs and coring analysis (electrical conductivity-resistivity effect) [182]. The fluids are designed to ensure that rotary drilling of subterranean formations is possible and economically viable.

The drilling fluid types used are primarily characterized into three broad groups according to the medium used for their preparation: water, oil and gas based drilling fluids. The water-based fluids are further subdivided into five based on their major constituents and dispersion: dispersed, non-dispersed, polymer fluids, low solids and salt water system (e.g. NaCl, $CaCl_2$ and seawater). While oil based mud is subdivided into two: Oil mud (e.g. all oil mud or invert emulsion fluid) and synthetic oil-based mud (SOBM) which is now more commonly used. It was designed to mirror the performance of a drilling mud with limited environmental hazard, unlike the conventional oil mud with high toxicity due to the presence of aromatic hydrocarbons and diesel.

The primary types of synthetic fluids used in the field are esters, ethers, poly alpha olefins and isomerized alpha olefins. They are preferred over water based muds because they are suitable for drilling water-sensitive formations. They provide shale stabilization, faster drilling with high rate of penetration, high temperature stability; are suitable for salt and low pore pressure formations, exhibit high lubricity and corrosion control property and can be stored over a longer period of time for re-use, with no problem of bacterial growth.

In general, drilling fluids are complex heterogeneous mixtures of various types of base fluids and chemical additives that must remain stable over a range of temperature and pressure conditions. They contain chemicals like dispersant/thinners, weighting agents, bentonite and fluid loss additives designed to control the pressure of the rock formation and at the same time prevent excessive aqueous fluid loss from the wellbore by forming a thin filtercake [183-185]. This is only achievable with fluid loss additives and suitable bridging particles which have a specific size range to create a solid framework for the ideal filter cake [186]. The muds are thus designed to create deformable particles to fill small gaps and improve the

seal by forming a tight filter cake that allows the hydrostatic pressure of the liquids to stabilize the borehole and prevents it from collapsing [187].

The mud to be used must be carefully selected based on the porosity and downhole pressure of the reservoir. It must be non-damaging which will allow production of more hydrocarbons from the reservoir and at the same time compatible with the formations being drilled. The pressure exerted by the mud column has to exceed the formation pressure in order to maintain overbalance and prevent the hole from collapsing and lower than the fracture pressure of the formation. If the formation strength is exceeded, artificial fracturing might occur, noticeable with what is known as a "kick". This might result in mud losses and formation damage that will requires the use of lost circulation materials to "kill the well" [188].

The types of drilling mud to be used that will give maximum production from the reservoir and additives of drilling fluid suitable for such operation is always designed on the basis of well log data [189], core analysis [190] and sensitivity analysis which is the study of effect of a selected parameter such as wettability of the reservoir, oil-wet (sandstone) or water-wet (mostly carbonates), formation water, stress, acid, pH, rate, etc., on the system performance aimed at evaluating the effect of inter-related parameters of the reservoir on production results [191].

Moreover, insoluble solids such as barite, hematite or bentonite which plug reservoir pores are not used in tight reservoirs with very low permeability in order to prevent formation damage caused by the invasion of filtrate and solids into the formation. Also, in salt formation, sized salt (NaCl) and $CaCO_3$ suspended in salt brine, sometimes with 2-4 % bentonite are often used which normally requires high dosages of viscosifying polymer and fluid loss polymer.

Oil-based systems are only used occasionally (disposal problem) for a variety of applications where fluid stability and inhibition are necessary such as high-temperature wells and where differential sticking and hole stabilization is a problem. The oil based muds are formulated with only oil as the liquid phase and are often used as coring fluids. Specialized oil-based mud additives include: emulsifiers and wetting agents (commonly fatty acids, amides consisting of N-alkylated polyether chains and amine derivatives), high molecular weight soaps, surfactants and lime for alkalinity. Others are organophilic clays which can be solved easily in oil, obtained by reaction of normal hydrophilic clays [bentonite, attapulgite which comprises of magnesium silicate, and sepiolite, a hydrated magnesium silicate that gives

stable viscosity up to 400 °C) with amine-treated organic materials. This is carried out by cation exchange of aliphatic amine salts with quaternary ammonium salts or base.

2.6.5 Well logging

This is the practice of making a detailed record of the geological formations penetrated by a borehole. The log (record) may be based either on visual analysis of samples brought to the surface (geological logs) or on physical measurements made by instruments lowered into the hole (geophysical logs).

2.6.6 Coring

Oil well coring is a modern method used for oil field prospecting and development for actualizing the objective of drilling an oil or gas well. This is used to locate hydrocarbon-bearing structure that will produce oil and gas in quantities sufficient to give adequate return on investment for drilling and completion of a well.

Coring involves an extensive investigation of formation chemistry in a well bore and its economic feasibility with the aftermath of recovery efficiency, which is defined as the ratio of the produced oil (PO) to the total oil in place (TOIP) [192]. Particularly, during the exploration phase of the field where simultaneous drilling and coring system is possible [193], coring presents an important means to calibrate the petrophysical model and gain additional information about the reservoir not obtainable by logs [194].

One of the most reliable sources of information on the lithology and fluid-bearing characterization of a reservoir is to sample the actual reservoir rock. A tool for retrieving samples from such well bore drilled in a subterranean formation includes a device used for retrieving a core from the well bore wall, a well bore isolation device that isolates an annular region proximate to the coring device; and a flow device that siphons fluids out of the isolation region [195]. The challenge of this method is to maintain the mechanical and /or chemical integrity of the core sample from its source to the surface prior to its examination in the laboratory. Sponge coring allows measurement of in-situ conditions, oil and water saturation, permeability, relative permeability, capillary pressure, and gas saturation with the

aid of different drill plug systems (see **Figure 18**) that can convert the core-head into a drill bit, thus allowing drilling of other formation without tripping even when retrieving the core [196].

Figure 18:Schematic of a drilling plug allowing simulteneous drilling and coring (from [196])

In 2006, *Carey* et al. retrieved a core sample that included casing, cement and shale cap rock from a 30-year old CO_2-flooding operation at the SACROC Unit located in West Texas

[197]. The core was investigated as part of a program to evaluate the integrity of Portland-cement based wellbore systems in CO_2-sequestration environments and thus confirmed that the recovered cement had air permeability in the tenth of a milliDarcy range with potential to retain its capacity in order to prevent significant flow of CO_2.

2.6.7 Well completion

Once a well has been drilled and tested, a decision is made whether to complete the well for production or plug it. Examination of the target reservoir rock porosity and permeability may indicate that the potential flow of oil and gas from the well will not justify the cost to complete the well. In that situation, the well is plugged with concrete in several stages, and the well was abandoned. But, in most cases, after a well has been drilled and oil was discovered, the well is then completed to obtain the maximum hydrocarbon production from the subterranean formations.

Completion of a well refers to the operations performed during the period from drilling into the pay zone until the time the well is put into production. These operations may include additional drilling-in, placement of downhole hardware, fishing, perforation (liner or casing perforation), corrosion control of downhole tools and sand control operations such as gravel packing; downhole cleaning, foam stabilization, water shutoff /leakoff inhibition. Also, other fluid mixtures are used which contain additives such as biocides, fluid-loss agents or oxygen scavengers. A fluid used to facilitate such operations is often called completion fluid.

After all the downhole debris is removed and the tools are in place, a cement slurry is finally pumped downward through the tubing within the casing and allowed to flow out at the well bottom as shown in **Figure 19**. It is then forced upward around the casing in the annular space between the outer wall of the casing and the wall of the bore hole.

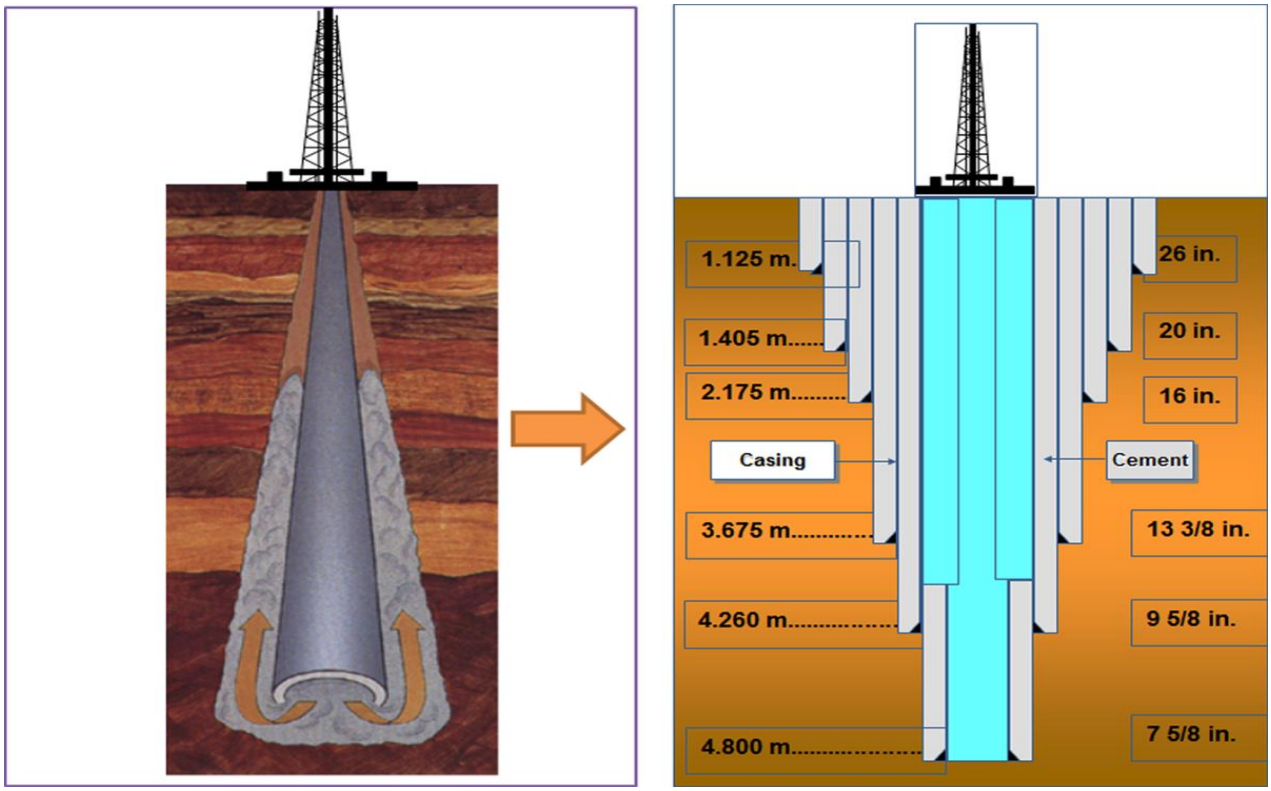

Figure 19: Schematic representation of the process of oil well cementing

The cement slurry thus pumped into place sets into a monolithic mass which prevents the flow of undesirable fluids from one formation to another; secures the casing in position, prevents unwanted shifting of the casing when the fluid being produced from a formation moves through it under considerable pressure. The cement also serves the important function of sealing off porous formations adjacent to the well bore. A schematic diagram activities showing most of the important downhole cementing tools is presented in **Figure 20**.

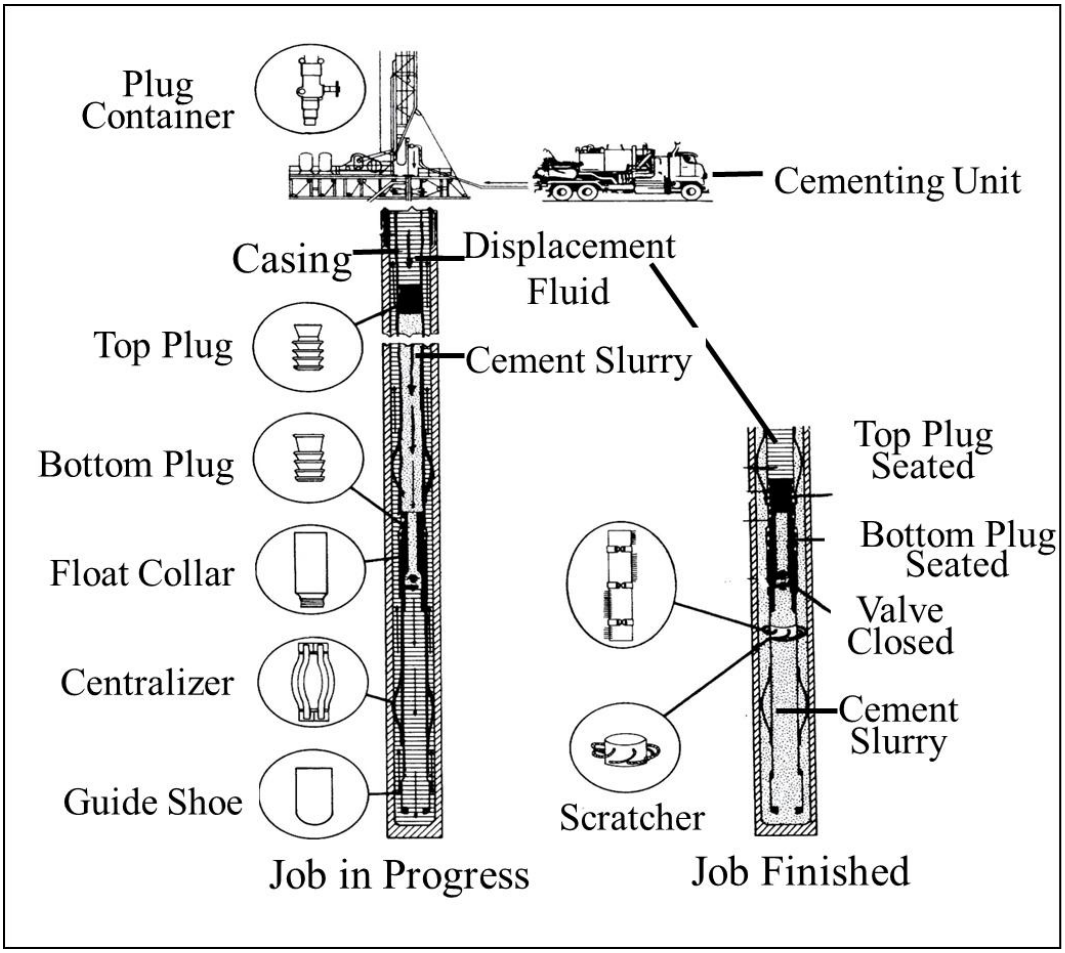

Figure 20: Schematic diagram of oil well cementing technology [from 98]

Down-hole equipment such as centralizers are used to ensure that satisfactory zonal isolation is obtained. If casing strings are cemented off-center, there is a high risk that a channel of drilling fluid or contaminated cement will be left where the casing contacts the formation. This will lead to an imperfect seal, as is shown in **Figure 21**.

Also, devices fitted with hinged collars and bow springs helps to keep the casing or liner in position at the center of the wellbore. This helps to ensure efficient placement of a cement sheath around the casing string.

Finally, the float Shoes and Collars (float valves) shown in the scheme (see **Figure 20**) will prevent backflow after the cement has been pumped into place.

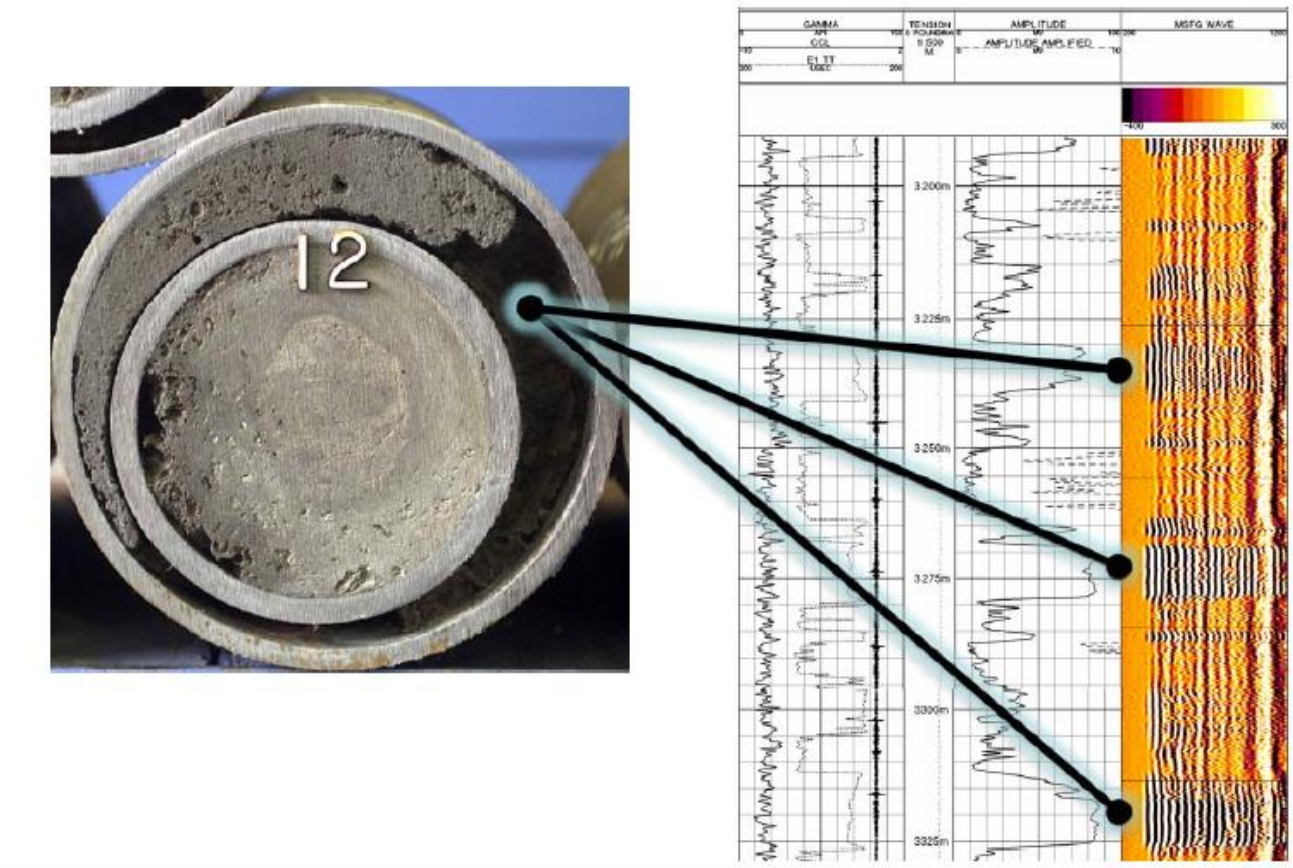

Figure 21: Poor cementing integrity in annulus (Courtesy of Halliburton open house seminar, Celle, 2010)

Most importantly, integrity of the cement sheath requires optimization of the placement of the fluids and thus mud removal in the well bore. Hence, cement slurry properties like mixability, stability, rheology, fluid loss, and thickening time should be taken into account when carrying out cement slurry design and testing. For example, loss of fluid from the slurry to the formation should be avoided because it will lead to premature thickening and setting of the cement, produce a set cement of non-uniform consistency and of reduced compressive strength.

The API fluid loss of neat cement slurry is generally in excess of 1,500 mL/30 min. A schematic diagram of the static fluid loss test for cement slurry according to American Petroleum Institute (API) specification with and without fluid loss additive (FLA) is shown in **Figure 22**. An API fluid loss of 50 mL/30 min is often required to maintain adequate slurry performance. To achieve this reduction, a suitable water soluble polymer known as

fluid loss additive which performs at the conditions occurring in a wellbore such as high temperature, pressure and salinity is indispensable for the slurry design [90, 198].

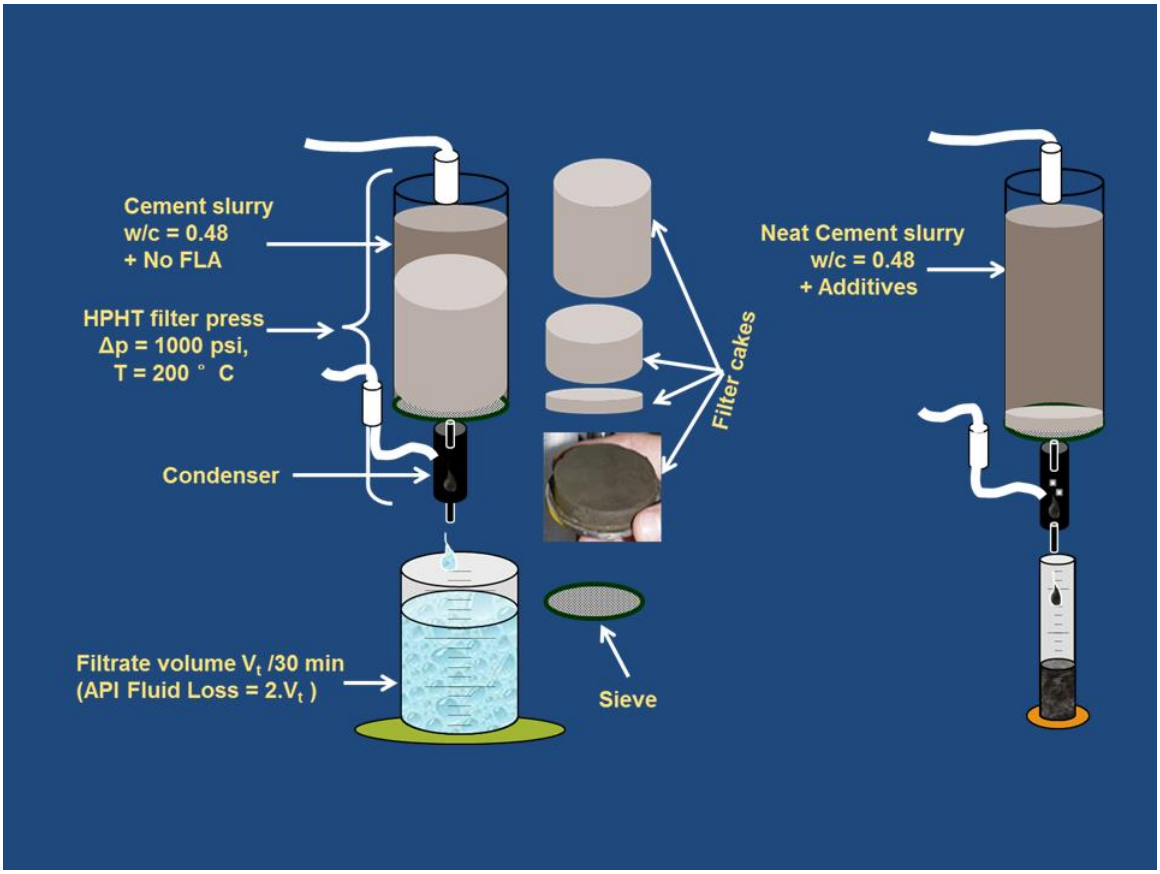

Figure 22: Schematic diagram of the static fluid loss test of a cement slurry with and without fluid loss polymer, according to American Petroleum Institute (API) specification

Once the casing is in place and complete zonal isolation has been achieved, a tool called a "perforating gun" is lowered into the wellbore to blast holes through the cemented casing (casing perforation or liner perforation), and into the reservoir. These holes are made in order to create a communication between the reservoir and the production casing. Tubing may then be lowered into the casing and a plug will be set above the perforations as a barrier between the production casing and the tubing. This allows natural pressure to push the hydrocarbons to the wellbore and to the surface unless a pump jack is necessary to raise the fluids to the surface.

2.6.8 Oil Production and Stimulation

In well construction, drilling through the impervious cap rock of the reservoir provides a pressure release point for the fluids in the reservoir to flow. When this fluid is recovered after perforation under its natural flow, it is termed “primary” recovery. This type of recovery is possible only when oil and gas coexist in a state at which their pressure is greater than the pressure at the well bore.

Primary recovery only produces less than 30 % of the total oil in place (TOIP), even when artificial lift (with the aid of installed pumps) is used to maintain the production when the pressure of the reservoir is reduced.

In order to extract more hydrocarbons from reservoirs, several secondary and tertiary approaches are used.

For carbonate and sandstone reservoirs, acidizing (acid fracturing) is mostly employed [199] while at present, hydraulic fracturing is widely used to improve recovery by pumping down hydraulic fluids into the well under high pressure until the reservoir rock is artificially fractured, most especially for shale oil and gas which present one of the largest potential at present e.g. the Barnett, Eagle Ford and Marcellus shales (see **Figure 23**).

The fracture created is maintained mostly with granular proppants (e.g. sand, ceramics, plastics, glass or composites) added to the fracturing fluid in order to keep the fracture propped open after the pumping of fluid has stopped and the pressure subsides, in order to avoid fracture closure.

Figure 23: Two Marcellus drilling sites at *beaver run reservoir* (from www.Marcellus-shale.us)

The purpose of fracturing induced cracks created in the formation is to increase reservoir permeability to facilitate the flow of oil and gas accomplished by pumping a large volume of fluid mixed with additives at high injection rates into the wellbore (see **Figure 24**).

These fluids are composed of at least 90 % water, 9.5 % sand and ~ 0.5 % additives, designed in such a way that it should breakdown after the fracturing job has been completed so that the constituents can be recovered easily.

Proper selection of the fracturing fluid is one of the important decisions carried out with respect to the wellbore chemistry [200]. To select the proper fluid, properties such as fluid loss control, fracture conductivity, pressure between the formation and the well bore, viscosity of the oil, reservoir composition and high enough viscosity to suspend and transport the proppant are considered.

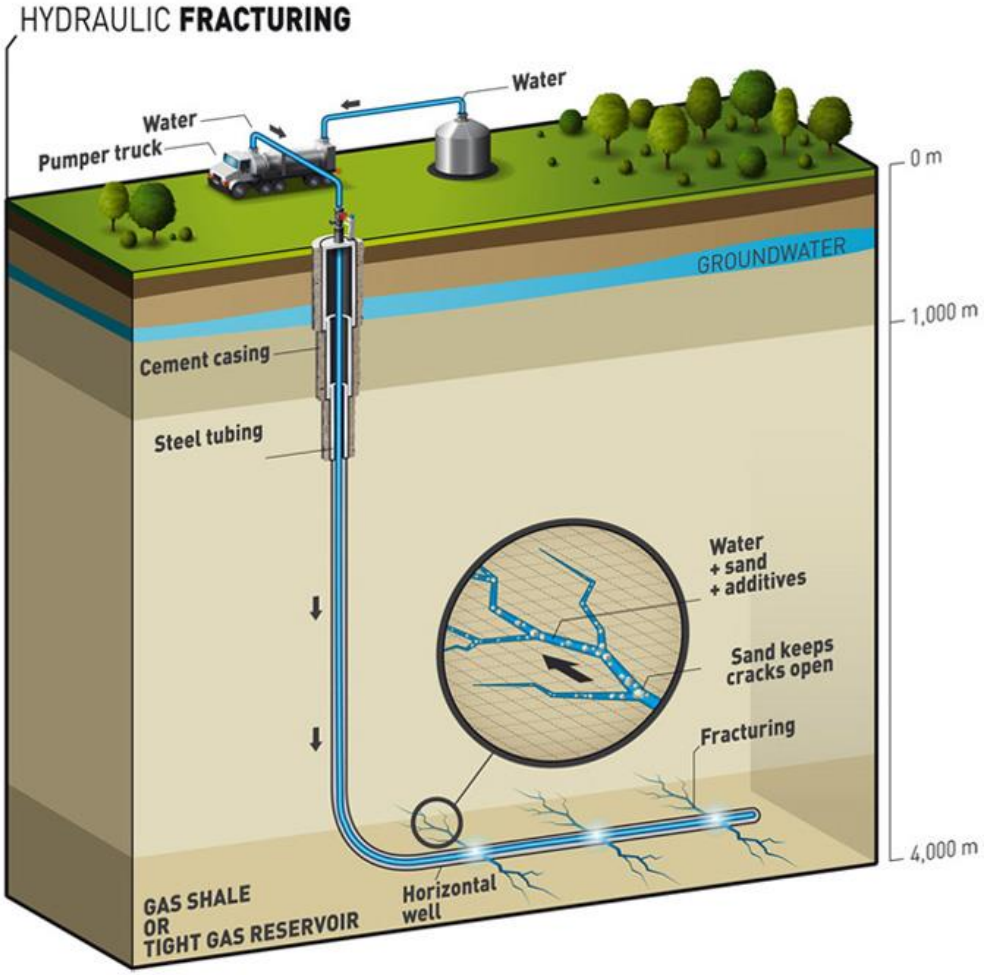

Figure 24: Schematic hydraulic fracturing operation [201]

The fluids used are categorized into four major parts: Gel fluids which are either linear or cross-linked gels; foam gels; and salt water containing potassium chloride and acids.

The fluids design must be: viscous enough to create a fracture of adequate depth; be able to transport large amounts of proppant into the fracture; maximize fluid travel distance to extend fracture length; minimize friction pressure losses during injection; cost effective; contain chemicals that are environmentally acceptable (often biodegradable); require minimal gelling agent to allow for easier degradation or clean-up by exhibiting a controlled break to a low viscosity fluid [202, 203].

One other factor considered in fracturing fluid selection is the use of organic polymers because of temperature limitations of the biopolymers.

RERERENCES

[1] The outlook for Energy by ExxonMobil: *A view to 2040*, http://www.exxonmobil.com/Corporate/files/news_pub_eo.pdf retrieved on August 27, **2013**.

[2] DeBruijn, G., Greenaway, R., Harrison, D., James, S., Mueller, F., Ray S., Riding M., Temple, L., Wutherich, K.: *High-Pressure, High-Temperature Technologies: oilfield review*, **2008**.

[3] Pike, W. J.: *How deep can we go?*, World Oil, April **2013**

[4] Sanz, P.F.; Dasari, G. R.: *Controls On In-situ Stresses Around Salt Bodies*, American Rock Mechanics Association Conference paper 10-169, **2010;** 44th U.S. Rock Mechanics Symposium and 5th U.S.-Canada Rock Mechanics Symposium

[5] Barker, J. W.; Feland, K. W.: *Drilling long salt sections along the US Gulf Coast*, SPE paper 24605 presented at the SPE Annual Technical Conference and Exhibition, Oct. 4–7, **1992** Washington DC

[6] Vidick, B., Acock, A., Dowell Schlumberger, Minimizing Risks in High-Temperature/High-Pressure Cementing: *The Quality Assurance/Quality Control Approach*, SPE paper 23074, Offshore Europe, 3-6 September **1991**, Aberdeen, United Kingdom

[7] Baker, A.C.; Price, M.: *Modeling the Performance of High-Pressure High-temperature Wells*, SPE paper 20903, European Petroleum Conference, **1990**, Hague, Netherlands

[8] Ravi, K.; Bosma, M.; Gastebled, O.: *Improve the Economics of Oil and Gas Wells by Reducing the Risk of Cement Failure*, SPE paper 74497, presented at the IADC/SPE Drilling Conference, 26–28 February **2002**, Dallas, Texas

[9] Goodwin, K.J. and Crook, R.J.: *Cement Sheath Stress Failure*, SPE paper 20453 presented at the Annual Technical Conference and Exhibition, 23-26 September, **1990**, New Orleans, Louisiana,

[10] Ravi, K., Bosma, M.; Gastebled, O.: *Safe and Economic Gas Wells through Cement Design for Life of the Well*, SPE paper 75700 presented at the Gas Technology Symposium, 30 April - 2 May, **2002,** Calgary, Alberta, Canada

[11] Ravi, K., McMechan, D. E., Reddy, B.R., Crook, R.: *A Comparative Study of Mechanical Properties of Density-Reduced Cement Compositions*, SPE paper 90068, SPE Annual Technical Conference and Exhibition, 26–29 September **2004**, Houston, Texas, U.S.A

[12] Pelipenko, S.; Frigaard, I. A.: *Mud removal and cement placement during primary cementing of an oil well*, J Eng. Maths, 48, **2004**, 1-26

[13] National Commission on the *BP Deepwater Horizon Oil Spill and Offshore Drilling*, Chief Counsel's Report, Washington: **2011**

[14] Plank, J., *Failed cement job caused environmental catastrophe at BP`s Macondo oil well*, Cement International, **2011**, 68 – 76.

[15] Smith, R. C.: *Successful Primary Cementing Can Be a Reality*, SPE distinguished author series, **1984**, 1851-1858

[16] Garnier A, Frauoulet B, Saint-Marc J.: *Characterization of Cement Systems to Ensure Sheath Integrity*, SPE paper 18754, SPE Offshore Tech. Conference, **2007**

[17] Bülichen, D., Plank, J.: *Role of Colloidal Polymer Associates for the Effectiveness of Hydroxyethyl Cellulose as a Fluid Loss Control Additive in Oil Well Cement*, J Appl Polym Sci 126, **2012**, E25-E32

[18] Bülichen, D.; Kainz, J.; Plank, J: *Working mechanism of methyl hydroxyethyl cellulose (MHEC) as water retention agent*, Cem Concr Res 42, **2012**, 953–959

[19] Poinot, T.; Govin, A.; Grosseau, P.: *Importance of Coil-overlapping for the effectiveness of hydroxypropylguars as water retention agent in cement-based mortars*, Cem Concr Res, 56, **2014**, 61-68

[20] Poinot, T.; Govin, A.; Grosseau, P.: *Impact of hydroxypropylguars on the early age hydration of Portland cement*, Cem Concr Res, 44, **2013**, 69-76

[21] Bülichen, D.; Plank, J.: *Mechanistic Study on Carboxymethyl Hydroxyethyl Cellulose as Fluid Loss Control Additive in Oil Well Cement*, J. Appl Polym Sci., **2012**, 124, 2340-2347

[22] Lewandowska, K.: *Comparative studies of rheological properties of polyacrylamide and partially hydrolyzed polyacrylamide solutions*, J. Appl Polym Sci., 103, **2007**, 2235-2241

[23] Plank, J.; Brandl, A.; Zhai, Y. N.; Franke, A.: *Adsorption behavior and effectiveness of poly(N,N-dimethylacrylamide-co-Ca 2-acrylamido-2-methylpropanesulfonate) as cement fluid loss additive in the presence of acetone-formaldehyde-sulfite dispersant*, J. Appl Polym Sci, 102, **2006,** 434 – 4347

[24] Ezzel, S.A.; McCormick, C. L.: *Water-Soluble Copolymers. 39. Synthesis and Solution Properties of Associative Acrylamido Copolymers with Pyrenesulfonamide Fluorescence Labels*, Macromol, 25, **1992**, 1881-1886

[25] Hill, A.; Candau, F.; Selb, J.: *Properties of Hydrophobically Associating Polyacrylamides: Influence of the method of the synthesis*, Macromol, 26, **1993**, 4521-4532

[26] Cram, S. L.; Brown, H. R.; Spinks, G. M.; Hourdet, D.; Creton, C.: *Hydrophobically Modified Dimethylacrylamide: Synthesis and Rheological Behavior*, Macromol, 38, **2005**, 2981-2989.

[27] Bishop, M.; Baron, A. R.: *Cement Hydration Inhibition with Sucrose, Tartaric acid and Lignosulfonate: Analytical and Spectroscopic Study*, J. Ind. Eng. Chem. Res., 45 (21), **2006**, 7042-7049

[28] Lummer, N. R.; Plank, J.: *Combination of lignosulfonate and AMPS®-co-NNDMA water retention agent - An example for dual synergistic interaction between admixtures in cement*, Cem Concr Res, 42, **2012**, 728-735

[29] Guo, S.; Bu, Y.: *Synthesis and Application of 2-Acrylamido-2-Methyl Propane Sulfonic Acid/Acrylamide/N,N-Dimethyl Acrylamide/Maleic Anhydride as a Fluid Loss Control Additive in Oil Well Cementing*, J. Appl. Polym. Sci. 127, **2013**, 3302–3309

[30] Lummer, N. R.; Dugonjic-Bilic, F.; Plank, J.: *Effect of High Temperature and the Role of Sulfate on Adsorption Behavior and Effectiveness of AMPS®-based Cement Fluid Loss Polymers*, J Appl Polym Sci, 121, **2011**, 1088-1095

[31] Chu, Q.; Luo, P.; Zhao, Q.; Feng, J.; Kuang, X.; Wang, D.: *Application of a New Family of Organosilicon Quadripolymer as a Fluid Loss Additive for Drilling Fluid at High Temperature*, J. Appl. Polym. Sci. 128, **2013**, 28–40

[32] Plank, J.; Dugonjic-Bilic, F.; Lummer, N. R.: *Impact of the Steric Position of Phosphate Groups in Poly (N,N-dimethylacrylamide-co-2-acrylamido-2-methylpropsnesulfonate-2-x-phosphonate) on its Adsorbed Conformation on Cement: Comparison of Vinyl Phosphoric Acid and 2-Acrylamido-2-methylpropane Phosphonate Modified Terpolymers*, J. Appl Polym sci, 115, **2010**, 1758-1768

[33] Plank, J.; Dugonjic-Bilic, F.; Lummer, N. R.: *Competitive Adsorption Between an AMPS®- Based Fluid Loss Polymer and Welan Gum Biopolymer in Oil Well Cement*, 116, **2010**, 2913-2919

[34] Wu, Y.-M.; Zhang, B.-Q.; Wu, T.; Zhang, C.-G.: *Properties of the forpolymer of N-vinylpyrrolidone with itaconic acid, acrylamide and 2-acrylamido-2-methyl-1-propane sulfonic acid as a fluid-loss reducer for drilling fluid at high temperatures*, Colloid Polym Sci, 279, **2001**, 836-842.

[35] Dugonjic-Bilic, F.; Plank, J.: *Polyelectrolyte Complexes from Polyethylene Imine/ Acetone Formaldehyde Sulfite Polycondensates: A Novel Reagent for Effective Fluid Loss Control of Oil Well Cement Slurries*, J. Appl Polym Sci., 121, **2011**, 1262-1275

[36] Plank, J.; Dugonjic-Bilic, F.; Lummer, N. R.: *Modification of the Molar Anionic Charge Density of Acetone-Formaldehyde-Sulfite Dispersant to Improve Adsorption Behavior and Effectiveness in the Presence of CaAMPS®-co-NNDMA Cement Fluid Loss Polymer*, J. Appl Polym Sci., 111, **2009**, 2018-2024

[37] Pires, R. V.; Oliveira, R. S.; Lucas, E. F.; Martins, A. L.: *Influence of Grafted Copolymer Structures (Polyacrylamide-g-polyoxide) on Drag-Reduction*, J. Appl Polym Sci., 119, **2011**, 2502-2510

[38] Patel, A.; Zhang, J. H.; Ke, M.; Panamarathupalayam, B.: *Lubricants and drag reducers for oilfield applications - chemistry, performance and environmental impact*, SPE paper 164049, presented at International Symposium on Oilfield Chemistry, April 8-10, **2013,** held in The Woodlands, Texas, USA

[39] Lahalih, S. M.; Ghloum, E. F.: *Rheological Properties of New Polymer Compositions for Sand Consolidation and Water Shutoff in Oil Wells*, J Appl Polym Sci, 104, **2007**, 2076–2087

[40] Jayakumar, S.; Lane, R. H.: *Delayed crosslink polymer gel system for water shutoff in conventional and unconventional oil and gas reservoirs*, SPE paper 164046, presented at International Symposium on Oilfield Chemistry, , April 8-10, **2013,** held in The Woodlands, Texas, USA

[41] Alvarez, F.; Flores, E. A.; Castro, L. V.; Hernandez, J. G.; Lopez, A.; Vazquez, F.: *Dissipative Particle Dynamics (DPD) Study of Crude Oil-Water Emulsions in the Presence of a Functionalized Copolymer*, Energy & Fuels, 25, **2011,** 562-567

[42] De Souza, C. E. C.; Alexandre Souza Lima, A. S.; Nascimento, R. S. V.: *Hydrophobically Modified Poly(ethylene glycol) as Reactive Clays Inhibitor Additive in Water-Based Drilling Fluids*, J Appl Polym Sci, 117, **2010**, 857–864

[43] Kredra-Krolik, K.; Mutelet, F.; Moise, J-C.; Jaubert, J-N. : *Deep Fuels Desulfurization and Denitrogenation Using n-Butyl-3-methylimidazolium Trifluoromethanesulfonate*, Energy & Fuels, 25, **2011**, 1559-1565

[44] Schlesinger, W. H.: *Biogeochemistry: An Analysis of Global Change*, Academic Press, San Diego, **1991**

[45] Stevenson, F. J.: *Humus Chemistry: Genesis, Composition*, Reactions, John Wiley & Sons, NY, **1994**

[46] Kucerik, J., Petar, M.; Klucakova, M.: *South-Moravian Lignite- Potential Source of Humic Substances*, Petroleum and Coal, 45, **2003**, 58-62

[47] Pettit, R. E.: *Organic Matter, Humus, Humate, Humic acid, Fulvic acid, and Humin.* Retrieved on 25th of July, **2013** from http://www.calciumproducts.com/articles/Dr._Pettit_Humate.pdf

[48] Velthorst, E.; Nakken-Brameijer, N.; Mulder, J.: *Fractionation of Soil Organic Matter*, Int. J. Environ. Ana. Chem., 73, **1999**, 237-251

[49] Moschopedis, S.E.: *Sulfomethylation of humic acids, lignites, and coals and products thereof*, US patent, 3,352,902, **1967**

[50] Schulz, J. G.; Cobler, J. A.: *Coal Suspensions and Process for Preparing same*, US patent 4,305,728, **1981**

[51] Tonelli, D.; Seeber, R.; Ciavatta, C.; Gessa, C.: *Extraction of humic acids from a natural matrix by alkaline pyrophosphate. Evaluation of molecular weight of fractions obtained by ultrafiltration*, Fresenius J. Ana. Chem., 359, **1997**, 555- 560

[52] Piccolo, A.: *The Supramolecular Structure of Humic Substances*, Soil Sci, 116, (11), **2001**, 810-832

[53] Cook, R. L.; Langford, C. H.: *Structural Characterization of a Fulvic Acid and a Humic Acid Using Solid-State Ramp-CP-MAS ^{13}C Nuclear Magnetic Resonance*, Environ. Sci. Technol., 32, **1998**, 719-725

[54] Janos, P.: *Separation methods in the chemistry of humic substances*, J. Chromatogr. A, 983, **2003**, 1-18

[55] Christl, I.; Knicker, H.; Knabner, K.; Kretzschmar, R.: *Chemical heterogeneity of humic substances: characterization of size fractions obtained by hollow-fibre ultrafiltration*, European Journal of Soil Science, 51, **2000**, 617-625

[56] Shinozuka, T.; Shibata, M.; Yamaguchi, T.: *Molecular Weight Characterization of Humic Substances by MALDI-TOF-MS*, J. Mass Spectrom. Soc. Jpn., 52, (1), **2004**, 29-32

[57] Li, L.; Zhao, Z.; Huang, W.; Peng, P.; Sheng, G.; Fu, J.: *Characterization of humic acids fractionated by ultrafiltration, Organic Geochemistry*, 35, **2004**, 1025-1037

[58] Li, L.; Jia, W.; Peng, P.; Sheng, G.; Fu, J.; Huang, W.: *Compositional and source characterization of base progressively extracted humic acids using pyrolytic gas chromatography mass spectrometry*, Applied Geochemistry, 21, **2006**, 1455-1468

[59] Buffle, J.; Greter, F.C.; Haerdi, W: *Measurement of complexation properties of humic acid and fulvic acids in natural waters with lead and copper ion-selective electrodes*, Anal. Chem. 49, **1977**, 216-222

[60] Thorn, k. A.; Younger, S. J.; Cox, L. G.: Order of Functionality Loss during Photodegradation of Aquatic Humic Substances, J. Environ. Qual., 39, **2010**, 1416-1428

[61] Caenn, R.; Chillingar, G. V.: *Drilling fluids: state of the art*, J Petrol Sci Eng, 14, **1996**, 221-230

[62] Firth Jr, W. C.: *Humates thinners for drilling fluids*, US patent 4, 235,727, 1**980**

[63] Firth Jr, W. C.: *Chrome humates as drilling mud additives*, US patent 5, 191,100, **1993**

[64] Russell, J. A.; Patel, B. B.: *Drilling fluid*, US patent 4,704,214, **1987**

[65] Clark, R. K.: *Impact of environmental regulations on drilling fluid technology*, J Pet Technol, 46, **1994**, 804-809

[66] Bhattacharya, A.; Misra, B. N.: *Grafting: a versatile means to modify polymers: Techniques, factors and applications*, Prog. Polym. Sci., 29, **2004**, 767-814

[67] Ranjan, R.; Brittain, W. J.: *Combination of Living Radical Polymerization and Click Chemistry for Surface Modification*, macromol, 40, **2007**, 6217-6223

[68] Fu, G. D.; Phua, S. J.; Kang, E. T.; Neoh, K. G.: *Tadpole-Shaped Amphiphilic Block−Graft Copolymers Prepared via Consecutive Atom Transfer Radical Polymerizations*, macromol, 38, **2005**, 2612-2619

[69] Misra, B. N.; Mehta, I. K.; Khetarpal, R. C.: *Grafting onto Cellulose. VIII. Graft Copolymerization of Poly (ethyl acrylate) onto Cellulose by Use of Redox Initiators. Comparison of Initiator Reactivities*, J Polym Sci., 22, **1984**, 2767-2775

[70] Khalil, M. I.; Mostafa, Kh. M.; Hebeish, A.: *Graft polymerization of acrylamide onto maize starch using potassium per sulfate as initiator*, Angew. Makromol. Chemie, 213, **1993**, 43-54

[71] Hosseinzadeh, H.: *Potassium persulfate induced grafting of polyacrylamide onto kappa-carrageenan*, J. Appl Polym Chem, 4 (10), **2009**, 9-20

[72] Chen, R. L.; Kokta, B. V.; Daneault, C.; Valade, J. L.: *Some Water-Soluble Copolymers from Lignin*, J. Appl Polym Sci., 32, **1986**, 4815-4826

[73] Chen, R.; Kokta, B. V.; Valade, J. L.: *Study on the Graft Copolymerization of Lignosulfonate and Acrylic Monomers*, J. Appl Polym Sci., 25, **1980**, 2211-2220

[74] Witono, J.R.; Noordergraaf, I.W.; Heeres, H. J.; Janssen, L.P.B.M.: *Graft copolymerization of acrylic acid to cassava starch - Evaluation of the influences of process parameters by an experimental design method*, Carbohydrate Polymers, 90, **2012**, 1522– 1529

[75] Binnemans, K.: *Handbook on the Physics and Chemistry of Rare Earths*, 36, **2006**, Elsevier, Amsterdam, The Netherlands

[76] Kubota, H.; Ogiwara, Y.: *Effect of Lignin in Graft Copolymerization of Methyl Methacrylate on Cellulose by Ceric Ion*, J. Appl Polym Sci., 13, **1969**, 1569-1575

[77] Machida, S.; Narita, H.; Katsura, T.: *Flocculation Properties of Cellulose-Acrylamide Graft Copolymer*, Angew. Makromol. Chemie, 20, **1971**, 47-56

[78] Kim, O-K, Griffith, J. R.: *Highly Branched Acrylamide Graft Copolymer*, J Appl Polym Sci, 13, **1975**, 151-160

[79] Vazquez, M. B.; Goni, I.; Gurruchaga, M.; Valero, M.; Guzman, G. M.: *Study of the Ceric Ion Behavior on the Initiation of Butyl Acrylate Polymerization onto Amylose*, J Polym Sci: Part A: Polym Chem., 25, **1987**, 1309-1314

[80] McCormick, C. L.; Park, L. S.: *Water-Soluble Copolymers. VII. Cerium (IV) Induced Graft Copolymerization of Acrylamide and Sodium-2-Arylamido-2-Methylpropane Sulfonate onto Dextran*, J. Polym Sci., 22, **1984**, 49-60

[81] Gupta, K. C.; Khandekar, K.: *Graft Copolymerization of Acrylamide-Methylacrylate Comonomers onto Cellulose Using Ceric Ammonium Nitrate*, J Appl Polym Sci, 86, **2002**, 2631-2642

[82] Zohuriaan-Mehr, M. J.; Pourjavadi, A.: *New Polysaccharide-g-polyacrylonitrile Copolymers: Synthesis and Thermal Characterization*, Polym. Adv. Technol., 14, **2003**, 508-516

[83] Biswal, D. R.; Singh, R. P.: *Flocculation Studies Based on Water-Soluble Polymers of Grafted Carboxymethyl Cellulose and Polyacrylamide*, J Appl Polym Sci, 102, **2006**, 1000-1007

[84] Eutamene, M.; Benbakhti, A.; Khodja, M.; Jada, A.: *Preparation and Aqueous Properties of Starch-grafted Polyacrylamide Copolymers*, Starch/ Stärke, 61, **2009**, 81-89

[85] Meister, J. J.; Patil, D. R.: *Properties and Applications of Lignin-Acrylamide Graft Copolymer*, J. Appl Polym Sci. 29, **1984**, 3457-3477

[86] Meister, J. J.; Patil, D. R.: *Solvent Effects and Initiation Mechanisms for Graft Polymerization on Pine Lignin*, Macromol., 18, **1985**, 1559-1564

[87] Meister, J. J.; Li, C. T.: *Synthesis and Properties of Several Cationic Graft Copolymers of Lignin*, Macromol, 25, **1992**, 611-616

[88] Philips, R. B.; Brown, W.; Stannett, V. T.: *The Graft Copolymerization of Styrene and Lignin. I. Hydrochloric Acid Lignin*, J. Appl. Polym Sci., 15, **1971**, 2929-2940

[89] Shadeghi, M.; Ghasemi, N.; Soliemani, F.: *Graft Copolymerization of Methacrylamide Monomer onto Carboxymethyl Cellulose in Homogeneous Solution and Optimization of Effective Parameters*, World Appl Sci J, 16, (1), **2012**, 119-125

[90] Nelson, E. B.: *Well Cementing*; Schlumberger Dowell: Sugar Land, TX, **1990**

[91] Taylor, H. F. W.: *Chemistry of Cements*, Vol I, Academic Press, London and NY, **1972**

[92] Sorrentino, F.: *Chemistry and engineering of the production process: State of the art*, Cem and Concr Res 41, **2011**, 616-623

[93] Lea, F. M.: *Chemistry of Cements and Concrete*, Fourth Edition, Chemical Publishing Company Inc., New York, **1988**

[94] Bogue, R. H.: *Chemistry of Portland cement*, New York, Reinhold, **1955**

[95] *Standard Specification for Portland cement*, American Society for Testing and Materials, ASTM C150-07, **2007**

[96] Paul; E. S.: *Guide for X-ray Powder Diffraction Analysis of Portland cement and clinker*, NISTIR 5755 National Institute of Standards and Technology, **1996**

[97] Plank, J., Stephan, D., Hirsch, C.: Bauchemie, Winnacker/Küchler: *Chemische Technik-Prozesse und Produkte, Band 7 (Industrieprodukte)*,Weinheim:Wiley-VCH, 5 Aufl., **2004**

[98] Smith, D. K.: SPE Monograph, Vol. 4: *Cementing*, Society of Petroleum Engineers, NY, **1990**

[99] Makar, J.; Luke, K.: *Thermal Stability of the Cement Sheath in Steam Treated Oil Wells*, J. Am. Ceram. Soc., 94 (12), **2011**, 4463-4470

[100] Jupe, A. C.; Wilkinson, A. P.; Luke, K.; Funkhouser, G. P.: *Class H cement hydration at 180 °C and high pressure in the presence of added silica*, Cem Concr Res, 38, **2008**, 660-666

[101] Meller, N.; Hall, C.; Kyritsis, K.; Giriat, G.: *Synthesis of cement based CaO-Al_2O_3-SiO_2-H_2O (CASH) hydroceramics at 200 and 250 °C: Ex-situ and in-situ diffraction*, Cem Concr Res, 37, **2007**, 823-833

[102] Barret, P.; Bertrandie, D. *J.: Fundamental hydration kinetic features of the major cement constituents:Ca_3SiO_5 and ß-Ca_2SiO_4* Chim. Phys., 83, **1986**, 765-775

[103] Barret, P.; Menetrier, D.; Bertrandie, D.: *Mechanism of C_3S dissolution and problem of the congruency in the very initial period and later on*, Cem. Concr. Res. **1983**, *13*, 728-738

[104] Neville, A. M.; Brooks, J. J.*: Concrete Technology*, Longman Scientific, USA, **1987**

[105] Durgun, E.; Manzano, H.; Pellenq, R. J. M.; Grossman, J. C.: *Understanding and Controlling the Reactivity of the Calcium Silicate phases from First Principles*, Chem. Mater., 24, **2012**, 1262−1267

[106] Nicoleau, L.; Nonat, A.; Perrey, D.: *The di- and tricalcium silicate dissolutions, Cem Concr Res*, 47, **2013**, 14-30

[107] Taylor, H. F. W.: *Cement chemistry*, Thomas Telford Publishing: London, UK, **1997**

[108] Juilland, P.; Gallucci, E.; Flatt, R.; Scrivener, K.: *Dissolution theory applied to the induction period in alite hydration*, Cem Concr Res, 40 (6), **2010**, 831-844

[109] Bullard, J. W.; Jennings, H. M.; Livingston, R. A.; Nonat, A.; Scherer, G. W.; Schweitzer, J. S.: *Mechanism of cement hydration*, Cem Concr Res, 1 (12), **2011**,1208-1223

[110] Scrivener, K. L. Nonat, A.: *Hydration of cementitious materials, present and future*, Cem Concr Res, 41 (7), **2011**, 651-665

[111] Stark, J.: *Recent advances in the field of cement hydration and microstructure analysis*, Cem Concr Res, 41 (7), **2011**, 666-678

[112] Edwards, C. L.; Lawrence B. Alemany, L. B.; Barron, A. R.: *Solid-State ^{29}Si NMR Analysis of Cements: Comparing different methods of relaxation analysis for determining spin-lattice relaxation times to enable determination of the C_3S/C_2S ratio*, Ind. Eng. Chem. Res. 46, **2007,** 5122-5130

[113] Bellmann, F.; Damidot, D.; Möser, B.; Skibsted, J.: *Improved evidence for the existence of an intermediate phase during hydration of tricalcium silicate*, Cem Concr Res 40, **2010**, 875-884

[114] Cody, A. M.; Lee, H.; Cody, R. D.; Spry, P. G.: *The effect of chemical environment on the nucleation, growth, and stability of ettringite $[Ca_3Al(OH)_6]_2(SO_4)_3 \cdot 26H_2O$*, Cem Concr Res, 34, **2004**, 869-881

[115] Hall, C.; Barnes, P.; Billimore, A.D.; Jupe, A.C.; Turrillas, X.: *Thermal decomposition of ettringite $Ca_6 [Al(OH)_6]_2 (SO_4)_3 \cdot 26H_2O$*, J. Chem. Soc., Faraday Trans., 92 (12), **1996**, 2125-2129

[116] Constantiner, D.; Farrington, S.A.: *Review of the thermodynamical stability of ettringite*, Cem. Concr. Aggreg., 21 (1), **1999**, 39-42

[117] Glasser, F. P.; Kindness, A.; Stronach, S. A.: *Stability & Solubility relationship in AFm phases, Part 1: Chloride, Sulfate and hydroxide*, Cem Concr Res, 29, **1999**, 861-866

[118] Glasser, F. P.; Damidot, D.; Atkins, M.: *Phase development of cement in relation to the secondary ettringite problem*, Adv. Cem. Res, 7, **1995**, 57-68

[119] Grangeon, S.; Claret, F.; Lerouge, C.; Warmont, F.; Sato, T.; Anraku, S.; Numako, C.; Linard, Y.; Lanson, B.: *On the nature of structural disorder in calcium silicate*

hydrates with a calcium/silicon ratio similar to tobermorite, Cem and Concr Res, 52, **2013**, 31–37

[120] Gallucci, E.; Zhang, X.; Scrivener, K. L.: *Effect of temperature on the microstructure of calcium silicate hydrate (C-S-H)*, Cem and Concr Res, 53, **2013**, 185–195

[121] Valori, A.; McDonald, P. J.; Scrivener, K.L.: *The morphology of C–S–H: Lessons from ^{1}H nuclear magnetic resonance relaxometry*, Cem and Concr Res, 49, **2013**, 65–81

[122] Pardal, X.; Brunet, F.; Charpentier, T.; Pochard, I.; Nonat, A.: *^{27}Al and ^{29}Si Solid-State NMR Characterization of Calcium-Aluminosilicate-Hydrate*, Inorg. Chem. 51, **2012**, 1827−1836

[123] Vandamme, M.; Ulm, F.-J.: *Nanoindentation investigation of creep properties of calcium silicate hydrates*, Cem and Concr Res, 52, **2013**, 38–52

[124] Dharmawardhana, C. C.; Misra, A.; Aryal, S.; Rulis, P.; Ching, W. Y.: *Role of interatomic bonding in the mechanical anisotropy and interlayer cohesion of CSH crystals*, Cem and Concr Res, 52, **2013**, 121–130

[125] Thomas, J. J.; Jennings, H. M.; Chen, J. J.: *Influence of Nucleation Seeding on the Hydration Mechanisms of Tricalcium Silicate and Cement,* J. Phys. Chem. C, 113, (11), **2009**, 4327-4334

[126] Chiang, W-S.; Fratini, E.; Baglioni, P.; Liu, D.; Chen, S-H. : *Microstructure Determination of Calcium-Silicate-Hydrate Globules by Small-Angle Neutron Scattering*, J. Phys. Chem. C, 116, **2012**, 5055−5061

[127] Bergold, S.T.; Goetz-Neunhoeffer, F.; Neubauer, J.: *Quantitative analysis of C–S–H in hydrating alite pastes by in-situ XRD*, Cem and Concr Res, 53, **2013**, 19–126

[128] Muller, A. C. A.; Scrivener, K. L.; Gajewicz, A. M.; McDonald, P. J.: *Densification of C−S−H Measured by ^{1}H NMR Relaxometry*, J. Phys. Chem. C, **2013**, 117, 403−412

[129] Bishop, M.; Bolt, S.G.; Barron, A. R.: *A New Mechanism for Cement Hydration Inhibition: Solid –State Chemistry of Calcium Nitrilotris (methylene) Triphosphonate*, Chem. Mater., 15, **2003**, 3074-3088

[130] Smith, B. J.; Roberts, L. R.; Funkhouser, G. P.; Gupta, V.; Chmelka, B. F.: *Reaction and Surface Interactions of Saccharides in Cement Slurries*, Langmuir 28 (40), **2012,** 14202-14217

[131] Peterson, V. K.: *Hydration of Tricalcium Silicate: Effect of $CaCl_2$ and Sucrose on Reaction Kinetics and Product Formation*, Chem. Mater. **2006**, 18, 5798- 5804

[132] Andersen, M. D.; Hans J. Jakobsen, H. J.; Skibsted, J.: *Incorporation of Aluminum in the Calcium Silicate Hydrate (C-S-H) of Hydrated Portland Cements: A High-Field ^{27}Al and ^{29}Si MAS NMR Investigation*, Inorg. Chem., 42, **2003**, 2280-2287

[133] Nachbaur, L.; Nkinamubanzi, P.C.; Nonat, A.; Mutin, J. C.: *Electrokinetic Properties which Control the Coagulation of Silicate Cement Suspensions during Early Age Hydration*, J. Colloid Interf Sci., 202, **1998**, 261-268

[134] Viallis-Terrisse, H.; Nonat, A.; Petit, J. C.: *Zeta-Potential Study of Calcium Silicate Hydrates Interacting with Alkaline Cations*, J. Colloid Interf Sci., 244, **2001**, 58-65

[135] Plassard, C:, Lesniewska, E:, Pochard, I.; Nonat, A.: *Nanoscale experimental investigation of particle interactions at the origin of the cohesion of cement*, Langmuir, 21, **2005**, 7263-7270

[136] Neves, M.I.B.; Oliva, V.; Mrabet, B.; Connan, C.; Chehimi, M.M.; Delamar, M.; Hutton, S.; Roberts, A.; Benzarti, K.: *Surface chemistry of cement pastes: a study by x-ray photoelectron spectroscopy*, Surf. Interface Anal., 33, **2002**, 834-841

[137] Ridi, F.; Luciani, P.; Fratini, E.; Baglioni, P.: *Water Confined in Cement Pastes as a Probe of Cement Microstructure Evolution*, J. Phys. Chem. B, 113, **2009,** 3080 – 3087

[138] Mishra, R. K.; Flatt, R. J.; Heinz, H.: *Force Field for Tricalcium Silicate and Insight into Nanoscale Properties: Cleavage, Initial Hydration and Adsorption of Organic Molecules*, J. Phys. Chem. C,117, **2013**, 10417-10432.

[139] Gutberlet, T.; Hilbig, H.; Beddoe, R. E.; Lohstroh, W.: *New insights into water bonding during early tricalcium silicate hydration with quasielastic neutron scattering*, Cem Concr Res, 51, **2013**, 104–108.

[140] Christensen, A.N.; Jensen, T.R.; Hanson, J. C.: *Formation of ettringite, $Ca_6Al_2(SO_4)_3(OH)_{12} \cdot 26\ H_2O$, AFt, and monosulfate, $Ca_4Al_2O_6(SO_4) \cdot 14H_2O$, AFm-14, in hydrothermal hydration of Portland cement and of calcium aluminium oxide-calcium sulphate dehydrate mixtures studied by in situ synchrotron X-ray powder diffraction*, J. Solid State Chem.,177, **2004**, 1944-1951

[141] Jahn, F.; Cook, M.; Graham, M.: *Exploration and Production, Development in Petroleum Science*, 55, 2 nd edition, Elsevier, Aberdeen UK, **2008**

[142] King, G. E.: *Hydraulic Fracturing 101: What Every Representative,Environmentalist, Regulator, Reporter, Investor, University Researcher, Neighbor and Engineer Should Know About Estimating Frac Risk and Improving Frac Performance in Unconventional Gas and Oil Wells*, SPE paper 152596, presented at Hydraulic Fracturing Technology Conference, **2012,** The Woodlands, USA

[143] Chilingar G.V., Buryakovsky L.A., Eremenko N.A. and Gorfunkel M.V.: *Geology and Geochemistry of Oil and Gas,* Published by Elsevier, **2005**

[144] Weggen, K.; Pusch, G.; Rischmüller, H.: *Oil and Gas*, Ullmann's Encyclopedia of Industrial Chemistry, **2000**

[145] *Scheme of an oil and gas reservoir*, retrieved on 2nd December **2013** from http://www.elateafrica.org/elate/specialtopics/ugandaoil/source.html

[146] Ramm, M.; Bjorlykke, K.: *Porosity/depth trends in reservoir sandstones: Assessing the quantitative effects of varying pore-pressure, temperature history and mineralogy, Norwegian shelf data*, Clay Minerals, 29, **1994**, 475-590

[147] Ramm, M.; Bjorlykke, K; Bloch, S.; Lander, R. H.; Bonnell. L.: *Anomalously high porosity and permeability in deeply buried sandstone reservoirs: Origin and predictability*, AAPG Bulletin, 86, **2002**, 301-328

[148] North, F. K.: *Petroleum Geology*, Allen and Unwin, Boston, **1985**

[149] Haeri-Ardakani, O.; Al-Aasm, I.; Coniglio, M.: *Petrologic and geochemical attributes of fracture-related dolomitization in Ordovician carbonates and their spatial distribution on southern Ontario, Canada*, Marine & Petroleum geology, 43, **2013**, 409-422

[150] Downey, M. D.: *Hydrocarbon seal rocks; In: The petroleum system from source to trap*; Magoon, L. B.; Dow, W.G.; Eds., Amer. Assoc. Petrol. Geol., Memoir 60, **1994,** 211-217

[151] Griffith, C. A.; Dzombak, D. A.; Lowry, G. V.: *Physical and chemical characteristics of potential seal strata in regions considered for demonstrating geological saline CO_2 sequestration*, Environ. Earth Sci., 64, **2011**, 925-948

[152] Biddle, K. T., Wielchowsky, C. C.: *Hydrocarbon Traps, : In The petroleum system from source to trap*; Magoon, L. B.; Dow, W.G.; Eds., Amer. Assoc. Petrol. Geol., Memoir 60, 211-217, **1994**

[153] *International Energy Agency*. World Energy Outlook, **2011**

[154] Barbot, E.; Vidic, N. S.; Gregory, K. B.; Vidic, R. D.: *Spatial and Temporal Correlation of Water Quality Parameters of Produced Waters from Devonian-Age Shale following Hydraulic Fracturing*, Environ. Sci. Technol., 47, **2013**, 2562−2569

[155] Dodd, C. G.; Conley, F. R.; Barnes, P. M.: *Clay minerals in petroleum reservoir sands and water sensitivity effects*, In Clays & Minerals Proc. Nat. Clay & Miner. Conf. Proc. 3rd ed.,Swinford Oxford: Pergamon, pg. 573, **1955**

[156] Amyx, J.; Bass, D.; Whiting, R.: *Petroleum Reservoir Engineering*, McGraw-Hill Book Company, Inc., New York, **1960**

[157] Agbalaka, C; Dandekar, A.Y; Patil, S.L; Khataniar, S.; Hemsath, J.R. : *The Effect of Wettability on Oil Recovery: A Review*, SPE paper 114496, presented at the SPE Asia & Gas Conference and Exhibition, Perth, Australia, October 20- 22, **2008**

[158] Salehi, M.; Johnson, S. J.; Liang, J. T.: *Mechanistic Study of Wettability Alteration Using Surfactants with Applications in Naturally Fractured Reservoirs*, Langmuir, 24 (24), **2008**, 14099-14107

[159] Fatemi, S. M.; Sohrabi, M.; Jamiolahmady, M.; Ireland, S.: *Experimental and Theoretical Investigation of Gas/Oil Relative Permeability Hysteresis under Low Oil/Gas Interfacial Tension and Mixed-Wet Conditions*, Energy & Fuels, 26, **2012**, 4366−4382

[160] Gandler G. L., Gbosi A., Bryant S. L., Britton L. N.: *Mechanistic Understanding of Microbial Plugging for Improved Sweep Efficiency*, SPE paper 100048, presented at SPE/DOE Symposium on Improved Oil Recovery 22-26 April **2006**, Tulsa, Oklahoma.

[161] Suganya, R.S: *Screening Optimization and Production of Biosurfactant from Bacillus and Pseudomonas species*, Int J Curr Pharm Res, 5 (1), **2013**, 19-23

[162] Banat, I. M.: *Biosurfactants production and possible use in microbial enhanced oil recovery and oil pollution remediation: a Review*, Bioresource Technol, 51, **1995**, 1-12

[163] Growcock, F. B.; Belkin, A.; Fosdick, M.; Irving, M.; O'Connor, B.; Brookey, T.: *Recent Advances in Aphron Drilling Fluids*, IADC/SPE paper 97982, **2006**, held in Miami, Florida, U.S.A

[164] Lee, L.; Patel, A. D.; Stamatakis, E.: *Glycol based Drilling Fluid,* US patent 6,291,405B1, **2001**

[165] Adachi, J.; Bailey, L.; Houwen, O. H.; Meeten, G. H.; Way, P. W.; Growcock, F. B.; Schlemmer, R. P.: *Depleted Zone Drilling: Reducing Mud Loss into Fractures*, IADC/SPE paper 87224, Drilling Conference, **2004,** presented in Dallas, Texas, USA

[166] Abdollahi, J.; Carlsen, I. M.; Mjaaland, S.; Skalle, P.; Rafiei, A.; Zarei, S.; *Underbalanced Drilling as a Tool for Optimized Drilling and Completion Contingency in Fractured Carbonate Reservoirs*, SPE/IADC Paper 91579, SPE/IADC Underbalanced Technology Conference and Exhibition, **2004,** presented in Houston, Texas

[167] Sweatman, R.; Kelley, S.; Heathman, J.: *Formation Pressure Integrity Treatments Optimize Drilling and Completion of HTHP Production Hole Sections*, SPE paper 68946, European Formation Damage Conference, **2001**, held in The Hague, The Netherlands,

[168] Montilva, J.; Mota, J.; Poletzky, I. C.; Sati, M.; Lovorn, R.; Grable, J.: *Next Generation Managed Pressure Drilling System Enables HP/HT Horizontal Wells in the Haynesville Shale*, IADC/SPE paper 151168, IADC/SPE Drilling Conference and Exhibition, March 6-8, **2012,** held in San Diego, California, USA

[169] Turner, D. R.; Harris, T. W. R.; Slater, M.; Yuratich, M. A.; Head, P. F.: *Electric Coiled Tubing Drilling*: A Smarter CT Drilling System, SPE/IADC paper 52791, SPE/IADC Drilling Conference, **1999,** presented in Amsterdam, Holland

[170] Bruno, M.; Reed, A.; Olmstead, S.: *Environmental Management, Cost Management, and Asset Management for High-Volume Oil Field Waste Injection Projects*, IADC/SPE paper 59119, IADC/SPE Drilling Conference, **2000,** held in New Orleans, Louisiana

[171] Fernandez, J. M.; Young, S.: *Environmentally Responsible Water-Based Drilling Fluid for HTHP Applications*, paper AADE-10-DF-HO-37, AADE Fluids Conference and Exhibition, **2010,** presented at Hilton Houston North, Texas

[172] Hille, M.:*Vinylsulfonate/Vinylamide Copolymers in Drilling Fluids for Deep, High-Temperature Wells*, SPE paper 13558, SPE Oilfield and Geothermal Chemistry Symposium, **1985,** held at Phoenix, Arizona

[173] Seright, R. S.; Fan, T.; Wavrik, K.; Wan, H.; Gaillard, N.; Favero, C.: *Rheology of a New Sulfonic Associative Polymer in Porous Media*, SPE paper 141355, presented in SPE Conference, **2011,** held at The Woodlands, Texas

[174] Saasen, A.; Løklingholm, G.: *The Effect of Drilling Fluid Rheological Properties on Hole Cleaning*, **,** IADC/SPE Paper 74558, IADC/SPE Drilling Conference, **2002,** held in Dallas, Texas

[175] *Offshore drilling rigs types*, retrieved on 1st of Nov. **2013** from http://www.psmag.com/politics/hurricanes-enter-the-offshore-oil-drilling-debate-4236/

[176] Fincher, R. W.; May, R.; Fontana, P.; Watkins, L.; Macfarlane, J. W.: *Subsea Wellbore Drilling System for Reducing Bottom hole Pressure*, US patent 6, 415,877 B1, **2002**

[177] Fossli, B.: *Arrangement and Method for Controlling and Regulating Bottom hole Pressures when Drilling Deepwater Offdhore Wells*, US patent 7,497,266B2, **2009**

[178] Donald, I.; Reid, J.: *Apparatus and Method for Processing Fluids from a Well*, US patent 8, 297,360B2, **2012**

[179] Horton, E. E.; Finn, L. D.; Maher, J.; Navarre, G.: *Dual Density Mud Return System*, US patent 0285698A1, **2012**

[180] Workshop handout on attributes of *Dual Gradient Drilling* in May **2013**; http://www.iadc.org/wp-content/uploads/2013/08/2013-May-09-DGD-System-Attributes-Handout-FINAL.pdf

[181] LWSA for Dual-Gradient Drilling JIP (Maurer Technology) retrieved on the 8th of Nov. 2013 from www.netl.doe.gov/KMD/cds/disk17/B-Microhole/ 1-29- 03.NPC Drilling Workship.ppt

[182] Darley, H. C. H.; Gray, G. R.: *Composition and Properties of Drilling and Completion Fluids*, Gulf Professional Publishing: Houston Texas, **1988**

[183] Patel, A. D.: *Water-Based drilling Fluids with High Temperature Fluid Loss Control Additive*, US patent 5,789,349, **1998**

[184] Elkatatny, S. M.; Mahmoud, M. A; Nasir-El-Din, H. A.: *Charaterization of Filter Cake Generated by Water-Based Drilling Fluids Using CT-Scan*, SPE Paper 144098, SPE European Formation Damage Conference, **2011,** presented at Noordwijk, The Netherlands,

[185] Aston, M.; Mihalik, P.; Tunbridge, J.; Clarke, S.: *Towards Zero Fluid Loss Oil Based Muds*, SPE Paper 77446, SPE Annual Technical Conference and Exhibition, , **2002,** San Antonio, Texas

[186] Tehrani, A.; Friedheim, J.; Cameron, J.; Reid, B.: *Design Fluids for Wellbore Strengthening – Is it An Art?*, paper AADE-07-NTCE-75, presented in AADE Fluids Conference and Exhibition, , **2007,** held at the Wyndham Greenspoint Hotel, Houston, Texas

[187] Watson, R. B.; Viste, P.; Lauritzen, J. R.: *The Influence of Fluid Loss Additives in High-Temperature Reservoirs*, SPE International Symposium and Exhibition on Formation Damage Control, 15-17 February, **2012**, presented at Lafayette, Louisiana, USA

[188] Adachi, J.; Bailey, L.; Houwen, O. H; Meeten, G. H.; Way, P. W.; Growcock, F.B.; Schlemmer, R.P.: *Depleted Zone Drilling: Reducing Mud Losses Into Fractures*, IADC/SPE paper 87224, IADC/SPE Drilling Conference, 2-4 March **2004,** held in Dallas, Texas, USA

[189] Giese, M.; Bratvold, R. B.: *Probabilistic Modeling for Decision Support in Integrated Operations*, SPE paper 127761, SPE Intelligent Energy Conference and Exhibition, **2010,** held in Utrecht, The Netherlands

[190] Goodfield, M.; Goodyear, S. G.; Townsley, P. H.: *New Coreflood Interpretation Method for Relative Permeabilities Based on Direct Processing of In-Situ Saturation*

Data, SPE paper 71490, SPE Annual Technical Conference and Exhibition, **2001,** held in New Orleans, Louisiana

[191] Smith, J. R.; Growcock, F. B.: *Wellbore Strengthening While Drilling Above and Below Salt in the Gulf of Mexico*, Paper AADE-08-DF-HO-21, AADE Fluids Conference and Exhibition, **2008,** held at the Wyndham Greenspoint Hotel, Houston, Texas

[192] Boukadi, F.H.; Al-Alawi, S.M: *Analysis and Prediction of Oil Recovery Efficiency in Limestone Cores Using Artificial Neural Networks*, Energy & Fuels, 11, **1997**, 1056-1060

[193] Struthers, B. W.; Collee, P. W.: *Bit-stabilized combination coring and drilling system*, US patent 5,568,838, **1996**

[194] Darling, T.: *Well logging and Formation Evaluation*, Gulf Professional Publishing, **2005**

[195] Ubani, C. E.; Adeboye, Y. B.; Oriji, A. B.: *Advances in Coring and Core Analysis for Reservoir Formation Evaluation*, Petroleum & Coal 54(1), **2012,** 42-51

[196] Coring pdf, retrieved on the 20th of October from http://www.halliburton.com/public/sdbs/sdbs_contents/brochures/web/h03023.pdf

[197] Carey; J. W.; Wigand, M.; Chipera, S. J.; WoldeGabriel, G.; Pawar, R.; Lichtner, P. C.; Scott C. Wehner, S. C.; Raines, M. A.; Guthrie Jr., G. D.: *Analysis and performance of oil well cement with 30 years of CO_2 exposure from the SACROC Unit*, West Texas, USA, Int. J. Greenhouse Gas Control, 1, **2007**, 75 – 85

[198] Fink, J. K.: *Oil Field Chemicals*, Gulf Professional Publishing, Burlington, MA **2003**

[199] Amro, M. M.: *Polymer-Acid Solutions*: *Their Use for the Enhancement of Oil Reservoir Stimulation*, J Appl Polym Sci, 110, **2008**, 1382-1387

[200] Castro, L.; Bass, C.; Pirogov, A.; Maxwell, S.: *A comparison of proppant placement, well performance, and estimated ultimate recovery between horizontal wells completed*

with multi-cluster plug & Perf and hydraulically activated frac ports in a tight reservoir, SPE paper 163820, presented at Hydrualic Fracturing Technology Conference, Feb. 04-06, **2013,** The Woodlands, TX, USA

[201] Schematic of a hydraulic fracturing, retrieved on the 4th of December **2013** from http://total.com/en/energies-expertise/oil-gas/exploration-production/strategic-sectors/unconventional-gas/presentation/new-applications-proven-techniques

[202] Berati, R.; Johnson, S. J.; McCool, S; Green, D. W.; Willhite, G. P.; Liang, J-T.: *Fracturing Fluid cleanup by Controlled Release of Enzymes from Polyelectrolyte Complex Nanoparticles*, J. Appl Polym Sci, 121, **2011**, 1292-1298

[203] Berati, R.; Johnson, S. J.; McCool, S; Green, D. W.; Willhite, G. P.; Liang, J-T.: *Polyelectrolyte Complex Nanoparticles for Protection and Delayed Release of Enzymes in Alkaline pH and at Elevated Temperature during Hydraulic Fracturing of Oil Wells*, J Appl Polym Sci, 126, **2012**, 587-592

3. RESULTS AND DISCUSSION- PUBLISHED PAPERS

This section contains three publications:

P**ublication 1#:** focuses on the synthesis of a **viscosifying graft copolymer**, its effects on cement slurry rheology, its performance in comparison to an AMPS®-NNDMA copolymer; its thermal stability and working mechanism as a high temperature fluid loss additive.

Publication #2: focuses on the synthesis of a **dispersing graft copolymer,** engineered and tailored to make the graft copolymer suitable for high density cement slurries that require a low water-to-cement ratio. The influence of specific molecular design on the cement flow properties and its performance and working mechanism as fluid loss additive in oil well cement exposed to high temperature (27- 200 °C) is presented.

P**ublication #3:** relates to the effects of sea water and NaCl solution on the performance of humic acid and lignite graft copolymers applied as fluid loss additives. Furthermore, it explains challenges for and limitation on the polymers when cementing salt formations and on offshore oil wells.

3.1 Synthesis, Effectiveness and Working Mechanism of Humic acid-{*sodium 2- acrylamido- 2-methylpropane sulfonate-co-N,N-dimethyl acrylamide-co-acrylic acid*} Graft Copolymer as High Temperature Fluid Loss Additive in Oil Well Cementing

Synopsis

This work relates to the synthesis of a viscosifying humic acid based graft copolymer as high temperature fluid loss additive for cementing oil and gas wells. The graft copolymer was synthesized by lateral grafting of AMPS®-co-NNDMA-AA onto humic acid backbone via aqueous free radical copolymerization. The graft copolymer exhibits a significantly higher molecular mass (M_w ~ 600,000 g/mol) than the humic acid backbone alone (M_w ~ 69,000 g/mol), thus confirming successful grafting reaction. The occurrence of grafting was further confirmed by SEC data (R_g), ineffectiveness of a blend of AMPS®-co-NNDMA-co-AA copolymer with humic acid; and elemental analysis that show the incorporation of N and S containing monomers into the graft copolymer. The graft copolymer provides water retention at >200 °C with a moderate viscosifying effect in cement slurry (see **Publication #1** and **appendix data**). In comparison, a conventional AMPS®/NNDMA copolymer shows no fluid loss control at 150 °C. The study demonstrates that by grafting lateral chains of AMPS®-co-NNDMA-co-AA onto humic acid, a copolymer with significantly high temperature stability is obtained.

These results were published in:

Journal of Applied Polymer Science,

O.T. Salami and J. Plank, 126, 1449 - 1460, **2012**.

Synthesis, Effectiveness, and Working Mechanism of Humic Acid-{sodium 2-acrylamido-2-methylpropane sulfonate-*co*-*N*,*N*-dimethyl acrylamide-*co*-acrylic acid} Graft Copolymer as High-Temperature Fluid Loss Additive in Oil Well Cementing

Oyewole Taye Salami, Johann Plank

Chair for Construction Chemistry, Institute for Inorganic Chemistry, Technische Universität München, Garching, Germany

Received 29 August 2011; accepted 31 December 2011
DOI 10.1002/app.36725
Published online 1 May 2012 in Wiley Online Library (wileyonlinelibrary.com).

ABSTRACT: Monomers of 2-acrylamido-2-methylpropane sulfonic acid (AMPS®), *N*,*N*–dimethyl acrylamide (NNDMA) and acrylic acid (AA) were grafted on humic acid as backbone by aqueous free radical copolymerization in such a manner that a graft copolymer possessing lateral terpolymer chains was obtained. Molar ratios between AMPS®, NNDMA, and AA were found to be 1 : 1.54 : 0.02 and the ratio between backbone and graft chain was 20 : 80 wt %. The synthesized fluid loss additive (FLA) was characterized by size exclusion chromatography (SEC), charge titration, and Brookfield viscometry. Thermogravimetric and SEC analysis revealed stretched backbone worm architecture for the polymer whereby humic acid constitutes the backbone decorated with lateral graft chains. Grafting was confirmed by SEC data (R_g) and by ineffectiveness of a blend of AMPS®-NNDMA-AA copolymer with humic acid. Their performance as high temperature FLA was studied at 150°C by measuring static filtration properties of oil well cement slurries containing 35% bwoc of silica fume and 1.2% bwoc AMPS®-*co*-itaconic acid retarder. At this temperature, 1.0% bwoc graft copolymer achieves API fluid loss value of 40 mL, thus confirming high effectiveness. The graft copolymer viscosifies cement slurries less than other common synthetic FLAs. The working mechanism of the graft copolymer was found to rely on adsorption onto surface of hydrating cement, as was evidenced by adsorption and zeta potential measurements. Adsorption is hardly affected by temperature and results in constriction of the filter cake pores. The study provides insight into performance of cement additives under the harsh conditions of high temperature and high pressure. © 2012 Wiley Periodicals, Inc. J Appl Polym Sci 126: 1449–1460, 2012

Key words: oil well cement; graft copolymer; humic acid; high temperature; fluid loss additive

INTRODUCTION

In oil well cementing, water-soluble polymers known as fluid loss additives are applied to provide water retention to cement slurries. They perform at demanding conditions occurring in well bores such as high temperature, pressure, and salinity.[1,2] Deep oil or gas wells are characterized by high bottom hole temperatures which may range up to 260°C (500°F). The principal function of filtration control additives is to control the loss of water from the cement slurry to porous formations, thereby preventing rapid dehydration and loss of pumpability of the cement slurry.[3]

Currently, a variety of different polymers is employed for the purpose of fluid loss control. At low temperatures (up to 100°C), unmodified or crosslinked polyvinyl alcohol (PVA) is used. Its working mechanism is based on film formation within the cement filter cake.[4,5] While in the medium temperature range (50–150°C) cellulose ethers, namely hydroxyethyl cellulose (HEC), and carboxymethyl hydroxyethyl cellulose (CMHEC) are prevalent.[6–8] Their effectiveness relies on the formation of large colloidal polymer associates once a specific "overlapping" concentration is transgressed (HEC), and on adsorption onto cement (CMHEC).[9] Additionally, polyethylene imine (PEI) has been applied for the same purpose, but was dropped by the industry in recent years because of its toxicity to fishes and other aquatic species. Interestingly, PEI achieves fluid loss control by forming large polyelectrolyte complexes with anionic dispersants such as acetone-formaldehyde-sulfite polycondensate.[10] For high temperature high pressure fluid loss control, synthetic sulfonated copolymers have become common. Among them are copolymers based on 2–acrylamido methane propane sulfonic acid (AMPS®),

Correspondence to: J. Plank (johann.plank@bauchemie.ch.tum.de).

© 2012 Wiley Periodicals, Inc.

TABLE I
Phase Composition (XRD, *Rietveld*), Specific Density, Specific Surface Area (*Blaine*) and d_{50} Value of API Class G Oil Well Cement Sample

C_3S (wt %)	C_2S (wt %)	C_3A_c (wt %)	C_4AF (wt %)	Free CaO (wt %)	$CaSO_4 \cdot 2H_2O$ (wt %)	$CaSO_4 \cdot 0.5\ H_2O$ (wt %)	$CaSO_4$ (wt %)	Specific density (kg/L)	Specific surface area (cm^2/g)	d_{50} value (μm)
59.6	22.8	1.2	13.0	<0.3	2.7[a]	0.0 [a]	0.7	3.18	3,058	11

[a] Measured by thermogravimetry.
C_3S, tricalcium silicate ($Ca_3(SiO_4)O$); C_2S, dicalcium silicate (Ca_2SiO_4); C_3A_c, cubic modification of tricalcium aluminate ($Ca_9Al_6O_{18}$); C_4AF, tetra calcium aluminate ferrite ($Ca_4Al_2Fe_2O_{10}$).

N-vinylacetamide and acrylamide, or AMPS® and *N,N*–dimethyl acrylamide.[11–14] Their effectiveness also relies on adsorption on cement.[15] A major drawback of these high molecular weight copolymers ($M_w > 1.5$ mio g/mol) is their pronounced viscosifying effect. This is highly undesirable, because deep wells which exhibit high temperatures require increased slurry densities (1.8–2.3 kg/L) to provide sufficient hydrostatic overburden pressure against the reservoir. Such cement slurries are characterized by low water and high cement content (water-to-cement ratio <0.40). FLAs such as the aforementioned which impact high viscosity to these already viscous cement slurries prompt addition of substantial dosages of dispersants to counteract this thickening effect. Such combinations are uneconomical and present a complicated admixture system. Hence, there is a need for a fluid loss additive with high temperature stable performance and at the same time with minor or no viscosifying effect. By grafting AMPS®-NNDMA-AA copolymer blocks onto a humic acid backbone, it was attempted to achieve a fluid loss additive possessing these properties. Additionally, its working mechanism was investigated via measurements of intrinsic viscosity, hydrodynamic size, filter cake permeability, adsorption on cement, and zeta potential. Temperature stability was further probed by exposing the aqueous polymer solution to 150°C (thermal ageing) over a period of 8 h and subsequent polymer characterization and performance testing.

EXPERIMENTAL

Materials

Oil well cement

An API Class G oil well cement ("black label" from Dyckerhoff AG, Wiesbaden, Germany) corresponding to American Petroleum Institute (API) Specification 10A was used.[16] Its clinker composition was determined through powder QXRD technique using *Rietveld* refinement (Table I). The amounts of gypsum ($CaSO_4 \cdot 2H_2O$) and hemi-hydrate ($CaSO_4 \cdot 0.5\ H_2O$) present in the cement sample were measured by thermogravimetry. Free lime (CaO) was quantified following the extraction method established by *Franke*.[17] Using a *Blaine* instrument, the specific surface area was found at 3058 cm^2/g. The specific density of this sample was 3.18 kg/L, as measured by Helium pycnometry. Its d_{50} value was 11 μm.

Silica flour

A commercial sample of silica flour (SSA-1 from Halliburton GmbH, Celle, Germany) containing (wt %) quartz 97.60, CaO 0.57, MgO 0.18, Al_2O_3 0.17, TiO_2 0.06 as determined by X-ray fluorescence analysis and LOI 1.40, was used. Its specific surface area (*Blaine method*) was 1857 cm^2/g, while the average particle size (d_{50} value) was 32.7 μm. Specific density of the silica flour was found to be 2.65 kg/L.

Synthesis of the graft copolymer

The humic acid-{AMPS®-NNDMA-AA} graft copolymer was prepared by aqueous free radical polymerization using sodium peroxodisulfate as initiator. In a typical reaction, 152 mL of a 14.5 wt % aqueous solution of caustic potash humic acid (pH 9.2, HA 2, Borregaard Lignotech, Sarpsborg, Norway) were placed in a 1 L four-necked flask equipped with a stirrer, thermometer and inlet for N_2 gas. 200 g of water were added into the flask. Prior to the addition of the monomers, the pH of the solution was adjusted to 12 by addition of 13.5 g of sodium hydroxide pellets. Next, 50 g of AMPS® (2404 monomer from Lubrizol, Rouen, France), 35 g of NNDMA (Sigma-Aldrich, Munich, Germany) and 1.2 g of acrylic acid (Merck KgaA, Darmstadt, Germany) were added in this order. These proportions result in a molar ratio of 1 : 1.46 : 0.07 between AMPS®, NNDMA, and acrylic acid, and the ratio between humic acid and the graft monomers is 20 : 80 (wt/wt). Moreover, 0.39 g of EDTA (Sigma-Aldrich, Munich, Germany) and 1 g of defoamer (TEGO ANTIFOAM MR 2123, an organo-modified polysiloxane from Evonik Goldschmidt GmbH, Essen, Germany) were added. While stirring, nitrogen gas was bubbled through the solution for 1 h. Then, the temperature was increased to 50°C and the first amount of $Na_2S_2O_8$ initiator (5.2 g) was added. After

TABLE II
Characteristic Properties of Humic Acid, Graft Copolymer, Thermally Aged Graft Copolymer and of SCR–500® Retarder as Obtained from SEC

Polymer	M_w (g/mol)	M_n (g/mol)	PDI (M_w/M_n)	Brookfield viscosity[a] (mPa s)	$R_{h(z)}$ (nm)	$R_{g(z)}$ (nm)
Humic acid	68,940	21,180	3.3	12	2.8	–
graft copolymer	615,000	192,900	3.2	40	38.1	71.2
aged graft copolymer	283,800	117,600	2.4	22	24.0	48.9
SCR-500® retarder	175,600	108,400	1.6	20	3.0	–

[a] Measured in 2.0 wt % solution using Brookfield viscometer model HAT, spindle # H 1 (humic acid) & H 2 (rest of samples).

50 min of reaction time, the second portion of initiator (5.2 g) was added. Grafting was continued for another 70 min while the temperature was increased to 60°C. There, the mixture was left to react for an additional hour before the temperature was again increased to 80°C to complete the reaction within an hour. The reaction was quenched by addition of 6.24 g sodium pyrosulfite ($Na_2S_2O_5$). The product yields a dark, viscous, odorless liquid which was diluted with 300 mL of DI water. The final product used in this study was a dark brown, 8 wt % aqueous solution possessing low viscosity and a pH value of 5.3. The characteristic properties of the graft copolymer are summarized in Table II.

Synthesis of AMPS®-NNDMA-AA copolymer

For comparison, a copolymer of AMPS®, NNDMA, and acrylic acid was prepared following the procedure for the graft copolymer except that no humic acid was present. Instead, for the initiation process, only 0.94 g of initiator was added for polymerization of the copolymer. The following procedure was identical with that of the graft copolymer. The reaction product was a colorless, 6.2 wt % aqueous solution possessing low viscosity and a pH value of 5.

Retarder

A commercial sample (SCR-500®) from Halliburton GmbH, Celle, Germany was used for high temperature retardation of cement. According to literature, this product is prepared by aqueous free radical copolymerization of AMPS® and itaconic acid at a molar ratio of 1 : 0.4.[18] The resulting colorless liquid is spray-dried to yield a white powder which was used in this study. The characteristic properties of SCR-500® are presented in Table II.

Instruments

Cement characterization

Phase composition of the cement sample was obtained by quantitative X-ray powder diffraction using a Bruker axs D8 Advance instrument from Bruker, Karlsruhe, Germany with Bragg-Bretano geometry. Topas 3.0 software was employed to quantify the amounts of individual phases present in the sample by following *Rietveld's* method of refinement.[19] The instrument was equipped with a scintillation detector using Cu K_α ($\lambda = 1.5406$ Å) radiation with a scanning range between 5° and 80° 2θ at a scanning speed of 0.5 s/step (with 0.008°/step). Specific density of the cement sample was measured on an Ultrapycnometer® 1000 (Quantachrome Instruments, Boynton Beach, FL/USA). Specific surface area of the sample was determined using a *Blaine* instrument (Toni Technik, Berlin, Germany). The average particle size (d_{50} value) was obtained from a laser-based particle size analyzer (1064 instrument from Cilas, Marseille, France).

Silica flour characterization

Oxide composition of SSA-1 silica flour was determined using an X-ray fluorescence spectrometer (Axios from PANalytical, Almelo, The Netherlands). Specific density, specific surface area, and average particle size (d_{50} value) of the silica sample were measured using the same instrumentation as described above for cement.

Polymer characterization

Viscosity of the polymer solutions was quantified using a *Brookfield* viscometer (Model HAT from Brookfield Engineering Labs, Middleboro, MA/USA) equipped with spindle # H1 or H2. Measurement was carried out at 100 rpm and room temperature. By multiplying the dimensionless reading with the correspondent factor, the values for viscosity (in mPa s) were obtained.

Also, the dynamic viscosities of cement filtrates obtained from the static filtration test were determined. First, kinematic viscosities of cement filtrates containing dosages from 0 to 1.6% bwoc of the graft copolymer were measured at 95°C on an *Ubbelohde* viscometer using 501 10/I, 501 20/II, and 501 30/III capillaries supplied by Schott Instruments, Mainz,

Germany. Totally, 15 mL of filtrate were filled into the reservoir of the capillary and the flow time was measured. From this, the kinematic viscosity of the filtrate was calculated according to eq. (1).

$$\upsilon = K\ (t - \zeta) \tag{1}$$

where K is the viscometer constant (0.1004 mm^2/s^2), t is the flow time, and ζ is the flow time dependant *Hagenbach-Couette* correction term, which is provided in the instrument instruction sheet. Multiplying the value obtained for the kinematic viscosity at 95°C with the specific density of the filtrate produced the value for the dynamic viscosity η_{dyn}, as is expressed by eq. (2).

$$\eta_{dyn} = \upsilon \cdot \rho \tag{2}$$

From this, the reduced viscosity of the filtrate η_{red} was calculated according to eq. (3). There, η_0 is the dynamic viscosity of the cement filtrate without polymer and c represents the respective concentration of polymer in the filtrate.

$$\eta_{red} = \frac{\eta_{dyn} - \eta_0}{\eta_0 \cdot c} \tag{3}$$

Molecular properties of the graft copolymer and of SCR-500® were determined via size exclusion chromatography (SEC). There, a Waters Alliance 2695 (Waters, Eschborn, Germany) separation module equipped with RI detector 2414 (Waters, Eschborn, Germany) and an 18 angle dynamic light scattering detector (Dawn EOS, Wyatt Technologies, Clinton, IA) was employed. The polymers were separated on a precolumn and two Aquagel–OH 60 columns (Polymer Laboratories, distributed by Varian, Darmstadt, Germany). Aqueous 0.2*M* $NaNO_3$ solution (adjusted with 50 wt % aqueous NaOH to pH 9) was used as an eluant at a flow rate of 1.0 mL/min. FLA solution (concentration: 10 mg/mL) was filtered through a 5-μm filter. A d_n/d_c value of 0.156 mL/g (value for polyacrylamide[20]) was used for calculation of M_w and M_n. Hence, the molecular weights measured are relative to polyacrylamide. Characterization of humic acid was carried out on another separation module (Waters Alliance 2695) equipped with RI detector 2414 and a 3 angle dynamic light scattering detector (mini Dawn from Wyatt Technologies, Santa Barbara, CA). The humic acid solution was filtered through a 0.2-μm filter and then separated on a Ultrahydrogel™ precolumn and three Ultrahydrogel™ columns (120, 250, and 500; Waters, Eschborn, Germany). Eluent was 0.1*M* aqueous $NaNO_3$ solution (adjusted to pH 12.0 with NaOH) pumped at a flow rate of 1.0 mL/min. The value of d_n/d_c used to calculate M_w and M_n for humic acid was 0.218 mL/g (value for lignin).[21]

The specific anionic charge amounts of the polymers used in this study were determined at room temperature in deionized water, 0.1*M* NaOH (pH 12.6) and cement pore solution, using a PCD 03 pH apparatus (BTG Mütek GmbH, Herrsching, Germany). Cement pore solution was freshly prepared by vacuum filtration of neat API Class G cement slurry (*w/c* ratio 0.44) using blue ribbon filter paper and a diaphragm vacuum pump (Vacuubrand GmbH, Wertheim, Germany). Charge titration was carried out according to a literature description employing a 0.001*N* solution of laboratory grade poly (diallyl dimethylammonium chloride) from BTG Mütek GmbH, Herrsching, Germany as cationic polyelectrolyte.[22] The values presented are the averages obtained from three different measurements. The standard deviation of this method was found to be ±5 C/g.

Thermal stability of the graft copolymer and the humic acid backbone was compared using thermogravimetric analysis (instrument STA 409 CD, NETZSCH Geraetebau GmbH, Selb, Germany) under nitrogen atmosphere at a heating rate of 10°C per min. Prior to analysis, aqueous solutions of the graft copolymer and of humic acid were dialyzed for 2 days using a Spectra/Por® dialysis membrane (MWCO 50,000) from Spectrum Laboratories, Rancho Dominguez, CA. The dialyzed copolymer and humic acid solutions were freeze dried and the polymer powders thus obtained were used. For thermal ageing of the graft copolymer, an OFITE roller oven was used. There, 300 mL of the graft copolymer solution were poured into a 500 mL teflon liner (OFITE part # 175 – 60) and placed into a stainless steel grade 316 ageing cell (OFITE part # 175 – 60). A pressure of 7 bar was applied to the cell which was rotated at 25 rpm in the roller oven. The oven was then heated up to a temperature of 150°C and left rotating for 8 h. After this time, the cell was removed from the oven and cooled with water to room temperature.

Cement slurry preparation

Cement slurries were prepared in accordance with the procedures set forth in *Recommended Practice for Testing Well Cements*, API Recommended Practice 10B, issued by the American Petroleum Institute, using API Class G oil well cement and deionized water.[23] At first, the cement was dry blended with silica flour at a weight ratio of 65: 35 to avert cement compressive strength retrogression occurring at temperatures above 115°C. This blend was mixed with DI water at a water-to-cement (*w/c*) ratio of 0.57 and a water-to-solids (*w/s*) ratio of 0.41 (solids = cement + silica flour) using a blade-type laboratory blender manufactured by Waring Products Inc. (Torrington,

CT). Generally, the graft copolymer solution was dissolved in the mixing water while powdery SCR-500® retarder was dry blended with cement. All admixture dosages are given in % by weight of cement (bwoc). In a typical experiment, the amount of mixing water required to achieve a *w/c* ratio of 0.57 excluding the amount of water present in the copolymer solution was placed in the cup of the Waring blender. This was followed by addition of the exact volume of copolymer solution holding the desired amount of copolymer. The cement: SSA-1 blend (65:35 wt %) was added within 15 s to the mixing water at 4000 rpm. Thereafter, stirring continued for additional 35 s at 1200 rpm. To ensure sufficient homogenization after mixing, all slurries were poured into a 500-mL slurry container and stirred for 20 min at 95°C in an atmospheric consistometer (model 1250 from Ametek Chandler Engineering, Broken Arrow, OK).

Rheology of the cement slurries was determined following API RP 10B procedure employing a model PVS Rheometer from Brookfield Engineering Laboratories, Middleboro, USA. This rheometer is capable of measuring viscosity at elevated temperatures above 100°C. Totally, 30 mL of the cement slurry homogenized in the atmospheric consistometer were poured into the rheometer cup. A pressure of 500 psi was applied and the sample was heated to 150°C. Thereafter, the shear stress (lbs/100 ft^2) was measured at shear rates of 1022, 511, 341, 170, 10.2, and 5.1 s^{-1} respectively using bob B5.

High temperature high pressure consistometer

HTHP thickening times of cement slurries were measured at 150°C under an applied pressure of 400 bar using a consistometer model 8240 (Ametek Chandler Engineering, Broken Arrow, OK). The cement slurries holding specified admixture dosages were prepared as described above, but without homogenization in the atmospheric consistometer. The slurries were poured into the HTHP consistometer cell and the time to reach 70 Bc (Bearden unit of consistency, a dimensionless unit) was taken as the cement slurry thickening time.

API static fluid loss

Static fluid loss at 150°C was measured using a 500-mL high pressure, high temperature (HP/HT) stainless steel filter cell manufactured by OFI Testing Equipment (Houston, TX). Design of this HP/HT filter cell and its operation are described in detail in a norm issued by the American Petroleum Institute (API).[23] After pouring the homogenized slurry obtained from the atmospheric consistometer at 95°C into the HT/HP cell preheated to 90°C, a condenser was attached to the filtrate collecting valve and a differential pressure of 70 bar N_2 was applied at the top of the cell. Within 40 min, the temperature was increased to the test temperature of 150°C using a heating jacket (OFI Testing Equipment, Houston, TX). Filtration proceeded through a 22.6 cm^2 (3.5 in^2) mesh metal sieve placed at the bottom of the cell. The fluid volume collected within 30 min was doubled as described by API RP 10B and regarded as API fluid loss of the corresponding cement slurry. The values reported for the respective API fluid loss test represents the average obtained from three separate measurements. Maximum deviation of individual values in the fluid loss tests was ±10 mL/30 min. Where complete dehydration of the cement slurry in <30 min occurred, the valve of the condenser was occasionally opened to ascertain the dehydration time.

Adsorption

The adsorbed amount of admixture (graft copolymer or retarder) was determined from the cement filtrate collected in the respective fluid loss test. Generally, the depletion method was applied, i.e., it was assumed that the decrease in the polymer concentration before and after contact with cement solely resulted from interaction with cement, and not from insolubility of the polymer. This assumption was confirmed through a solubility test. For this purpose, 35 g/L of the graft copolymer and of the retarder respectively (this concentration correlates to a polymer dosage of 2.0% bwoc) were dissolved in cement pore solution and stored for three days. No precipitation was observed. The amount of individual polymer retained was calculated from the difference in the equilibrium concentration of the polymer present in the liquid phase before and after contact with cement (depletion method). A High TOC II apparatus (Elementar, Hanau, Germany) equipped with a CO_2 detector was used for quantification of the carbon content present in the solutions. Maximum deviation of the adsorbed amount was found at ±0.1 mg polymer/g cement. Quantification of adsorbed amounts of the individual polymers was done as follows: Since the retarder is colorless while the graft copolymer is dark brown, UV–vis spectroscopy was used to determine the graft copolymer concentration while adsorbed amount of retarder was obtained by subtracting the carbon content originating from the graft copolymer from the total organic carbon content found in the filtrate and converting this value into concentration of retarder. For this purpose, a standard addition plot of both polymer solutions holding a fixed dosage of 0.029% bwoc (0.5 g/L) retarder and increasing dosages of graft copolymer was taken at 600 nm using a spectroflex 6100 spectrophotometer (WTW Wissenschaftlich-Technische

TABLE III
Standard Addition Plot of UV–Vis Absorbance Measured at 600 nm and at Increased Dosages of Graft Copolymer at a Fixed Dosage of 0.029% bwoc (0.5 g/L) of SCR–500® Retarder

Graft copolymer dosage (g/L)	Absorbance @ 600 nm
0.5 graft copolymer only (w/o retarder)	0.491
0.0	−0.001
0.5	0.496
1.0	1.019
1.5	1.463

Werkstätten GmbH, Weilheim, Germany). This standard plot of absorbance vs. graft copolymer concentration was used to determine the concentration of the copolymer based on the equation $y = 0.983x + 0.007$ ($R^2 = 0.999$). Where y represents the absorbance, x the concentration of the graft copolymer, and R is coefficient of determination. The data for the standard plot are given in Table III.

Zeta potential measurement

Titration of the graft copolymer to the cement/silica flour slurry (c : s = 65 : 35 wt/wt) was performed at room temperature on an electro acoustic spectrometer (DT-1200 from Dispersion Technology, Bedford Hills, NY). Immediately after mixing the slurries were poured into the cup of the spectrometer and measured without homogenization in the atmospheric consistometer. The resulting zeta potential values were recorded and the accuracy of this method was ±1 mV.

RESULTS AND DISCUSSION

Properties and structure of the graft copolymer

The synthesized graft copolymer was first dialyzed and then characterized by size exclusion chromatography (Fig. 1). According to this analysis, the graft copolymer exhibits a significantly higher molar mass ($M_w \sim 600{,}000$ g/mol) than the humic acid backbone ($M_w \sim 69{,}000$ g/mol), thus confirming successful grafting (Table II). In accordance with this finding, the particle size (hydrodynamic diameter) as determined by size exclusion chromatography increased from 5.6 nm for the unmodified humic acid to ~ 80 nm after the grafting reaction. Similarly, the *Brookfield* viscosity of a 2 wt % aqueous solution shows a substantial increase for the graft copolymer in comparison to that of individual humic acid. Finally, elemental analysis confirmed the incorporation of N and S containing monomers into the graft copolymer. The difference between calculated and actual elemental composition of the graft copolymer is attributed to the removal of impurities, unreacted monomers and salts during dialysis. Also, the elemental analysis data provided in Table IV suggest that relative to the feeding molar ratios, only 87.5% of AMPS®, 92.4% of NNDMA, and 19.6% of acrylic acid fed were incorporated into the graft copolymer. Hence, the actual molar composition of the graft chain is 1 : 1.54 : 0.02. This differs from the feeding molar ratio which was 1 : 1.46 : 0.07.

According to literature, the phenolic group present in humic acid allows grafting of monomers through a hydrogen abstraction mechanism initiated by strong oxidants such as e.g., peroxodisulfates or Ce^{4+}. For example, acrylic acid and other monomers have been demonstrated to graft well onto humic acid or caustic lignite (the latter possesses some building blocks which are similar to these contained in humic acid).[24–29] Successful occurrence of grafting was confirmed by SEC data and performance testing. The copolymer made from AMPS®, NNDMA and acrylic acid only (no humic acid present!) under identical conditions with those for the graft copolymer exhibits a molecular size as expressed by the

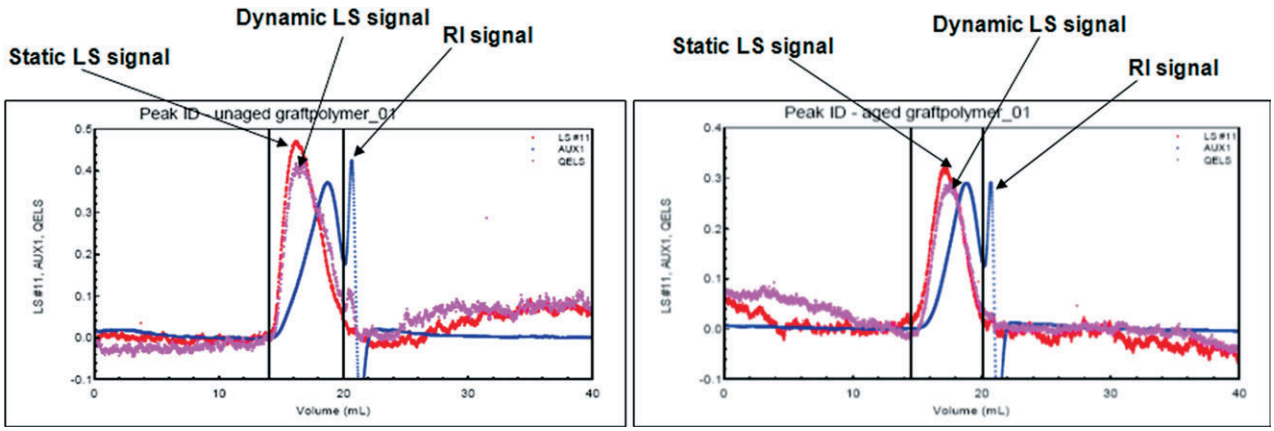

Figure 1 Size exclusion chromatograms of graft copolymer as obtained from synthesis (left) and after ageing for 8 h @ 150°C (right); eluent: 0.2*M* $NaNO_3$, pH = 9. [Color figure can be viewed in the online issue, which is available at wileyonlinelibrary.com.]

TABLE IV
Elemental Analysis Data for Graft Copolymer, Humic Acid, and Graft Chain

Elements	Graft copolymer found (%)	Graft copolymer calculated (%)	Humic acid found (%)	Graft chain calculated (%)
C	39.0	43.4	38.7	44.9
H	7.0	6.0	3.7	6.6
O	36.0	27.1	41.5	23.2
N	6.6	7.3	1.0	8.9
S	6.0	6.8	0.8	8.2
Na	4.9	6.7	0.5	8.3
K	0.5	2.8	13.8	-

O content always calculated as difference to 100 %.

$R_{g(z)}$ value which is considerably smaller than that of the graft copolymer (21.2 nm for the copolymer vs. 71.2 nm for the graft copolymer). Thus, it is evident that the graft copolymer possesses a larger number of side chains. Additionally, fluid loss performance of the graft copolymer at 150°C in cement slurry was compared with that of a mere blend of humic acid with the AMPS®/NNDMA/AA copolymer at a 20:80 wt ratio. There, the graft copolymer produced an excellent API fluid loss of 25 mL whereas the blend showed practically no fluid loss control (~ 200 mL) for the cement slurry. This experiment demonstrates that under the conditions selected, indeed a reaction between humic acid, AMPS®, NNDMA, and acrylic acid had occurred and that not just a simple mixture of humic acid and an AMPS®/NNDMA/AA copolymer is present. Accordingly, the graft copolymer is composed of a humic acid backbone and AMPS®-*co*-NNDMA-*co*-AA graft chains which are linked to the backbone via oxygen atoms from phenol groups (Fig. 2). Note that the chemical formula used there for humic acid was taken from literature.[30] With humic acid being a natural polymer, variations in its composition may occur.

Using thermogravimetric analysis and data from SEC, an attempt was made to develop a more precise structural model for the graft copolymer. Thermogravimetry revealed that at incremental increase of temperature, individual humic acid shows a gradual and almost linear decomposition with temperature (Fig. 3). Opposite to this, after an initial loss of ~ 6.5% water, the graft copolymer shows very high resistance to degradation up to a temperature of ~ 380°C. Beyond this temperature, rapid breakdown of the graft copolymer occurs. Obviously, humic acid present in the graft copolymer is protected from thermal degradation by the lateral graft chains made of AMPS®-NNDMA-acrylic acid. The overall architecture of the graft copolymer is that of a stretched backbone worm, as is illustrated in Figure 4. There, the graft chains present the teeth of a rather linear main chain. A similar model has been proposed for the solved conformation of polycarboxylate comb polymers bearing polyethylene oxide

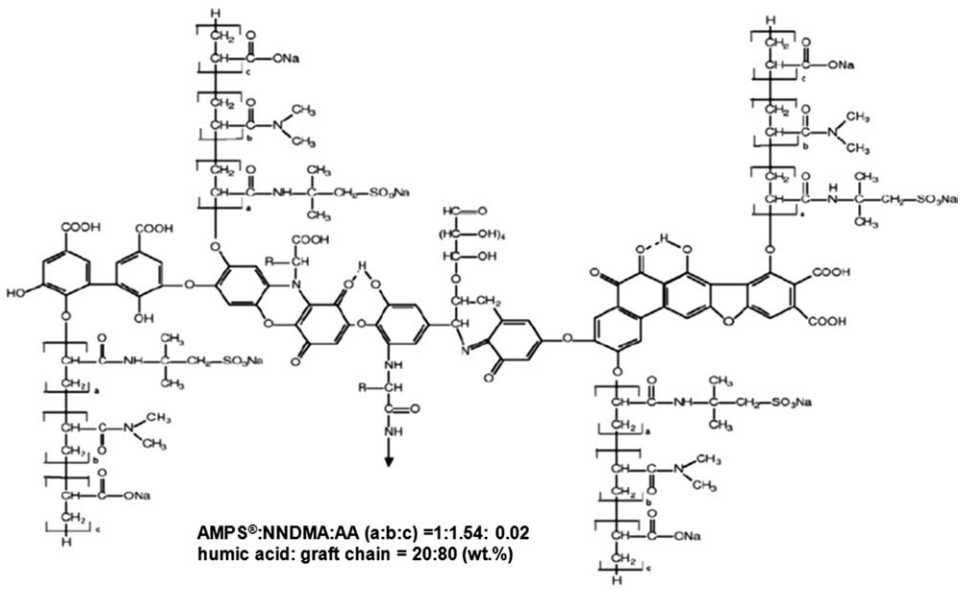

Figure 2 Structural representation of synthesized graft copolymer; structure of humic acid after.[30]

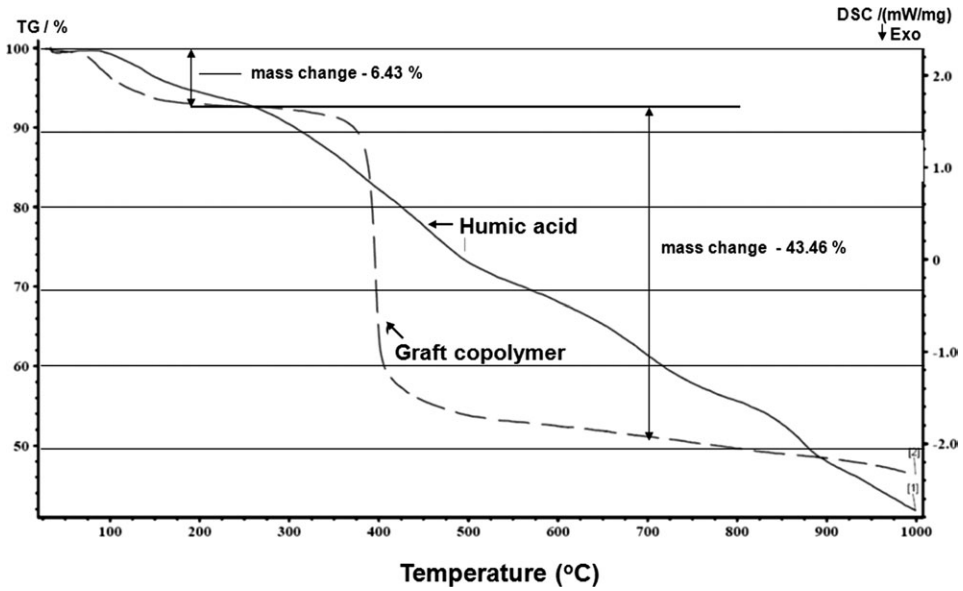

Figure 3 Thermogravimetric analysis of the humic acid backbone and of the graft copolymer.

graft chains (sodium polymethacrylate-*g*-PEO comb copolymers).[31–33] This specific structure is believed to be responsible for the superior thermal stability of the graft copolymer.

Another evidence for the existence of a stretched backbone worm structure is provided by data obtained from SEC. There, a value of $\sim$ 1.8 was obtained for the ratio of R_g/R_h (the so-called *Burchard* parameter). According to *Burchard,* values of 1.5–2.05 represent linear molecules, while at >2.2, stiff chains exist.[34]

Fluid loss performance of the graft copolymer

At first, the dosage of SCR-500® retarder required to delay the set of cement sufficiently to obtain slurry which is fluid and pumpable over several hours was determined. The target was to achieve a thickening time (pumping time) at 150°C for at least 4 h.

Static filtration properties of cement/silica flour slurries containing increased dosages (0–1.6% bwoc) of the graft copolymer and a fixed dosage of 1.2% bwoc of SCR–500® retarder were determined at 150°C (slurry density 1.93 kg/L). The results are shown in Figure 5.

Generally, API fluid loss decreases exponentially with increasing graft copolymer dosage. The minimum concentration of FLA needed to achieve an API fluid loss below 100 mL/30 min lies at 0.8% bwoc. This value presents a relatively low dosage, considering the harsh temperature conditions. In comparison, conventional CaAMPS®-NNDMA copolymers which are routinely used on HTHP wells require substantially higher dosages to achieve the same fluid loss as will be shown later in Table VI. The graft copolymer reaches its maximum effectiveness at a dosage of 1.2 % bwoc. From there, a filtrate volume of less than 30 mL/30 min is achieved. In a separate test, SCR–500® retarder was found to provide no fluid loss control at all (slurry dehydration occurred in less than 2 min). Thus, it was confirmed that filtration control was solely the effect of the graft copolymer.

Effect on rheology

Table IV presents results on the viscosifying properties of the synthesized graft copolymer in the presence of SCR–500® retarder. It shows that the graft copolymer generally increases slurry viscosity, but much less than conventional synthetic FLA polymers such as e.g., CaAMPS®-NNDMA copolymer.[15] Thus,

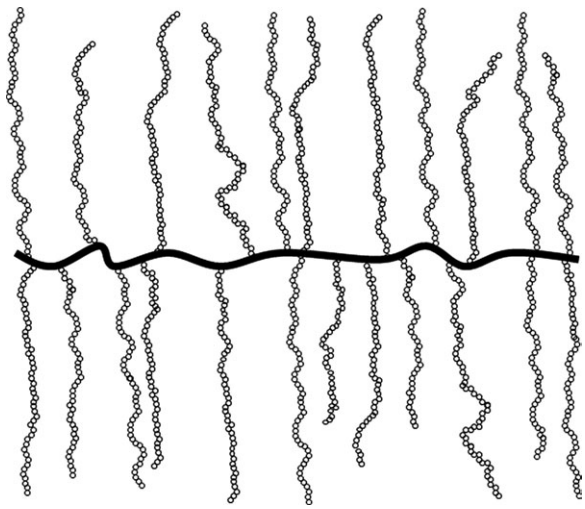

Figure 4 Model of the synthesized graft copolymer exhibiting the structure of a stretched backbone worm decorated with lateral graft chains.

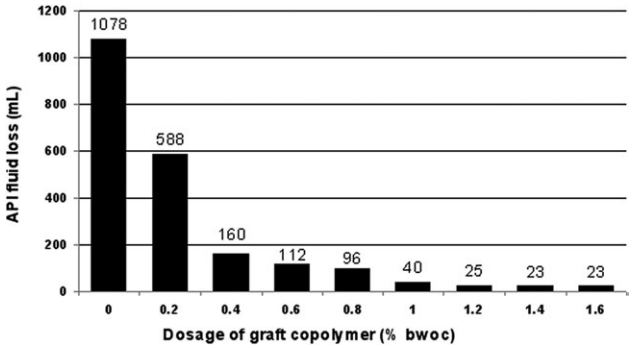

Figure 5 API fluid loss of Class G cement/silica (65:35% wt./wt.) slurries containing increased dosages of graft copolymer and 1.2% bwoc of SCR-500® retarder, measured at 150°C.

the graft copolymer behaves more advantageous in high density cement slurries. Still, caution needs to be exercised when the dosage of this FLA exceeds ~ 1.5% bwoc. Fortunately, such excessive dosages are not required to achieve sufficient fluid loss control with this polymer.

High temperature stability

To ascertain the high temperature stability of the graft copolymer, a sample of the aqueous solution was exposed at 150°C for 8 h in a roller oven and subsequently used in a static filtration test at 150°C. The results are presented in Table V. Interestingly, the same API fluid loss values were obtained for the graft copolymer before and after thermal exposure. This result instigates that the graft copolymer is high temperature stable with respect to fluid loss performance, while the rheology of its aqueous solution (Table II) and of the cement slurry (Table V) is lower in comparison to that of the unaged sample. This effect is owed to partial depolymerization of the graft copolymer, as was evidenced by size exclusion chromatography (see Fig. 1 and Table II). The molecular weights of the aged FLA were reduced by ~ 40% as a result of thermal exposure. This effect also became apparent from the Brookfield viscosity of their aqueous solutions and a reduction in the steric size (R_h) of the solved macromolecule (see Table II). Also, the aged graft copolymer solution exhibited a lighter color than the unaged sample. From this observation it was concluded that the humic acid was partially oxidized and fragmented while the graft chains remained essentially unaffected. In spite of this partial depolymerization, the graft copolymer still maintained its high effectiveness as cement fluid loss additive.

Mechanistic study

To uncover the working mechanism of this graft copolymer as fluid loss additive, a series of experiments were devised. First, the correlation between API fluid loss, filter cake permeability, dynamic filtrate viscosity, and filtercake pore size obtained at 150°C in the presence of varied dosages (0–1.6% bwoc) of the graft copolymer and of 1.2% bwoc of retarder was studied. The results are presented in Table VI. The dynamic filtrate viscosity was found to be always very low and independent of dosage. This means that filtrate viscosity has no impact on the fluid loss performance of the graft copolymer whereas filter cake permeability decreases linearly with API fluid loss. For example, permeability decreases from 1044 μD to 2.2 μD while API fluid loss is reduced from 1078 mL to 25 mL/30 min (see Table VI). This clearly emphasizes that the graft copolymer works by reduction of filter cake permeability.

TABLE V
Rheology (Shear Stress) of API Class G Cement/Silica Slurries Containing 0–1.6% bwoc of the Graft Copolymer and 1.2% bwoc of SCR-500® Retarder, Measured at 150°C and at Different Shear Rates

	Shear stress (lbs/100 ft^2) at shear rate (rpm) @ 150ºC					
Graft copolymer dosage (% bwoc)	300	200	100	6	3	600
0.0[a]	60	40	17	1	0	115
0.2[a]	55	30	11	1	0	98
0.4[a]	50	36	13	2	1	99
0.6[a]	57	38	16	2	1	109
0.8	90	68	54	5	4	152
1.0	168	106	57	7	6	268
1.2	181	126	70	10	8	>300
1.4	>300	245	130	19	17	>300
1.6	>300	>300	211	30	25	>300
For comparison: CaAMPS®-NNDMA copolymer[15]						
0.5	92	70	41	2	2	176
0.8	154	110	71	6	4	274
1.0	199	136	83	9	6	>300

[a] Low viscosity of the cement slurry causes solids settling.

TABLE VI
Rheology (Shear Stress) and API Fluid Loss of API Class G Cement/Silica Slurries Containing 1.2% bwoc of the Graft Copolymer Before and After Thermal Exposure to 150°C over 8 h[a]

Graft copolymer	300	200	100	6	3	600	API fluid loss @ 150°C (mL)
Unaged	181	126	70	10	8	>300	25
Aged 8 h @ 150°C	123	70	35	2	1	220	24

[a] Slurry also includes 1.2% bwoc of SCR-500® retarder.

To probe the reason behind the reduction in filter cake permeability, adsorption of the graft copolymer on the cement/silica solids was investigated.

Adsorption of the graft copolymer

Since the graft copolymer is an anionic polyelectrolyte similar to AMPS®-*co*-NNDMA fluid loss additive which exhibits an adsorptive working mechanism,[15] it was speculated that this graft copolymer may function according to the same principle. Thus, adsorbed amounts of the graft copolymer and of the retarder were determined by UV–vis spectroscopy and TOC measurement, as described in the experimental section. The results are displayed in Figure 6.

Generally, the adsorbed amount of the retarder is quite constant (variation range 5.4–7.1 mg/g of cement) and is independent of its dosage and that of the graft copolymer. While the adsorbed amount of the graft copolymer clearly increases with dosage. The adsorbed amount first increases linearly until it levels out at a dosage of ~ 1.5% bwoc. There, a saturated adsorbed amount of ~ 15 mg/g cement was observed. This behavior is best described by a Langmuir type adsorption isotherm which includes monolayer formation of the adsorbed polymer.

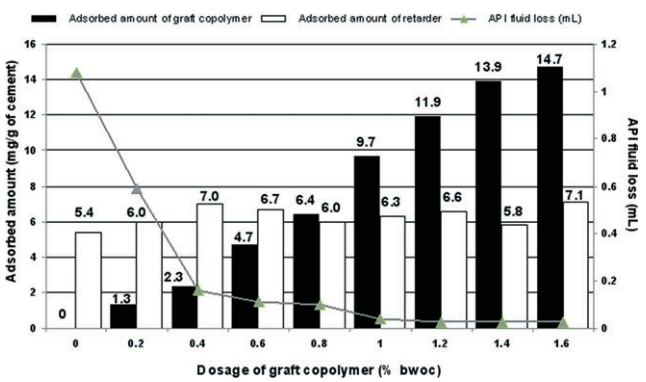

Figure 6 Adsorbed amounts of graft copolymer and retarder respectively and corresponding API fluid loss of the cement/silica slurry holding 1.2% bwoc of retarder as a function of graft copolymer dosage, measured at 150°C. [Color figure can be viewed in the online issue, which is available at wileyonlinelibrary.com.]

Adsorption was confirmed to be the sole reason for FLA depletion through a solubility test. For this purpose, 2% bwoc of the graft copolymer were dissolved in this cement pore solution and left to rest for 3 days. No precipitation of the FLA was observed after this period.

Another observation from Figure 6 is that the adsorbed amount of FLA still increases even when API fluid loss remains stable below 30 mL. This effect can be explained as follows: API filtrates of <30 mL/30 min are produced by dehydration of the first layers of the cement slurry next to the sieve. Formation of this early filtrate (the "spurt loss") is always necessary to produce a filter cake which is tight and seals the slurry against further dehydration. There is no possibility to avoid this initial spurt loss. Thus, using this test protocol, it is impossible to achieve API fluid loss values of less than 25 mL/30 min.

Next, the adsorptive working mechanism of the FLA was further investigated via zeta potential measurement and determination of its calcium binding capacity.

Zeta potential measurement

The zeta potential curve obtained for the cement/silica flour slurry under titration of the graft copolymer solution is displayed in Figure 7. Without copolymer, the slurry exhibits a positive charge of ~ +4 mV. Stepwise addition of the anionic graft copolymer reverses the positive charge to negative values until a point of saturation is achieved. This trend towards negative charges confirms that polymer adsorption onto the surfaces of cement and silica occurs.[35]

Specific anionic charge and calcium binding capacity

For the unaged graft copolymer, aged graft copolymer, and humic acid, their specific anionic charges in deionized water, 0.1*M* NaOH (pH 12.6) and cement pore solution were determined. The results are exhibited in Figure 8.

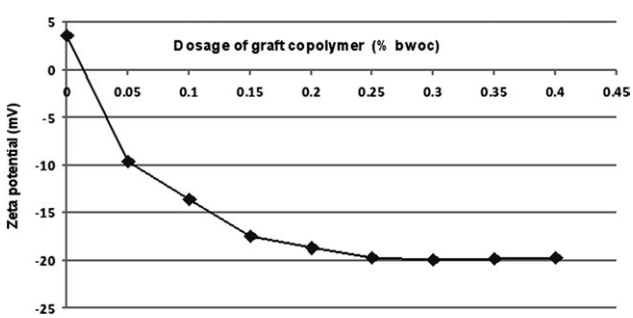

Figure 7 Zeta potential of cement/silica slurry titrated with increased dosages of graft copolymer.

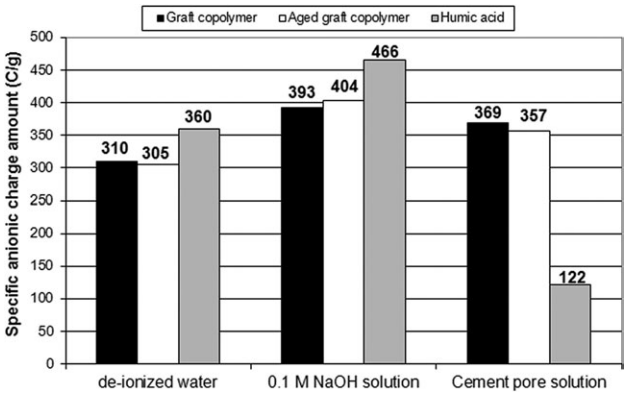

Figure 8 Specific anionic charge amounts of the graft copolymer, aged graft copolymer, and humic acid in DI water, 0.1*M* NaOH (pH 12.6) and cement pore solution.

Generally, in all fluid systems, the aged and unaged graft copolymers exhibit comparable anionic charge amounts. This again indicates that during the ageing process, the humic acid backbone is fragmented while no significant degrafting of side chains takes place. Additionally, all samples exhibit higher specific anionic charge amounts in 0.1*M* NaOH than in DI water. This effect is owed to increased deprotonation at high pH. Whereas in cement pore solution (which contains $\sim$ 0.6 g/L of Ca^{2+}), anionic charges of all samples dropped, with the effect on humic acid being particularly strong. A possible explanation for this behavior is strong calcium complexation.[22]

To probe into this, the calcium binding capacities of humic acid and of aged and unaged graft copolymer were determined in NaOH (pH 12.6) in presence and absence of 0.6 g/L Ca^{2+} ions (Table VII). It was found that the specific anionic charge amount of humic is most strongly affected by Ca^{2+} (reduction of 84 %). At this Ca^{2+} concentration of 0.6 g/L, humic acid partially comes out of solution as a brown precipitate consisting of calcium humate. While for the unaged and aged graft copolymers, the specific anionic charge amounts only decrease by 12% and 28% respectively, with no precipitation. This signifies much lower calcium binding capacity for the graft copolymers. For comparison, the anionic charge of CaAMPS®-NNDMA copolymer is reduced by 4% only.[36] This instigates that the interaction between Ca^{2+} and the graft copolymer mainly occurs at the humic acid backbone and less at the lateral chains.

The experiments demonstrate that the grafting process produces a copolymer with greatly enhanced solubility in the presence of Ca^{2+}. This property is a prerequisite for the effectiveness of the graft copolymer in cementitious systems.

Additionally, the graft copolymer is fully compatible and effective with a synthetic retarder based on AMPS®-*co*-itaconic acid. They do not perturb each other, which differentiates it from other cement fluid loss additives such as e.g., CaAMPS®-*co*-NNDMA.[37]

The adsorptive mechanism of the graft copolymer is highly surprising since it is well known that ettringite, a cement hydrate formed from tricalcium aluminate and calcium sulfate present in cement, presents the main mineral for adsorption of anionic admixtures.[38] However, ettringite is not stable at temperatures exceeding $\sim$ 80°C and therefore is practically absent at 150°C which was the test temperature here. Therefore, the graft copolymer has to adsorb onto another mineral substrate which most likely are calcium silicate hydrates. In cement pore solution they were found to develop a slightly positive charge which increases with temperature as a result of increased Ca/Si ratio.[39] This effect renders them a potential substrate for polymer adsorption.

TABLE VII
API Fluid Loss, Dynamic Filtrate Viscosity, and Filter Cake Permeability of Cement/Silica Flour Slurries Containing Different Dosages of Graft Copolymer and 1.2% bwoc of SCR-500® Retarder, Measured at 150°C

Graft copolymer dosage (% bwoc)	Dynamic filtrate viscosity (mPa·s)	Filtercake permeability (μD)	API fluid loss (mL)
0.0	0.44	1044	1078[a]
0.2	0.39	448	588[a]
0.4	0.41	96	160
0.6	0.45	50	112
0.8	0.63	71	96
1.0	0.48	5.1	40
1.2	0.49	2.2	25
1.4	0.49	2.0	23
1.6	0.50	2.0	23
For comparison: CaAMPS®-NNDMA copolymer[15]			
0.8	4.3	4,905	554[a]
1.0	6.0	4,432	410[a]

[a] Calculated (dehydration occurred in less than 30 min).

TABLE VIII
Specific Anionic Charge Amount of Humic Acid, Unaged, and Aged Graft Copolymer Respectively, Measured in 0.1*M* NaOH (pH 12.6) in Presence and Absence of 0.6 g/L Ca^{2+} Ions

Polymer	Specific anionic charge amount (C/g)		Reduction of anionic charge by Ca^{2+} ions
	NaOH @ pH 12.6	NaOH @ pH 12.6 plus 0.6 g/L Ca^{2+}	
Humic acid	466	76	84%
Graft copolymer	393	345	12%
Aged graft copolymer	404	293	28%
CaAMPS®-NNDMA copolymer[15,38]	368	352	4%

CONCLUSIONS

Monomers of AMPS®, NNDMA, and acrylic acid were successfully grafted on humic acid, as was evidenced by SEC analysis (R_g value) and comparative performance testing of the graft copolymer and a mere blend of humic acid with an AMPS®/NNDMA/AA copolymer prepared under similar conditions as the graft copolymer. The latter provided excellent fluid loss control while the blend showed no fluid loss control at all. The working mechanism of humic acid-{AMPS®-*co*-NNDMA-*co*-AA} graft copolymer as cement fluid loss additive was found to rely on reduction of filtercake permeability. This reduction is achieved by adsorption of the graft copolymer on cement and possibly silica particles. Adsorption was evidenced by zeta potential measurement showing increased negative loading onto solid particles present in the cementing formulation. Through strong adsorption which is hardly affected by temperature, the polymer constricts the pores of the filter cake. The study also shows that this graft copolymer exhibits only a moderate viscosifying effect on the cement slurry, and thus qualifies for high density slurries which are required on high temperature high pressure wells. Additional research is in progress to validate which cementitious phases are responsible for the adsorption of the graft copolymer.

References

1. Fink, J. K. Oil Field Chemicals; Gulf Professional Publishing: Burlington, MA, 2003.
2. Nelson, E. B.; Guillot, D. Well Cementing; Schlumberger Dowell: Sugar Land, TX, 2006.
3. Smith, D. K. Cementing; Society of Petroleum Engineers; SPE Monograph: New York, 1990.
4. Audebert, R.; Hendricks, H.; Janca, J.; Maroy, P. US Patent Number 5,597,050, 1997.
5. Plank, J.; Dugonjic-Bilic, F.; Recalde Lummer, N.; Salami, T. J Appl Polym Sci 2010, 117, 2290.
6. Hook, F. E. US Patent Number 3,483,007, 1969.
7. Vijn, J. P.; Dao, B.; Melbouci, M. US Patent Number 6,730,636, 2004.
8. Raines, R. H. US Patent Number 4,629,573, 1986.
9. Buelichen, D.; Plank, J. SPE International Symposium on Oilfield Chemistry, The Woodlands/TX, paper SPE 141182, 2011.
10. Plank, J.; Dugonjic-Bilic, F. J Appl Polym Sci 2011, 121, 1262.
11. Udarbe, R. G.; Hancock-Grossi, K. US Patent Number 6,136,935, 2000.
12. Stephens, M., US Patent Number 5,294,651, 1994.
13. Persinski, L.; Cook, L. J.; Adams, S. L. US Patent Number 4,015,991, 1977.
14. Rao, S. P.; Burkhalter, J. F. US Patent Number 4,555,269, 1985.
15. Plank, J.; Brandl, A.; Zhai, Y. N.; Franke, A. J Appl Polym Sci 2006, 102, 4341.
16. American Petroleum Institute. API Specification 10A, 24th ed.; American Petroleum Institute: Washington, 2010.
17. Franke, B. Z Anorg Allgem Chem 1941, 247, 180.
18. Rodrigues, A. K. European Patent Number 0,633,390, 1999.
19. McCusker, L. B.; Von Dreele, R. B.; Cox, D. E.; Louër, D.; Scardi, P.,J Appl Crystallogr 1999, 32, 36.
20. Huglin, M. B. In Polymer Handbook, 3rd ed.; Brandrup, J.; Immergut, E. H., Eds.; Wiley: New York, 1989.
21. Gupta, P. R.; Goring, D. A. I. Can J Chem 1969, 38, 270.
22. Plank, J.; Sachsenhauser, B. Cem Concr Res 2009, 39, 1.
23. American Petroleum Institute. API Recommended Practice 10B-2, 1st ed.; American Petroleum Institute: Washington, 2005.
24. Lewis, S.; Chatterji, J.; King, B.; Brennels, D. C. US Patent Number 7,523,748, 2009.
25. Lewis, S.; Chatterji, J.; King, B.; Brennels, D.C., US Patent Number 7,388,045, 2008.
26. Fry, S. E.; Childs, J. D. US Patent Number 4,703,801, 1987.
27. Fry, S. E.; Childs, J. D. US Patent Number 4,676,317, 1987.
28. Huddleston, D. A.; Williamson, C. D., US Patent Number 5,028,271, 1991.
29. Huddleston, D. A.; Williamson, C. D. US Patent Number 4,938,803, 1990.
30. Stevenson, F. J. Humus Chemistry: Genesis, Composition, Reactions; Wiley-Interscience: New York, 1982.
31. Gay, C.; Raphael, E. Adv Colloid Interfac 2001, 94, 229.
32. Borget, P.; Galmiche, J.-F.Le Meins; Lafuma, F. J Colloids Surf A, 2005, 260, 173.
33. Giraudeau, C.; d'Espinose de Lacaillerie, J.-B.; Sougguir, Z.; Nonat, A; Flatt, R. J. J Am Ceram Soc 2009, 92, 2471.
34. Burchard, W. Adv Polym Sci 1983, 48, 1.
35. Mollah, M. Y. A.; Adams, W. J.; Schennach, R.,Adv Cem Res 2000, 12, 153.
36. Plank, J.; Recalde Lummer, N.; Dugonjic-Bilic, F. J Appl Polym Sci 2010, 116, 2913.
37. Tiemeyer, C.; Plank, J. J Appl Polym Sci 2011, doi:10.1002/app.35535
38. Plank, J.; Hirsch, C. Cem Concr Res 2007, 37, 537.
39. Nachbaur, L.; Nkinamubanzi, P.-C.; Nonat, A.; Mutin, J.-C. J Colloid Interface Sci 1998, 202, 261.

3.2 Preparation and Properties of a Dispersing Fluid Loss Additive based on Humic Acid Graft Copolymer Suitable For Cementing High Temperature (200 °C) Oil Wells

Synopsis

This work relates to the synthesis of a humic acid based graft copolymer providing simultaneous water retention and dispersing properties in cement slurries at 200 °C.

The dispersing graft copolymer exhibits a much lower molecular weight (~ 323, 000 g/mol) than viscosifying graft copolymer (~ 600,000 g/mol). The dispersing effect originates from its specific molar composition: AMPS®-co-NNDMA-co-AA =1:0.31:0.03 which differs from that of the viscosifying graft copolymer (m.r = 1:1.54:0.02). It possesses highly flexible, dangling lateral chains.

The polymer adsorbs strongly onto cement and effectively constricts filter cake pores at 200 °C. The polymer is essentially suitable for high density cement slurries exhibiting particularly low water-to-cement ratios, as required for high pressure reservoirs.

The results were published in:

Journal of Applied Polymer Science,

O: T. Salami and J. Plank, 129, 2544 - 2553, **2013**

Journal of Applied Polymer Science

Preparation and Properties of a Dispersing Fluid Loss Additive based on Humic Acid Graft Copolymer Suitable for Cementing High Temperature (200°C) Oil Wells

Oyewole Taye Salami, Johann Plank
Institute for Inorganic Chemistry, Technische Universität München, Garching, Germany
Correspondence to: J. Plank (E-mail: johann.plank@bauchemie.ch.tum.de)

ABSTRACT: A humic acid graft copolymer possessing both water-retention and dispersing properties in cement slurry was synthesized by grafting lateral chains of 2-acrylamido-2-methylpropane sulfonic acid (AMPS®), *N*,*N*-dimethylacrylamide (NNDMA), and acrylic acid (AA) onto a backbone of humic acid using aqueous free radical polymerization. The graft copolymer is composed of 20 wt % humic acid backbone and 80 wt % graft chain (molar ratio AMPS/NNDMA/AA = 1 : 0.31 : 0.03), it exhibits a M_w of 323 kDa and is highly anionic in cement pore solution. The influence of this specific molecular design on cement flow properties is unraveled. When tested at 200°C, the graft copolymer achieved very low cement fluid loss values (~50 mL) at low rheology. This behavior differentiates it from most common synthetic high temperature fluid loss additives which excessively viscosify cement slurries. The working mechanism of the graft copolymer was found to rely on adsorption onto the surface of hydrating cement. © 2013 Wiley Periodicals, Inc. J. Appl. Polym. Sci. 129: 2544–2553, 2013

KEYWORDS: adsorption; copolymers; grafting; oil and gas; rheology

Received 24 May 2012; accepted 23 December 2012; published online 30 January 2013
DOI: 10.1002/app.38980

INTRODUCTION

Crude oil (petroleum) and natural gas are among the most abundant fossil resources found in geological formations beneath the earth's surface in depths of up to 9000 m. For their recovery, oil and gas wells have to be constructed by drilling through multiple geological formations using water or oil-based drilling fluids. Water-based drilling muds use functional water-soluble polymers for water retention, e.g. for polymers based on *N*-vinylpyrrolidone.[1] In mature oilfields, aqueous solutions of viscosifying polymers are used for tertiary oil recovery (so-called chemical flooding).[2]

Since recent, an increasing number of oil and gas wells is characterized by excessively high temperatures (up to 260°C), high pressures (up to 1700 bar), and saline reservoir fluids that may contain numerous electrolytes such as NaCl, $CaCl_2$, $MgCl_2$, and $MgSO_4$ at total concentrations of up to 40 wt %. These wells need to be sealed by cementing a metal pipe (so-called casing) into the borehole.[3,4] The primary objective of cementing such casing is to achieve complete zonal isolation. It prevents migration of fluids and gases between formations and of influxes into the borehole. Consequently, the cement sheath needs to withstand the various stresses occurring during the life of an oil well.[5,6]

Cement dispersed in water presents a classical colloidal system whereby the cement particles attain an overall negative surface charge, as is evidenced by zeta potential measurement.[7,8] The silicate phases C_3S and C_2S present in cement clinker produce a negative charge while the aluminates (C_3A and C_4AF) exhibit a positive charge. Thus, the charge distribution on the surface of cement is heterogeneous and provides anchoring sites for both cationic and anionic polyelectrolytes. Since silicates and thus negatively charged surfaces are prevalent in cement, anionic cement additives are most commonly used because they require less dosage to cover the fewer positively charged sites of the aluminate hydrates by adsorption.[9]

The addition of fluid loss additives (FLAs) to oil well cement slurries is of paramount importance to prevent loss of water (dehydration) of the cement slurry while it is being pumped down hole and placed between the porous formation and the casing. Currently, synthetic sulfonated copolymers present common high temperature (HT) fluid loss additives. Among them are for polymers based on 2-acrylamido methane propane sulfonic acid (AMPS®), *N*-vinylacetamide and acrylamide, or AMPS and *N*,*N*-dimethyl acrylamide.[10,11–14] Their effectiveness is known to rely on adsorption on the surface of cement.[15] A major drawback for these high molecular weight copolymers

© 2013 Wiley Periodicals, Inc.

(M_w > 1.5 mio g/mol) is their excessive viscosifying effect. This is highly undesirable, because deep wells which exhibit ultra-high temperatures require increased slurry densities (>1.9 kg/L) to provide sufficient hydrostatic overburden pressure against the reservoir. Such cement slurries are characterized by low water and high cement content (water-to-cement ratio < 0.40). FLAs such as the aforementioned impart even more viscosity to those already highly viscous cement slurries which renders it extremely difficult to pump them over distances of e.g. 16 km. Consequently, substantial additions of dispersants are required to counteract this thickening effect. Such combinations are highly uneconomical and present a complex admixture system which is difficult to handle in the field.

Owed to the recent trend for constructing ultra-deep HT/HP wells, admixture technology suitable for those conditions is required. Relative to fluid loss additives, copolymers which exhibit stable performance at high temperature and possibly a dispersing effect are most desirable.

It is known that copolymerization provides an excellent way for the tailoring of macromolecules with specific chemical structures and for the control of properties such as hydrophilic/hydrophobic balances, rigidity, solubility, polarity, etc. These properties are regulated by the nature and distribution of the monomeric units along the copolymer chains and depend on the physico-chemical properties of the co-monomers used.[16,17] Here, highly anionic AMPS-NNDMA-AA terpolymer blocks were grafted onto a humic acid backbone with tailor-made co-monomer composition that involves a significant amount of pronounced hydrophilic AMPS and acrylic acid monomers which produce flexible units and ionize completely in aqueous solution, in contrast to the less polar NNDMA monomer which renders the polymer chain more rigid and less hydrophilic as a result of the steric effect induced by the CH_3 groups linked to the amide. On the basis of this concept, a dispersing fluid loss additive was designed, synthesized and characterized. Its performance in oil well cement slurries was compared to that of a viscosifying graft copolymer presented in an earlier article.[18]

Exceptional temperature stability was probed by performance testing at 200°C, and the influence of the specific graft chains on the flow behavior of cement was established. In addition, its working mechanism was verified from filter cake permeability, adsorption, and zeta potential measurements.

EXPERIMENTAL SECTION

Materials

Oil Well Cement. An API Class G oil well cement ("*black label*" from Dyckerhoff AG, Wiesbaden, Germany) corresponding to American Petroleum Institute (API) Specification 10A was used.[19] Its clinker composition was determined through powder Q-XRD technique using *Rietveld* refinement (Table I). The amounts of gypsum ($CaSO_4{\cdot}2H_2O$) and hemi-hydrate ($CaSO_4{\cdot}0.5{\cdot}H_2O$) were measured by thermogravimetry. Free lime (CaO) was quantified following the extraction method established by *Franke*.[20] The specific surface area was determined using a Blaine instrument (Toni Technik, Berlin, Germany), and the specific density was measured by helium pyconometry (Quantachrome Instruments, Boynton Beach, FL). The average particle size (d_{50} value) was obtained using a laser granulometer (1064 instrument from Cilas, Marseille, France).

Table I. Phase Composition (XRD, *Rietveld*), Specific Density, Specific Surface Area (*Blaine*), and d_{50} Value of API Class G Oil Well Cement Sample

C_3S (wt %)	59.6
C_2S (wt %)	22.8
C_3A_c (wt %)	1.2
C_4AF (wt %)	13.0
Free CaO (wt %)	<0.3
$CaSO_4{\cdot}2H_2O$ (wt %)	2.7[a]
$CaSO_4{\cdot}0.5\ H_2O$ (wt %)	0.0[a]
$CaSO_4$ (wt %)	0.7
specific density (kg/L)	3.18
Specific surface area (cm^2/g)	3058
d_{50} value (μm)	11

C_3S: tricalcium silicate ($Ca_3(SiO_4)O$); C_2S: dicalcium silicate (Ca_2SiO_4); C_3A_c: cubic modification of tricalcium aluminate ($Ca_9Al_6O_{18}$); C_4AF: tetra calcium aluminate ferrite ($Ca_4Al_2Fe_2O_{10}$).
[a]Measured by thermogravimetry.

Silica Flour. A commercial sample of silica flour (SSA-1 from Halliburton GmbH, Celle, Germany) containing (wt %) quartz 97.60, CaO 0.57, MgO 0.18, Al_2O_3 0.17, TiO_2 0.06 (determined by X-ray fluorescence) and LOI 1.40 was used. Its specific surface area (Blaine *method*) was 1857 cm^2/g, while the average particle size (d_{50} value) was 32.7 μm. Specific density of the silica flour was found to be 2.65 kg/L.

Synthesis of the Dispersing Graft Copolymer. The humic acid graft copolymer was prepared by grafting AMPS, NNDMA, and AA onto a humic acid backbone via aqueous free radical copolymerization using sodium persulfate as initiator. In a typical experiment, 117 mL of a 14.5 wt % aqueous solution of commercial potassium humate (HA 2 from Borregaard Lignotech, Sarpsborg, Norway) and 160 mL of DI water were placed in a 1-L four-necked flask equipped with stirrer, thermometer, and N_2 inlet. The pH of the solution which initially was 9.2 was adjusted to 12 by feeding of 13.5 g of sodium hydroxide pellets into the flask. Next, in this order: 50 g of AMPS (2404 monomer from Lubrizol, Rouen, France), 15 g of NNDMA (Sigma-Aldrich, Munich, Germany), 1.2 g of acrylic acid (Merck KgaA, Darmstadt, Germany), 0.30 g of EDTA (Sigma-Aldrich, Munich, Germany), and 1 g of defoamer (TEGO ANTIFOAM MR 2123, an organo-modified polysiloxane from Evonik Goldschmidt GmbH, Essen, Germany) were added to the solution of potassium humate. The feed molar ratios of AMPS, NNDMA, and AA were 1 : 0.63 : 0.07, and the weight ratio between backbone and graft chain was 20 : 80. While stirring, nitrogen gas was bubbled through the solution for 1 h. Then, the temperature was increased to 50°C and the first amount of $Na_2S_2O_8$ initiator (4.0 g) was added. After 50 min of reaction time, the second portion of the initiator (4.0 g) was added. Grafting was continued for another 70 min, while the temperature was increased to 60°C. There, the mixture was left to react for an additional

hour before the temperature was again increased to 80°C for another hour to complete the reaction. Finally, the liquid was cooled to room temperature and the reaction was quenched by addition of 4.8 g sodium pyrosulfite ($Na_2S_2O_5$). The product yields a dark, viscous, odorless liquid which was diluted with 300 mL of DI water. Thus, a dark brown, 14 wt % aqueous solution possessing low viscosity and a pH value of 7.0 was obtained. The characteristic properties of the graft copolymer are summarized in Table III.

Synthesis of a Comparative Graft Copolymer. For comparison, a viscosifying graft copolymer possessing a similar molecular weight as the dispersing graft copolymer, but a different monomer composition was synthesized following the same procedure as described in a previous article for a viscosifying graft copolymer.[18] In the present preparation, the same feed molar ratios of AMPS, NNDMA, and AA of 1 : 1.46 : 0.07 as used for the previous viscosifying graft copolymer were used (50 g of AMPS, 35 g of NNDMA, and 1.2 g of AA). Also, the weight ratio between the humic acid backbone and the graft chain was kept constant at a weight ratio of 20 : 80. In the preparation, nitrogen gas was bubbled through the stirred solution for 1 h after the flask has been charged with the monomers, sodium hydroxide, EDTA, and defoamer, as presented in Ref. 18. Next, temperature was increased to 60°C and the first amount of $Na_2S_2O_8$ initiator (20.8 g) was added. After 50 min of reaction time, the second portion of the initiator (20.8 g) was added accordingly. Grafting was continued for another 70 min while the temperature was increased to 70°C. There, the mixture was left to react for an additional hour before the temperature was again increased to 80°C for another hour to complete the reaction. Finally, the liquid was cooled to room temperature and the reaction was quenched by addition of 6.25 g of sodium pyrosulfite ($Na_2S_2O_5$). The product yields a dark, highly viscous, odorless liquid which was diluted with 300 mL of DI water to obtain a dark brown, 7.3 wt % aqueous solution with a pH value of 4.0. The characteristic properties of this graft copolymer are summarized in Table III.

Cement Retarder. A commercial sample, HR®-25 from Halliburton GmbH, Celle, Germany containing tartaric acid was used.

Instruments and Procedures

Q–XRD was performed on a Bruker axs D8 Advance instrument (Bruker, Karlsruhe, Germany) with Bragg-Bretano geometry using Cu K_α ($\lambda = 1.5406$ Å) radiation and using Topas 3.0 software. X-ray fluorescence was performed on a spectrometer from PANalytical, Almelo, NL.

For size-exclusion chromatographic (SEC) analysis, a Waters Alliance 2695 (Waters, Eschborn, Germany) separation module equipped with RI detector 2414 (Waters) and an 18 angle dynamic light scattering detector (Dawn EOS, Wyatt Technologies, Clinton, IA) was used. The polymer was separated on a precolumn and two Aquagel–OH 60 columns (Polymer Laboratories, distributed by Varian, Darmstadt, Germany). Aqueous 0.2*M* $NaNO_3$ solution (pH 9 w/50 wt % aqueous NaOH) was used as eluant (flow rate 1.0 mL/min). A d_n/d_c value of 0.156 mL/g (value for polyacrylamide[21]) was used for calculation of M_w and M_n. The specific anionic charge amounts of the polymers were determined in DI water, 0.1*M* NaOH (pH 13) and cement pore solution (CPS), using a PCD 03 pH apparatus (BTG Mütek GmbH, Herrsching, Germany). Cement pore solution was freshly prepared by vacuum filtration of neat API Class G cement slurry (w/c ratio 0.44). Charge titration was carried out according to a literature description.[22]

Cement slurries were prepared in accordance with the procedures set forth in *Recommended Practice for Testing Well Cements*, API Recommended Practice 10B, issued by the American Petroleum Institute, using API Class G oil well cement and deionized water. At first, cement was dry blended with SSA-1 silica flour at a weight ratio of 65 : 35. This blend was mixed with DI water at a water-to-cement (w/c) ratio of 0.48 and a water-to-solids (w/s) ratio of 0.31 (solids = cement + silica) using a blade-type laboratory blender manufactured by Waring Products (Torrington, CT). In general, the graft copolymer solution was added to the mixing water while powdery HR-25 retarder was dry blended with cement.

Rheology of the slurries was determined on a FANN 35SA (Fann Instruments Company, Houston, TX) rotational viscometer, equipped with RI rotor sleeve, B1 bob and F1 torsion spring. HTHP thickening times of cement slurries were measured at 200°C under 400 bar pressure using a consistometer model 8240 (Ametek Chandler Engineering, Broken Arrow, OK). After mixing, the slurries were poured into the HTHP consistometer cell and the time to reach 70 Bc (Bearden unit of consistency) was designated as cement slurry thickening time. Stirred cement fluid loss was measured at 200 C using an HTHP stirred fluid loss cell (model 7120 from Chandler Engineering, Tulsa, OK) following a norm issued by the American Petroleum Institute (API).[23]

Adsorbed amounts of admixtures were determined from the cement filtrate collected in the respective fluid loss test applying the depletion method, i.e. it was assumed that the decrease in the polymer concentration before and after contact with cement solely resulted from interaction with cement. This assumption was confirmed through a solubility test of the admixtures in cement pore solution over 3 days. No precipitation was observed. A High TOC II apparatus (Elementar, Hanau, Germany) equipped with a CO_2 detector was used for quantification of the carbon content present in the filtrated solutions. Quantification of adsorbed amounts of the individual polymers was done by using the nitrogen content as a marker for the graft copolymer and the difference between the nitrogen content and the TOC value for quantification of the retarder.

Zeta potential measurement was performed at room temperature on an electro acoustic spectrometer (DT-1200 from Dispersion Technology, Bedford Hills, NY) using the cement slurry (w/c ratio of 0.48) mixed according to API RP 10B procedure, except that no homogenization was carried out in the atmospheric consistometer.

RESULTS AND DISCUSSION

Polymer Characterization

The free radical copolymerization process used here produces a relatively homogeneous graft copolymer which exhibits a polydispersity index of ~2.4 (see SEC diagram in Figure 1). From

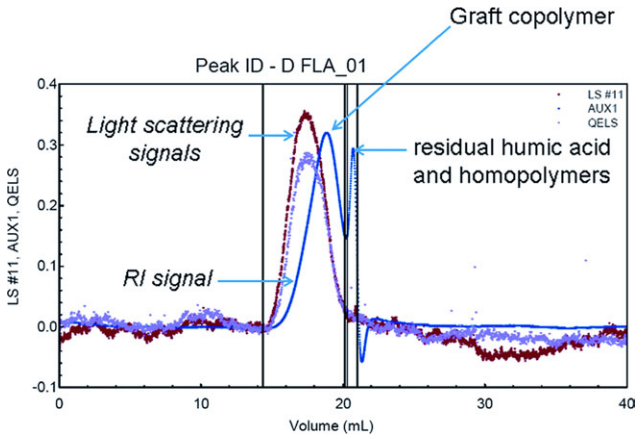

Figure 1. Size-exclusion chromatogram of the graft copolymer as obtained from synthesis. [Color figure can be viewed in the online issue, which is available at wileyonlinelibrary.com.]

SEC data, a turnover rate for the monomers of 83% was calculated, indicating an incomplete reaction.

Next, chemical composition of the graft copolymer (prepared from AMPS: NNDMA: AA at a molar ratio of 1 : 0.63 : 0.07) was determined. Elemental analysis of the purified copolymer confirmed successful incorporation of S and N containing monomers into the graft copolymer (see Table II). According to this data, 92.94 wt % of AMPS, 45.83 wt % of NNDMA, and 39.53 wt % of AA were incorporated. This suggests a molar ratio of 1 : 0.31 : 0.03 for the graft chain which differs from the feed molar ratio of 1 : 0.63 : 0.07. The difference is explained by the fact that AMPS and NNDMA exhibit alternating polar factors (AMPS: $Q,e = 0.39, 0.22$; NNDMA: $Q,e = 0.41, -0.26$) and thus tend to polymerize at a 2 : 1 molar ratio. Whereas acrylic acid, due to its similar Q and e values (0.82, 0.81) tends to preferentially undergo homopolymerization.[24] On the basis of this analysis, a chemical structure is proposed for the graft copolymer (Figure 2).

Molecular properties of the synthesized dispersing graft copolymer were determined by SEC (Table III). A comparison of its properties with those of a viscosifying graft copolymer composed of AMPS:NNDMA:AA at a molar ratio of 1 : 1.54 : 0.02 prepared according to a literature description[18] revealed that the dispersing graft copolymer which is characterized by a significantly lower NNDMA content exhibits much lower molecular weights (e.g. M_w: 323,200 vs. 577,400 Da). Consequently, the *Brookfield* viscosity of its aqueous solution is significantly lower than that of the viscosifying graft copolymer.

In cement pore solution, the specific anionic charge amount of the graft copolymer was found to be 3545 μeq/g which indicates a strongly anionic additive as a result of the large number of carboxylate, sulfonate, and phenolate functionalities. For comparison, the viscosifying graft copolymer prepared according to[18] exhibits a slightly higher anionic charge of 3826 μeq/g.

Fluid Loss Control Performance

To determine the effectiveness of the graft copolymer for fluid loss control, dynamic filtration properties of cement/silica flour slurries (slurry density 1.94 kg/L) containing increased dosages (0.4–1.8 % bwoc) of the graft copolymer at a fixed addition of 2.0% bwoc of HR®-25 retarder were measured at 200°C under stirring condition. The results are exhibited in Figure 3.

In general, API fluid loss values decrease exponentially with increasing graft copolymer dosage. The minimum concentration of FLA needed to achieve an API fluid loss value of below 100 mL/30 min lies at 1.0% bwoc. This value represents a relatively low dosage, considering the harsh temperature conditions. The data confirms high effectiveness of the dispersing graft copolymer in fluid loss control application under the very severe condition of 200°C.

Dispersing Property

Rheology of cement/silica slurries containing the dispersing and the viscosifying graft copolymer, and of a commercial lignite-based graft copolymer manufactured according to a patent description[25] (HALAD®-413 from Halliburton GmbH, Celle, Germany) were compared at 95°C. At this temperature, no addition of HR®-25 retarder was required, thus the values indicate the effect of individual polymers. The results are displayed in Table IV. The graft copolymer exhibits remarkable cement dispersion with increased dosages, while addition of the viscosifying graft copolymer results in excessively high viscosity values which are unacceptable for field use. Thus, the viscosifying polymer relies on combination with a dispersant to facilitate its field application. In addition, a comparison with the lignite-based commercial graft copolymer shows that the latter also possesses a viscosifying effect. This data confirms the novelty of the graft copolymer describe here.

One might speculate whether the different behaviors of the new dispersing and the previous viscosifying graft copolymer are solely owed to their different molecular weights which are presented in Table III. For clarification, a modified viscosifying graft copolymer was synthesized as comparative polymer following exactly the description used for preparation of the previous viscosifying polymer,[18] except that a higher initiator dosage and an increased temperature (60–70°C) were used to obtain a polymer with a M_w of ~331 kDa which was comparable to that of the dispersing graft copolymer (~323 kDa), but much lower

Table II. Elemental Analysis Data for Graft Copolymer, Humic Acid, and Graft Chain

Elements	Graft copolymer found (%)	Humic acid found (%)	Graft copolymer calculated[a] (%)	Graft chain calculated [b] (%)
C	38.0	38.7	39.9	40.5
H	6.3	3.7	5.4	5.8
O	36.0	41.5	28.7	25.3
N	6.0	1.0	6.2	7.4
S	7.9	0.8	8.5	10.5
Na	1.9	0.5	8.5	10.5
K	1.2	13.8	2.8	-

Note: O content calculated as difference to 100%.
[a]Calculation based on number of moles of monomers added. [b]Calculation based on weight proportion of monomers and humic acid added (80:20 wt %).

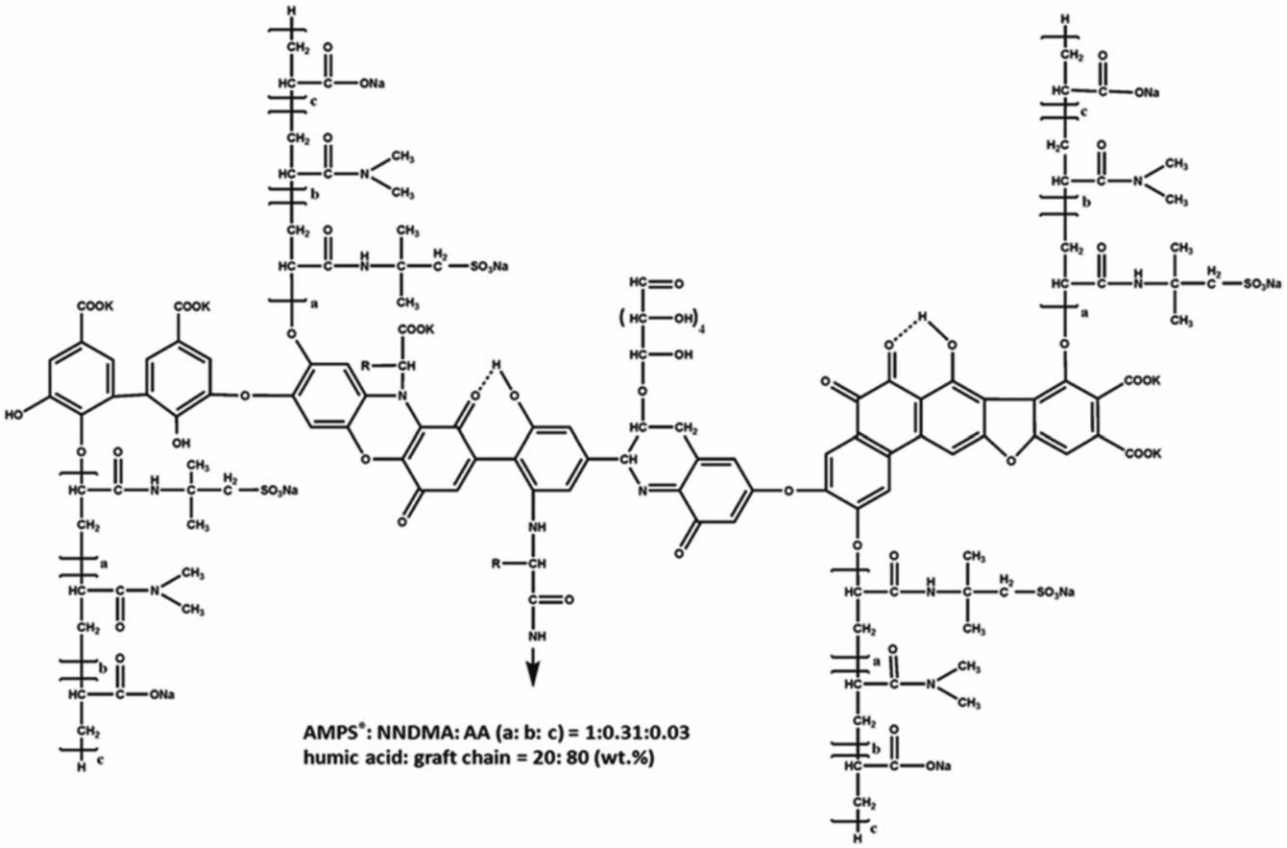

Figure 2. Proposed chemical structure of the synthesized graft copolymer.

than that of the previous viscosifying graft copolymer which exhibited an M_w of ~577 kDa (Table III).

Furthermore, rheological measurements of cement/silica slurries holding the modified viscosifying graft copolymer were performed, and the results were compared with those obtained from the dispersing and the high molecular weight viscosifying graft copolymer (Table IV). It was found that the modified graft copolymer, despite its molecular weight being comparable to that of the dispersing graft copolymer, still exhibited a very significant viscosifying effect. This result clearly signifies that the molar composition and the properties derived thereof present the key factor for the interaction of such graft copolymers with cement, and not the molecular weight.

We attribute the differences in the behaviors of the dispersing and the comparative graft copolymer to their distinctly different molecular architectures and rigidity of the side chains. First, it is well established that in free radical copolymerization, higher initiator concentration and higher temperature result in shorter chain lengths. Hence, the comparative polymer can be expected to contain a higher number of shorter lateral chains, thus leading to a graft copolymer with significantly higher grafting density than the dispersing copolymer which possesses fewer, but longer side chains. A graphical sketch of the different architectures of the two graft copolymers is presented in Figure 4.

Another aspect which can impact the influence of both polymers on the rheology of cement slurries is the different conformational flexibility of their side chains. It is well established that a high AMPS content produces copolymer chains with a high degree of hydrophilicity and anionic character over a wide range of pH because of the strongly ionizable sulfonate group.

Table III. Characteristic Properties of Different Graft Copolymers and of Humic Acid, as Obtained from SEC

Polymers	M_w (g/mol)	M_n (g/mol)	PDI (M_w/M_n)	*Brookfield*[a] viscosity (mPa·s)
Dispersing graft copolymer	323,200	133,400	2.4	14
Viscosifying graft copolymer[b]	577,400	266,300	2.2	40
Comparative graft copolymer[c]	331,300	130,200	2.5	24
Humic acid	68,940	21,180	3.3	12

[a]Measured in 2.0 wt % aqueous solution @ 100 rpm using spindle no. H 1. [b]Prepared according to literature.[18] [c]Prepared according to literature[18] but at increased initiator dosage and temperature.

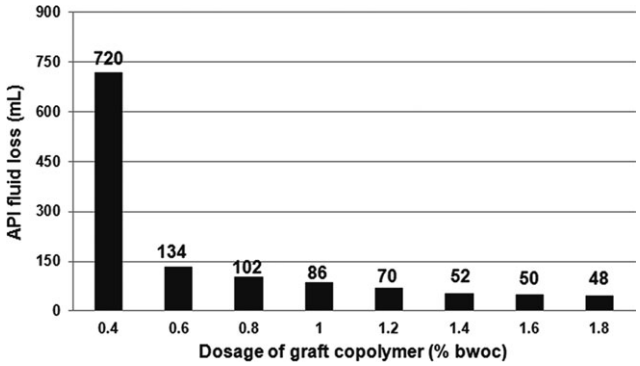

Figure 3. API fluid loss of Class G cement/silica (65 : 35% wt/wt) slurries containing increased dosages of graft copolymer and of 2.0% bwoc of HR-25 retarder, measured at 200°C and 70 bar differential pressure under stirred condition.

In addition, such lateral chains exhibit high conformational flexibility and coiling in aqueous solution. Whereas, high NNDMA contents produce relatively stiff polymer chains, as a result of dominant steric interaction between the amide CH_3 functionalities.[26] Hence, the comparative graft copolymer which possesses a very high amount of NNDMA in its side chains can be expected to present a rather rigid macromolecule, with stiff lateral chains attached to the main chain. Such conformation is favorable for generating a viscosifying effect in solution. In addition, it is known that polymer chains that are rich in NNDMA exhibit a strong water sorption and swelling behavior.[27] Contrary to this, the dispersing graft copolymer possesses highly flexible, dangling lateral chains because its main monomer component is AMPS and not NNDMA. As a result, this polymer cannot viscosify aqueous solutions and solid suspensions, as is also indicated by its significantly lower Brookfield viscosity (Table III). Instead, with its highly flexible lateral chains, it can easily anchor on multiple sites on the surface of hydrating cement and thus produce a dispersing effect.

All these observations allow to conclude that the specific molar composition of the lateral chains chosen here presents the very criteria for obtaining such dispersive graft copolymer.

Effect of Combined Retarder and Graft Copolymer on Rheology

In practical oil well cementing at bottom hole temperatures of 200°C, addition of sufficient amounts of HT-effective retarders is necessary to delay the set of cement sufficiently long to achieve a pumping time (cement thickening time as determined on the HT/HP consistometer) of at least 4 h. This was found to occur at a dosage of 2.0% bwoc of HR®-25 retarder.

In previous studies, it has been established that upon combination of one admixture with another, their functional properties can change drastically as a result of additive-additive interaction.[28,29] To investigate such potential pertubance, the rheology of cement/silica slurries containing both the graft copolymer and HR®-25 retarder was examined. The results are presented in Table V. The data signifies that the presence of the retarder causes cement slurry viscosity to increase with increased graft copolymer dosage. This trend is opposite to what was observed for the individual graft copolymer. It suggests that some interaction between both admixtures occurs, as was confirmed later. However, at dosages of 1.0–1.4% bwoc that present the dosage range of graft copolymer required to achieve a field practical cement fluid loss, rheology is still lower than for the viscosifying or the lignite-based copolymer. It is also sufficiently low to allow pumping of the slurry.

Working Mechanism of the Graft Copolymer

A series of experiments was devised to uncover the mechanism of this graft copolymer as fluid loss additive. First, the correlation between API fluid loss, filter cake permeability and dynamic filtrate viscosity as obtained at 200°C from slurries containing both the graft copolymer and HR®-25 retarder (2.0% bwoc) were established. The results are presented in Table VI. According to this data, the dynamic filtrate viscosity of the slurries is fairly independent of graft copolymer dosage. This means that filtrate viscosity has no significant impact on the fluid loss performance. Conversely, filter cake permeability decreases rapidly with dosage and a direct relationship with API fluid loss is apparent. For example, permeability decreases from 422 μD at 0.4 % graft copolymer dosage to ~10 μD when $\geq$1.4% of copolymer was added. At the same time, API fluid loss is reduced from 720 mL to ~50 mL/30 min (see Table VI). This signifies that the working mechanism of this graft copolymer relies on reduction of filter cake permeability.

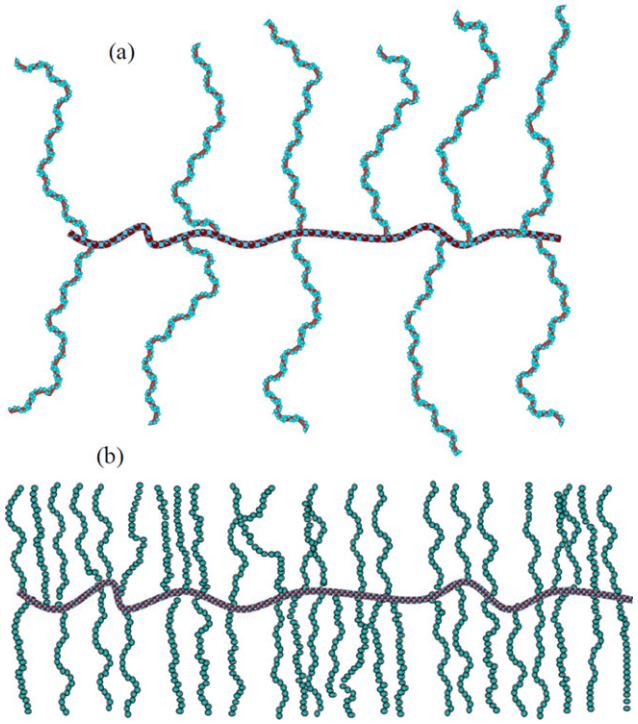

Figure 4. Illustration of molecular architectures of (a) dispersing graft copolymer possessing few and flexible side chains and (b) the comparative viscosifying copolymer possessing numerous and stiff lateral chains. [Color figure can be viewed in the online issue, which is available at wileyonlinelibrary.com.]

Table IV. Rheology (Shear Stress) of API Class G Cement/Silica Slurries (w/c = 0.48) Containing Addition of Various Graft Copolymers, Measured at 95°C and at Different Shear Rates

	Shear stress values (lbs/100 ft^2) @ 95°C at shear rate (rpm)					
Copolymer dosages (% bwoc)	300	200	100	6	3	600
Dispersing graft copolymer (M_w = 323,200 Da)						
0.0	200	173	124	59	58	248
0.2	191	165	121	46	42	237
0.4	138	82	49	23	21	206
0.6	89	58	28	7	5	165
0.8	80	53	24	5	4	158
1.0	74	51	20	2	1	135
Viscosifying graft copolymer (M_w = 577,400 Da)						
0.2	172	132	98	30	28	265
0.4	160	124	84	38	33	272
0.6	>300	252	165	52	48	>300
0.8	>300	>300	200	64	57	>300
1.0	Too thick to test					
Lignite-based graft copolymer (HALAD®-413)						
0.2	224	181	161	43	32	>300
0.4	234	178	134	22	14	>300
0.6	>300	239	163	49	35	>300
0.8	>300	204	149	44	34	>300
1.0	280	201	125	37	25	>300
Comparative viscosifying graft copolymer(M_w = 331,300 Da)						
0.2	183	135	122	74	65	228
0.4	196	138	105	50	48	>300
0.6	>300	220	149	49	47	>300
0.8	>300	>300	>300	82	69	>300
1.0	Too thick to test					

Table V. Rheology (Shear Stress) of API Class G Cement/Silica Slurries (w/c = 0.48) Containing the Dispersing Graft Copolymer and 2.0% bwoc of HR®-25 Retarder, Measured at 95°C and at Different Shear Rates

	Shear stress values (lbs/100 ft^2) @ 95°C at shear rate (rpm)					
Graft copolymer dosage (% bwoc)	300	200	100	6	3	600
0.0	131	109	67	19	17	>300
0.4	150	83	41	4	3	>300
0.6	180	129	54	6	4	>300
0.8	259	144	68	8	6	>300
1.0	244	140	64	8	5	>300
1.2	>300	179	96	11	7	>300
1.4	>300	258	150	17	12	>300
1.6	>300	215	135	14	9	>300
1.8	>300	248	143	14	8	>300
Viscosifying graft copolymer according to[18]						
0.2	Too thick to test					
0.4	Too thick to test					
Lignite-based graft copolymer according to Ref. 34						
1.0	>300	>300	250	29	16	>300

Table VI. API Fluid Loss, Dynamic Filtrate Viscosity, and Filtercake Permeability of API Class G Cement/Silica Slurries (w/c = 0.48) Containing Different Dosages of Dispersing Graft Copolymer and 2.0% bwoc of HR®-25 Retarder, Measured at 200°C

Graft copolymer dosage (% bwoc)	Dynamic filtrate viscosity (mPa s)	Filtercake permeability (μD)	API fluidloss (mL)
0.4	0.30	422	720[a]
0.6	0.31	52	134
0.8	0.31	33	102
1.0	0.32	24	86
1.2	0.32	16	70
1.4	0.33	9	50
1.6	0.36	9	52
1.8	0.37	8	48

[a]Dehydration of cement slurry in less than 30 min.

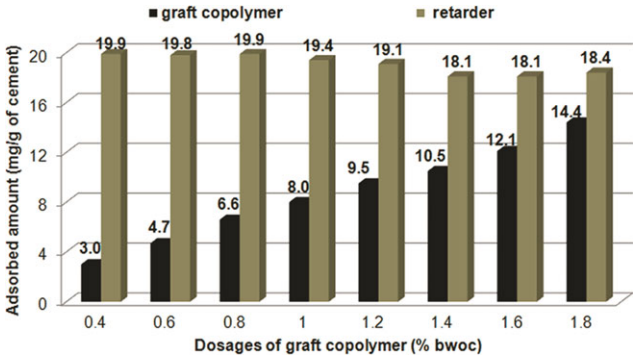

Figure 5. Adsorption of graft copolymer and of HR-25 retarder (dosage: 2.0% bwoc), measured from cement filtrates collected at 200°C. [Color figure can be viewed in the online issue, which is available at wileyonlinelibrary.com.]

To investigate the reason behind the reduced filter cake permeability, adsorption of the graft copolymer and of the retarder on the cement/silica solids was investigated.

Adsorption Behavior

Since the graft copolymer is an anionic polyelectrolyte with dispersing property, it was speculated that this graft copolymer may function by adsorption on cement, as has been demonstrated before for AMPS-based copolymers.[15] Thus, the adsorbed amounts of the graft copolymer and of the retarder in the combination were analyzed. The results are displayed in Figure 5. In general, the adsorbed amount of the graft copolymer increases almost linearly. No saturation plateau (complete surface coverage) is achieved at the dosages tested. This signifies strong electrostatic attraction of this highly anionic polymer on the positive surface of cement. Another observation from Figure 5 is that the adsorbed amount of the copolymer still increases even when API fluid loss remains stable at ~50 mL (see Figure 3). This effect can be explained as follows: API filtrates of < 50 mL/30 min are produced by dehydration of the first layers of the cement filter cake. Release of this "spurt loss" is always necessary to produce a tight filter cake. Thus, continued adsorption beyond the dosage of 1.4% does not contradict the working mechanism by adsorption.

Conversely, the working mechanism of the retarder was found to rely on precipitation from cement pore solution. Precipitation (plausibly of calcium tartrate) occurred almost instantaneously when HR-25 retarder was added to cement pore solution. At retarder dosages up to 1.2% bwoc, the amount precipitated was quite constant (19–20 mg/g cement) and independent of graft copolymer dosage. Above this concentration, the retained amount of retarder decreased by ~1 mg/g of cement. This effect is owed to partial co-precipitation of the retarder and the graft copolymer, as was confirmed by a decreased total organic nitrogen (TON) content of unadsorbed graft copolymer in presence and absence of the retarder (see Table VII). There, it was found that at graft copolymer dosages above 1.0 % bwoc, significant co-precipitation of the unadsorbed graft copolymer with the retarder occurs.

At 200°C, an adsorptive working mechanism of the graft copolymer appears to be almost impossible because ettringite, a cement hydrate formed from tricalcium aluminate and calcium sulfate present in cement, presents the main mineral for adsorption of anionic admixtures [9]. However, ettringite is known to be stable only at temperatures up to ~ 80°C to 115°C.[30–33] Thus, it is practically absent at 200°C as was evidenced by XRD patterns obtained from dry cement/silica specimens cured at 200°C (XRD diagrams not shown here). Apparently, the graft copolymer adsorbs onto other hydrate phases formed under the hydrothermal conditions existing at 200°C. The specifics of this mineralization process and its consequences for the anchoring possibilities of anionic polyelectrolytes will be the subject of another study.

Table VII. Co-precipitation of HR®-25 Retarder and of Graft Copolymer in Cement Pore Solution Derived From TON Measurement

Graft copolymer dosage (% bwoc)	TON[a] of graft copolymer only (mg/L)	TON of graft copolymer in presence of HR®-25 retarder (mg/L)	Reduction in TON[a] content (mg/L)	Reduction in graft copolymer concentration (%)
0.8	743	715	28	3.9
1.0	1054	960	94	9.8
1.2	1190	936	254	27.1

[a]TON means total organic nitrogen concentration in supernatant.

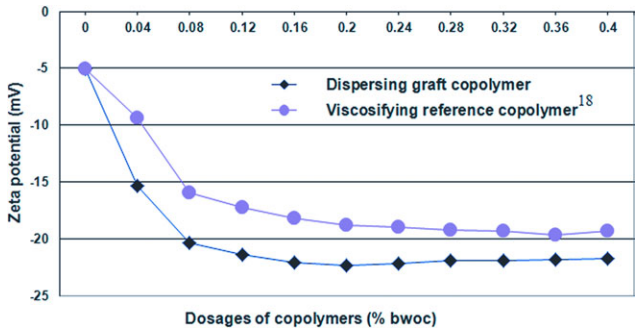

Figure 6. Zeta potentials of cement/silica slurries (w/c = 0.48) with added graft copolymers. [Color figure can be viewed in the online issue, which is available at wileyonlinelibrary.com.]

Electro Kinetic Properties

The zeta potentials of cement/silica slurries titrated with individual dispersing and viscosifying graft copolymer solutions are displayed in Figure 6. The neat cement slurry (no polymer present) exhibits a charge of −5 mV. Stepwise addition of the anionic graft copolymers further decreases the charge to more negative potentials until a point of saturation is achieved. The dispersing graft copolymer shows more pronounced negative zeta potentials than the viscosifying graft copolymer. Thus, it induces a higher electrostatic repulsion between the cement particles. This behavior explains its superior capability to disagglomerate cement particles. The curves confirm the adsorptive mechanism for the graft copolymer. Apparently, with increased polymer dosage, more and more of the FLA is loaded onto the surface of cement until a state of saturation (adsorption equilibrium) is reached. There, the zeta potential attains a constant value.

CONCLUSION

A humic acid-(AMPS-*co*-NNDMA-*co*-AA) graft copolymer that presents a dispersing cement fluid loss additive has been synthesized using aqueous free radical copolymerization. It reduces cement fluid loss effectively, even at temperatures as high as 200°C. A low NNDMA and high AA content provides dispersing properties to this polymer which are most advantageous when formulating cement slurries of high density as required on ultra-deep wells. Its working mechanism was found to rely on reduction of filtercake permeability which is achieved by adsorption of the graft copolymer on cement and possibly silica particles. Adsorption was confirmed by TOC and zeta potential measurements. Apparently, this adsorptive anchoring of the graft copolymer is hardly affected by temperature. Through this mechanism, the copolymer constricts the pores of the filtercake and thus reduces the loss of water from the cement slurry.

The study shows that cement additives such as the graft copolymer described here can be engineered to make them suitable for high density cement slurries required on ultra-high temperature high pressure wells possessing particularly low water to cement ratios. Here, the tailored composition of the lateral chains contained in the graft copolymer translates into a specific molecular architecture and conformational behavior which provides the desired dispersing effect. As the oil industry in their quest to explore the crude oil resources for the next decades is venturing into ever deeper reservoirs, more of such additives will be required and the performance envelope needs to be pushed to withstand temperatures even as high as 260°C.

ACKNOWLEDGMENTS

We thank Lubrizol Company for providing samples of the AMPS monomer, Dyckerhoff AG for the API Class G "black label" cement and Halliburton GmbH for the HR-25 retarder.

REFERENCES

1. Wu, Y. M.; Zhang, B. Q.; Wu, T.; Zhang, C.G. *J. Colloid. Polym. Sci.* **2001**, *279*, 836.
2. Wang, W.; Liu, Y.; Gu, Y. *J. Colloid. Polym. Sci.* **2003**, *281*, 1046.
3. Fink, J. K. Oil Field Chemicals; Gulf Professional Publishing: Burlington, MA, **2003**.
4. Nelson, E. B; Guillot, D. Well Cementing; Schlumberger Dowell: Sugar Land, TX, **2006**.
5. Smith, D. K., Cementing; Society of Petroleum Engineers; SPE Monograph: New York, **1990**.
6. Garnier, A.; Frauoulet, B.; Saint-Marc, J. Paper SPE 18754, SPE Offshore Tech. Conference, Texas, **2007**.
7. Yoshioka, K.; Tazawa, E.-I.; Kawai, K.; Enohata, T. *Cem. Concr. Res.* **2002**, *32*, 1507.
8. Hodne, H.; Saasen, A. *Cem. Concr. Res.* **2000**, *30*, 1767.
9. Plank, J.; Hirsch, C. *Cem. Concr. Res.* **2007**, *37*, 537.
10. Persinski, L.; Cook, L. J.; Adams, S. L. U.S. Patent No. 4,015,991, **1977**.
11. Engelhardt, F.; Riegel, U.; Hille, M.; Wittkus, H. U.S. Patent No. 4,309,523, **1982**.
12. Rao, S. P.; Burkhalter, J. F. U.S. Patent No. 4,555 269, **1985**.
13. Stephens, M. U.S. Patent No. 5,294,651, **1994**.
14. Udarbe, R. G.; Hancock-Grossi, K. U.S. Patent No. 6,136,935, **2000**.
15. Plank, J.; Brandl, A.; Zhai, Y.; Franke, A. *J. Appl. Polym. Sci.* **2006**, *102*, 4341.
16. Vazquez, B.; San Roman, J.; Peniche, C.; Cohen, M. E. *Macromolecules* **1997**, *30*, 8440.
17. Gallardo, A.; Lemus, A. R.; San Roman, J.; Cifuentes, A.; Diez-Masa, J. C. *Macromolecules* **1999**, *32*, 610.
18. Salami, O. T.; Plank, J. *J. Appl. Polym. Sci.* DOI: 10.1002/app.36725.
19. American Petroleum Institute. API Specification 10A, 24th ed.; American Petroleum Institute: Washington, **2010**.
20. Franke, B. *Z. Anorg. Allgem. Chem.* **1941**, *247*, 180.
21. Huglin, M. B.; In Polymer Handbook, 3rd ed.; Brandrup, J., Immergut, E. H., Eds.; Wiley: New York, **1989**, 409 p.
22. Plank, J.; Sachsenhauser, B. *Cem. Concr. Res.* **2009**, *39*, 1.

23. American Petroleum Institute. API Recommended Practice 10B-2, 1st ed.; American Petroleum Institute: Washington, **2005**.
24. Odian, G. Principles of Polym.erization. Wiley: New York, **1991**.
25. Huddleston, D. A.; Williamson, C. D. U.S. Patent No. 4,938,803, **1990**.
26. Reber, A. C.; Khanna, S. N.; Ottenbrite, R. *Polym. Adv. Technol.* **2007**, *18*, 978.
27. Caykara, T.; Akcakaya, I. *J. Appl. Polym. Sci.* **2007**, *104*, 2140.
28. Plank, J.; Dugonjić-Bilić, F.; Recalde Lummer, N. *J. Appl. Polym. Sci.* **2010**, *116*, 2913.
29. Plank, J.; Brandl, A.; Lummer, N. *J. Appl. Polym. Sci.* **2007**, *106*, 3889.
30. Damidot, D.; Glasser, F. P. *Cem. Concr. Res.* **1993**, *23*, 221.
31. Hall, C.; Barnes, P.; Billimore, A. D.; Jupe, A. C.; Turrillas, X. *J. Chem. Soc. Faraday. Trans.* **1996**, *92*, 2125.
32. Shimada, Y.; Young, J. F. *Adv. Cem. Res.* **2001**, *13*, 77.
33. Constantiner, D.; Farrington, S. A. *Cem. Concr. Aggreg.* **1999**, *21*, 39.
34. Lewis, S.; Chatterji, J.; King, B. J.; Brenneis, D. C. U.S. Patent No. 7,842,652, **2010**.

3.3 Influence of Electrolytes on the Performance of a Graft Copolymer Used as Fluid Loss Additive in Oil Well Cement

Synopsis

This work relates to the effect of salts (NaCl and sea water) on the performance of humic acid and lignite based graft copolymers. It focuses on the influence of individual ions (Ca^{2+}, K^{+}, Na^{+}, Mg^{2+}, OH^{-}, SO_4^{2-}, Cl^{-}, CO_3^{2-}) on admixtures.

It was found that in cementing systems mixed from sea water, the electrolytes present in sea water affect the fluid loss performance of the graft polymer strongly whereas 20 % NaCl dissolved in the mixing water produce comparable fluid loss results than in fresh water.

The results suggest that relatively minor concentrations of specific ions such as e.g. Mg^{2+} can severely impact the effectiveness of oil well cement additives.

The mechanism behind poor performance in the presence of sea water and mitigating measures to counteract their effect were investigated. Here, the negative effect of Mg^{2+} is owed to coprecipitation and entrapment of the graft copolymer into the precipitate of $Mg(OH)_2$ which is formed in the alkaline pore solution of cement.

The study recommends that specific ion sensitivities of oil well cement additives should be identified when designing cement slurries.

The results were submitted on Jan 3, **2014** to

Journal of Petroleum Science and Engineering,

O.T. Salami and J. Plank

*Manuscript
Click here to download Manuscript: Journal of Petroleum Engineering and Science-Salami.doc Click here to view linked References

Influence of Electrolytes on the Performance of a Graft Copolymer Used as Fluid Loss Additive in Oil Well Cement

*Oyewole Taye Salami, Johann Plank**

Prof. Dr. Johann Plank, Chair for Construction Chemicals, Institute for Inorganic Chemistry,

Technische Universität München, Garching, Germany

Address:

Technische Universität München

Lichtenbergstr. 4

85747 Garching

Germany

Phone: ++49 89 289 13150

Fax: ++49 89 289 13152

E-mail address: johann.plank@bauchemie.ch.tum.de

Key words: oil well cement; electrolytes; sea water; graft copolymer; fluid loss additive

Abstract

The influence of electrolytes contained in sea water and 20 wt.% NaCl solution on a high temperature fluid loss additive (FLA) for oil well cement was investigated. The FLA was comprised of a humic acid-{*sodium 2-acrylamido-2-methylpropane sulfonate-co-N,N-dimethyl acrylamide-co-acrylic acid*} graft copolymer which was tested at 27 °C and 150 °C. Its performance was compared with that of an industrial lignite-based copolymer. It was found that seawater, in spite of its relatively low electrolyte content (~3.6 wt.%), affects fluid loss performance of the graft copolymer strongly whereas 20 % NaCl dissolved in the mixing water exhibit a minor effect only. Mg^{2+} present in sea water was identified as cause for poor admixture performance. Experiments demonstrate that in the highly alkaline environment of cement, Mg^{2+} precipitates as voluminous $Mg(OH)_2$ which entraps significant amounts of the graft copolymer. Delayed addition of the graft copolymer to the cement slurry presents a mitigation strategy to overcome the negative effect of Mg^{2+} present in sea water.

1. Introduction

The global oil and gas industry is challenged to increase production in order to meet the rising world energy demand. One key area being explored now are the reservoirs below massive salt formations. Among the most promising candidates are the deepwater areas in the Gulf of Mexico, the North Sea, offshore Brazil, in the North Caspian Sea, and off North and West Africa (Hunter et al., 2010; Sanz and Dasari, 2010; Martins et al., 2011).

Typically, such salt formations are composed of ~ 96 wt.% NaCl (halite) while the remaining ~ 4 wt.% include sylvite (KCl) and various magnesium and/or calcium salts (Heerema, 2009). For example, the Zechstein formation which runs across Europe from UK, Netherlands, Germany, Poland to Ukraine contains a significant amount of magnesium salts, especially bischofite, $MgCl_2 \cdot 6H_2O$ (Geluk et al., 2007). Such salt formations can vary from salt domes to massive beds with thicknesses up to 1,500 m (Barker and Feland, 1992).

Wells constructed in these areas encounter reservoir fluids containing high electrolyte contents from NaCl, $CaCl_2$, $MgCl_2$ and $MgSO_4$, with total salt concentrations as high as 40 wt.%. Besides, bottom hole temperatures can reach 170 °C.

The challenge for cementing such wells is that the chemical admixtures commonly applied to control the properties of the cement slurry have to perform well in the presence of such high amounts of electrolytes. However, salt tolerant additives are rare because most admixtures were designed for fresh water slurries, and often perform poorly in saline environment (Whisonant, 1988). For example, in offshore cementing sea water is commonly used as mixing water for cement. It is however well established that sea water perturbs the effectiveness of most cement admixtures, although its salt content is only slightly higher than that in fresh water. Surprisingly,

the reason for the adverse effects of various salts on these admixtures is still mostly unknown. It is thus imperative to investigate and understand the interactions of oil well cement additives with various electrolytes.

Here, as a representative example for oil well cement additives, a humic acid {sodium 2-acrylamido-2-methylpropane sulfonate-co-N,N-dimethyl acrylamide-co-acrylic acid} graft copolymer which presents a dispersing fluid loss additive was tested at 27 °C and 150 °C respectively in cement slurries prepared from fresh water, sea water and 20 wt.% NaCl. Moreover, the impact of these electrolytes in general and of specific ions in particular on the functionality and interaction of this graft copolymer with cement was examined. Based on these findings, a simple method to mitigate the negative effect of specific salts is proposed.

2. Experimental

2.1 Materials

2.1.1 Oil well cement and silica flour

An API Class G oil well cement ("*black label*" from Dyckerhoff AG, Wiesbaden/Germany) corresponding to American Petroleum Institute (API) Specification 10A was used (API, 2010). Its clinker composition is given in **Table 1.** A commercial sample of silica flour (SSA-1 from Halliburton GmbH, Celle/Germany) was included into the cementing system to prevent high temperature induced strength retrogression. Average particle size (d_{50} value) of SSA-1 was 32.7 µm.

2.1.2 Chemicals

2-acrylamido-2-methylpropane sulfonic acid (AMPS®) monomer was obtained from Lubrizol, Rouen, France; N,N-dimethyl acrylamide (NNDMA, Sigma Aldrich, Munich, Germany), acrylic acid (AA), magnesium chloride hexahydrate ($MgCl_2 \cdot 6H_2O$), sodium chloride (NaCl), calcium chloride dihydrate ($CaCl_2 \cdot 2H_2O$), sodium hydrogen carbonate ($NaHCO_3$), potassium bromide (all from Merck KgaA, Darmstadt, Germany) and sodium sulphate (Na_2SO_4, Applichem Chemical Synthesis Services, Darmstadt, Germany) were used as per obtained.

2.1.3 Graft copolymer

The humic acid graft copolymer was prepared by grafting 2-acrylamido-2-methylpropane sulfonic acid (AMPS®), N,N-dimethyl acrylamide (NNDMA) and acrylic acid (AA) onto a humic acid backbone via aqueous free radical copolymerization using sodium persulfate as initiator following a literature description (Salami and Plank, 2013). This dispersing graft copolymer is composed of 20 wt.% humic acid backbone and 80 wt.% graft chains. The molar ratio of the monomers in the graft chain was AMPS®/NNDMA/AA = 1:0.31:0.03. The resulting graft copolymer solution constitutes a dark brown liquid with a solid content of 19 wt.% and a pH value of 7. The molecular weights of the graft copolymer measured via SEC were 309,900 g/mol (M_w) and 161,400 g/mol (M_n) with a corresponding polydispersity index (PDI) of 1.9. The proposed chemical structure of the graft copolymer is shown in **Figure 1.**

2.1.4 *Industrial graft copolymer*

For comparison, a commercial lignite – based graft copolymer marketed by Halliburton Co., Houston/TX was studied. Its synthesis is described in a patent (Huddleston and Williamson, 1991). According to this literature, the graft copolymer contains ~ 20 wt.% of a lignite backbone and ~ 80 wt.% of graft chains composed of AMPS® and dimethyl acrylamide (NNDMA). The molecular weights of the lignite graft copolymer obtained from SEC are 394,000 g/mol (M_w) and 265,000 g/mol (M_n) respectively, with a corresponding polydispersity index (PDI) of 1.5.

2.1.5 *Cement Retarder*

As cement retarder, a combination of a self-synthesized AMPS®-itaconic acid copolymer and of a commercial product, HR®-25 which is composed of natural 2R, 3R- tartaric acid, was used. The AMPS®-itaconic acid copolymer was prepared at a molar ratio of 1: 0.4 via free radical copolymerization according to literature (Rodrigues, 1999) yielding a viscous, yellowish aqueous solution with a solid content of 39 wt.% and a pH value of 4. The molecular weights of the copolymer measured via SEC were: M_w = 175,600 g/mol; M_n = 108,600 g/mol and PDI (M_w/M_n) = 1.6.

2.1.6 *Synthetic seawater*

Sea water prepared according to the American Standard for Testing Materials (ASTM D1141) was used. The composition of this synthetic sea water is given in **Table 2**. The resulting ion concentrations (mg/L) were: Na^+ 10,900; Mg^{2+} 1,300; Ca^{2+} 418; K^+ 403; Cl^- 19,800; SO_4^{2-} 2,800; HCO_3^- 152; Br^- 67.

2.1.7 Cement slurry preparation and testing

Cement slurries were prepared in accordance with the procedures set forth in *Recommended Practice for Testing Well Cements*, API Recommended Practice 10B, issued by the American Petroleum Institute, using API Class G oil well cement (API, 2005a). Fresh and salt water cement slurries were prepared using fresh water, sea water and 20 % by weight of water (bwow) NaCl as mixing water. At first, cement was dry blended with SSA-1 silica flour at a weight ratio of 65:35. This blend was mixed with DI water, sea water or 20 % NaCl solution at a water-to-cement (w/c) ratio of 0.48 and a water-to-solids (w/s) ratio of 0.31 (solids = cement + silica) using a blade-type laboratory blender manufactured by Waring Products Inc. (Torrington, CT/USA). Within 15 s, the cement/silica blend was added to the mixing water placed in the cup of the Waring blender and mixed for 35 s at 12,000 rpm. All dosages of admixtures (FLA, retarder) are stated in % by weight of cement (bwoc). The aqueous solutions of the graft copolymer and of the AMPS®-*co*-itaconic acid retarder were added to the mixing water while powdery HR®-25 retarder was dry blended with cement (unless stated otherwise which was the case in the delayed addition experiment). To ensure sufficient homogenization after mixing, all slurries were stirred for 20 min at 94 °C in an atmospheric consistometer (model 1250 from Chandler Engineering, Tulsa, OK/USA).

The rheology of the homogenized cement slurries was measured at 94 °C on a FANN 35SA (Fann Instruments Company, Houston, Texas, USA) rotational viscometer, equipped with RI rotor sleeve, B1 bob (radius: 17.3 mm, height: 38.0 mm) and F1 torsion spring. The values of the viscometer reading were recorded for 6 speeds of the rotor (3, 6, 100, 200, 300 and 600 rpm).

Static cement fluid loss was measured at 27 °C and 150 °C respectively using a 500 mL high temperature, high pressure (HTHP) stainless steel filter press cell (model 7120 from Chandler

Engineering, Tulsa/OK, USA) following a norm issued by the American Petroleum Institute (API, 2005b).

Cement pore solutions (CPS) of the slurries were collected via vacuum filtration from the API Class G cement/silica blend (65:35 wt. %; w/c ratio 0.48) suspended in various mixing fluids.

2.1.8 Cation and anion analysis

The concentration of sulfate ions present in the cement pore solutions were determined using ion chromatography (ICS-2000 apparatus, Dionex, Idstein/Germany) while the concentrations of cations (K, Ca, Mg and Na) were obtained from an atomic absorption spectroscope Model 1100B (Perkin Elmer, Überlingen, Germany). Prior to measurement, the filtrates containing the ions were diluted and acidified with 0.1 M HCl in order to prevent the formation of $CaCO_3$ precipitate.

2.1.9 Adsorption of polymers on cement/silica

Adsorbed amounts of the graft copolymer on cement & silica particles were determined from the filtrates collected in the respective fluid loss tests (at 150 °C) applying the depletion method, i.e. it was assumed that the decrease in the polymer concentration before and after contact with cement solely resulted from adsorption on cement/silica mineral surfaces. This assumption was confirmed through a solubility test whereby 10.42 g/L of graft copolymer (equivalent to a dosage of 0.5 % bwoc) were dissolved in CPS. After storage over three days, no precipitate had occurred. A High TOC II apparatus (Elementar, Hanau/Germany, equipped with a CO_2 and N_2

detector was used for quantification of the carbon and nitrogen contents present in the filtrated solutions containing the admixtures. The concentration of the graft copolymer was quantified via total nitrogen (TN) analysis while the concentration of AMPS®-co-itaconic acid present in the filtrates was obtained by subtracting the carbon content of the graft copolymer from the total carbon content present in the filtrate. The adsorbed amounts were calculated from the difference in the equilibrium concentration of the polymer present in the liquid phase before and after contact with cement/silica. Before conducting the TOC and TN analysis, the alkaline cement/silica slurry filtrates containing the unadsorbed polymers were diluted with 0.1 M HCl at a ratio of 1:20 (v. /v.) and the final pH of the solution was 1.0.

3. Results and Discussion

3.1 Performance of graft copolymer at room temperature

Firstly, performance of the copolymer in cement slurries prepared from fresh water, sea water and 20 % NaCl water at room temperature was tested. The results are displayed in **Figure 2**. The graft copolymer appears to be equally effective in all three cementing systems, with a slightly lower performance in the sea water system. At a dosage of only 0.2 % bwoc, API fluid loss values of $\leq$ 50 mL/30 min are achieved. Such values are considered as excellent in field applications.

3.2 Effect of electrolytes on performance of graft copolymer at high temperature

To determine the influence of the salts on the performance of the graft copolymer at elevated temperature, static fluid loss values of the three cementing systems prepared from fresh water, sea water and 20 % NaCl were measured at 150 °C. All slurries were prepared from the cement/silica blend and contained the combination of AMPS®-co-itaconic acid and HR®-25 retarders. The result is presented in **Figure 3**. Addition of the graft copolymer to the fresh water and 20 % NaCl slurries at varied dosages and fixed concentrations of 0.5 % bwoc each of AMPS®-co-itaconic acid and HR®-25 retarders results in excellent API fluid loss values of less than 50 mL while in the sea water system, an exceptionally high dosage (1.2 % bwoc) of the graft copolymer is required to achieve ~ 50 mL in API fluid loss. This result is surprising, because the electrolyte content contained in sea water is significantly less than that in the NaCl solution (3.6 vs. 20 wt.%). Apparently, sea water holds a species of electrolyte which is especially harmful to the performance of the graft copolymer, while even large amounts of NaCl have practically no negative impact, compared to the fresh water system.

To probe whether the sensitivity of the graft copolymer towards sea water was an exception or represented a more general behavior of cement fluid loss polymers, an industrial lignite – based graft copolymer which is commonly used in the field was incorporated into the study. The results are shown in **Figure 4**. Apparently, this graft copolymer is even more negatively affected by sea water than the humic acid – based graft copolymer. This finding suggests that the adverse effect of sea water is not limited to one specific additive, but is of more general nature.

3.3 Mechanistic study

Next, a series of experiments was devised to uncover the perturbation resulting from sea water. For this purpose, rheology and fluid loss values of cement slurries containing 0.2 % bwoc of the graft copolymer and with 0.5 % bwoc of the retarders. The slurries were prepared from sea water or sea water from which individual electrolytes have been removed. The results are presented in **Table 3.** There it is shown that both API fluid loss values and rheology of the slurries do not change much when individual NaCl, $CaCl_2$ or Na_2SO_4 are removed from the sea water. However, a huge improvement in both API fluid loss and rheology is observed when $MgCl_2$ was omitted from the sea water formulation exhibited in **Table 2**. In the absence of $MgCl_2$ in the sea water, the API fluid loss value was excellent with only 32 mL whereas in fully formulated sea water, a value of 1,423 ml/30 min was obtained. The negative effect of $MgCl_2$ was further ascertained by addition of $MgCl_2$ to the 20 wt.% NaCl brine which led to a significant increase in fluid loss from 44 mL (for 20 % NaCl) to 1,120 mL, thus confirming the deleterious effect of the Mg^{2+} cation. Furthermore, the rheology of the cement slurry containing additional $MgCl_2$ in the 20 wt.% NaCl solution exhibited a sharp increase in viscosity which was even higher than what was observed for pristine sea water (see **Table 3**).

To elucidate the mechanism for the negative impact of $MgCl_2$ on the performance of the graft copolymer, its adsorption on the cement/silica was determined.

3.4 Adsorption behaviour

In previous work it has been established that in fresh water, the fluid loss control effect of the graft copolymer is based on its adsorption onto cement/silica and subsequent constriction of the

filter cake pores (Salami and Plank 2013). Through this mechanism less water is released from the filter cake. Here, the adsorbed amounts of the graft copolymer in fresh water, 20 wt.% NaCl and sea water cement/silica slurries were compared. The results are displayed in **Figure 5.** In fresh water and NaCl loaded cement slurries, the adsorbed amounts of the graft copolymer increase nearly linear with dosage. Whereas in the sea water system, the adsorbed amounts remain relatively low. The results signify that electrolytes generally decrease the adsorbed amount of the graft copolymer. This effect is minor for the 20 % NaCl system and more severe for the sea water slurry. Furthermore, it should result in decreased fluid loss performance. However, it cannot fully explain the extremely negative effect of sea water on fluid loss, as shown in **Figure 3**. In sea water, the adsorbed amounts of the graft copolymer are too high to explain the poor filtration control observed in **Figure 3**. Hence, it was necessary to identify another reason for the effect of sea water. As a next, the concentration of ions present in the pore solutions of the individual fluid systems was determined, with a focus on the Mg^{2+} concentration.

3.5 Pore solution chemistry

Analysis of the pore solutions collected from the three cementing systems was performed via AAS and ion chromatography. The result is presented in **Table 4**. There, the most significant observation is the huge difference in the Mg^{2+} concentration of the sea water system. Based on the $MgCl_2$ content of the synthetic sea water, an Mg^{2+} concentration of ~ 1,300 mg/L was expected. Whereas in the pore solution collected from the sea water cementing system, only 28 mg Mg^{2+}/L were found, which represents a reduction of 98 % versus the initial concentration. Obviously, Mg^{2+} ions are depleted from the ionic soup, and this appears to be the reason behind

the poor performance of the graft copolymer in the presence of Mg^{2+}. Hence, as a next step the interaction between Mg^{2+} and the graft copolymer was studied.

3.6 Interaction of $Mg(OH)_2$ with graft copolymer

To access the behaviour of Mg^{2+} towards the graft copolymer under the pH conditions of oil well cement (pH ~12.5), a portion of $MgCl_2$ equivalent to that present in sea water (116 mmol) was added to DI water under stirring. This produced a clear solution of pH = 6. Subsequently, through addition of 50 wt.% aqueous sodium hydroxide, the pH was increased to 12.5 which is comparable to that in a cement slurry. There, instant precipitation of a white solid occurred which was identify via XRD as $Mg(OH)_2$ (brucite). Next, an aqueous solution of the graft copolymer holding the same amount of $MgCl_2$ as before was adjusted to pH =12.5. Again, precipitation of a brown solid was observed (see **Figure 6**). Such precipitate did not occur when a solution of the graft copolymer only (no $MgCl_2$ present) was adjusted to alkaline pH. A similar precipitation test was performed where $MgCl_2$ was replaced by the amount of $CaCl_2$ (14 mmol) present in the sea water. There, no precipitate was found, both in the absence and in the presence of the graft copolymer. According to literature, the solubility of calcium hydroxide at 25 °C (1.26 g/L) is considerably higher than that of magnesium hydroxide which is 9.0×10^{-3} g/L only (Holleman and Wiberg, 1995). Apparently, in the alkaline cement slurry only magnesium hydroxide is precipitated while calcium hydroxide remains in solution. Consequently, this experiment allows to conclude that precipitating $Mg(OH)_2$ might remove some of the graft copolymer from the cement slurry via coprecipitation.

Next, the concentration of the graft copolymer before and after coprecipitation with $Mg(OH)_2$ was quantified by measuring the total organic carbon content of the supernatant. There, a significant reduction of the polymer concentration by 45 % was found (from 3.03 to 1.67 g/L). Elemental analysis of the precipitate revealed that it indeed presented a co-precipitate of the graft copolymer with magnesium hydroxide. The X-ray diffraction spectrum of the precipitate (not shown here) also identified $Mg(OH)_2$ in the coprecipitate. Furthermore, this precipitation test was repeated, except that this time the copolymer was added in a delayed mode after $Mg(OH)_2$ had precipitated at high pH. Here, despite thorough mixing of the polymer with the precipitate, no reduction of the polymer concentration was found. This experiment suggests that the voluminous precipitate of $Mg(OH)_2$ presumably entraps a significant amount of graft copolymer because of its sheer size (hydrodynamic radius of graft copolymer, R_h = 22 nm, according to SEC measurement). While electrostatic attraction between colloidal $Mg(OH)_2$ and the anionic polyelectrolyte does not seem to play a role.

To confirm whether the precipitation of magnesium hydroxide occurring *in-situ* during the mixing process of the cement slurry is indeed solely responsible for the loss of performance of the graft copolymer, all additives were added *after* the cement/silica slurry has been mixed in the blender (delayed addition mode). A comparison of the results for early addition (graft copolymer present in the mixing water) versus delayed addition (copolymer added to the cement slurry) in sea water is shown in **Table 5**. At delayed addition, the performance of the graft copolymer is comparable to that in fresh water and in 20 % NaCl. The API fluid loss obtained at a dosage of 0.2 % bwoc at delayed addition is 50 mL whereas at early addition, practically no fluid loss control is achieved (API fluid loss is 1,423 mL). This experiment confirms that the performance of the graft copolymer is not perturbed when co-precipitation with $Mg(OH)_2$ is avoided.

Another observation from **Table 5** is that at delayed addition, rheology of the cement slurry is considerably lower. This indicates that a substantial portion of the dispersing graft copolymer is removed by co-precipitation, and thus cannot exercise its full potential for dispersion.

3.7 Effect of temperature on Mg^{2+} tolerance of graft copolymer

A comparison of the results for fluid loss performance presented in **Figure 2** (27 °C) and **Figure 3** (150 °C) suggests that the graft copolymer is negatively affected by sea water (or Mg^{2+}, to be more specific) only at elevated temperature. This is however contradicted by the coprecipitation experiments performed at room temperature (**Figure 6**) where significant removal of the graft copolymer became apparent. This observation stimulated another experiment where fluid loss performance of the graft copolymer in the three cementing systems was determined at 0.1 % dosage only (as compared to ≥ 0.2 % in **Figure 2**). There, it became clear that also at room temperature, sea water produces much higher fluid loss values, and that NaCl reduces fluid loss performance slightly as well (**Figure 7**). These findings are in perfect agreement with the adsorbed amounts exhibited in **Figure 5** and suggest that Mg^{2+} generally impedes the performance of this fluid loss polymer, independent of temperature.

4. Conclusion

A humic acid AMPS®-NNDMA-AA graft copolymer was tested at 150 °C in fresh water, sea water and 20 wt.% salt water cement slurries. It was found that sea water significantly perturbs the effectiveness of the graft copolymer. There, about a six-fold dosage is required to achieve

fluid loss values comparable to those in fresh water and 20 % NaCl solution. According to our experiments, this negative effect can be attributed to entrapment of the graft copolymer into the voluminous $Mg(OH)_2$ precipitate which is formed from Mg^{2+} present in sea water under the highly alkaline pH conditions of cement. Whereas, other electrolytes present in sea water such as e.g. SO_4^{2-}, Cl^-, CO_3^{2-}, HCO_3^-, K^+, Na^+ or Ca^{2+} do not perturb effectiveness of the copolymer. The results suggest that the humic acid-AMPS®-NNDMA-AA graft copolymer presents an economical admixture for cementing systems based on fresh water or NaCl brines. However, caution is required when offshore wells are cemented using sea water as mixing water. There, delayed addition of the admixture to the cement slurry presents a viable remedy. Alternatively, different fluid loss polymers possessing high Mg^{2+} tolerance should be applied. The results signify that relatively minor concentrations of specific ions (here: ~ 1,300 mg/L of Mg^{2+} can severely impact the effectiveness of oil well cement additives. To uncover such specific ion sensitivities it is thus recommended to first test the behavior of admixtures against individual ion rather than using fully formulated salt brines which is common practice at present.

Acknowledgement

The authors wish to thank Lubrizol Company for providing the AMPS® monomer, Dyckerhoff AG for the API Class G "black label" cement and Halliburton Celle GmbH for HR®-25 retarder and silica flour SSA-1.

References

API, 2005a. API Recommended Practice 10B, 1st ed.; American Petroleum Institute: Washington.

API, 2005b. API Recommended Practice 10B2, 1st ed.; American Petroleum Institute: Washington.

API, 2010. API Specification 10A, 24th ed.; American Petroleum Institute: Washington

Barker, J.W. and Feland, K.W., 1992. Drilling long salt sections along the US Gulf Coast, SPE paper 24605, Annual Technical Conference and Exhibition, Washington DC.

Geluk, M.C., Paar, W.A. and Fokker, P.A., 2007. Geology of the Netherlands, <www.knaw.nl/publicaties/ pdf/20011075-17.pdf>, accessed July 13, 2013, pp 283-294

Heerema, S., 2009. A magmatic model for the origin of large salt formation, J. Creation, 23: 116-118.

Holleman, A.F., and Wiberg, N., 1995. Lehrbuch der Anorganischen Chemie, 101. Auflage, Walter de Gruyter, Berlin

Huddleston, D.A., and Williamson, C.D, 1991. Vinyl grafted lignite fluid loss additives, US patent 5 028 271.

Hunter, B., Tahmourpour, F. and Faul, F., 2010. Cementing Casing Strings Across Salt Zones: An Overview of Global Best Practices. SPE paper 122079, SPE Drilling and Completion, 25: 426 - 437.

Martins, A.L., Aranha, P.E., Folsta, M.G., Simao, C.A., Batalha, N.A. and Pinto, G.H.V.P., 2012. Integrated Cementing hydraulics Design for Massive Salt Zones, SPE paper 151031, Latin American and Caribbean Petroleum Engineering Conference, Mexico City, Mexico.

Rodrigues, A.K., 1999. Set retarding cement additive, EP 0 633 390.

Salami, O.T and Plank, J., 2013. Preparation and Properties of a Dispersing Fluid Loss Additive based on Humic Acid Graft Copolymer Suitable for Cementing high Temperature (200 °C) Oil Wells, J. Appl. Polym. Sci., 129, 2544-2553.

Sanz, P.F. and Dasari, G.R., (2010). Controls On In-situ Stresses Around Salt Bodies, SPE paper 10169, 44th U.S. Rock Mechanics Symposium and 5th U.S.-Canada Rock Mechanics Symposium, Salt Lake City, Utah.

Whisonant, B.J., Rae, P.J. and Ramsey, L.K., 1988. New Materials Improve the Cementation of Salt Formations in the Williston Basin, SPE paper 17512, Casper, Wyoming.

Table 1

Phase composition (XRD, *Rietveld*), specific density, specific surface area (*Blaine*) and d_{50} value of API class G oil well cement sample

C_3S (wt.%)	C_2S (wt.%)	C_3A_c (wt.%)	C_4AF (wt.%)	Free CaO (wt.%)	$CaSO_4 \cdot 2H_2O$ (wt.%)	$CaSO_4 \cdot 0.5\ H_2O$ (wt.%)	$CaSO_4$ (wt.%)	specific density (kg/L)	specific surface area (cm^2/g)	d_{50} value (µm)
59.6	22.8	1.2	13.0	<0.3	2.7 [a]	0.0 [a]	0.7	3.18	3,058 [b]	11

[a] measured by thermogravimetry. [b] measured with *Blaine* instrument

C_3S: tricalcium silicate ($Ca_3(SiO_4)O$); C_2S: dicalcium silicate (Ca_2SiO_4); C_3A_c: cubic modification of tricalcium aluminate ($Ca_9Al_6O_{18}$); C_4AF: tetra calcium aluminate ferrite ($Ca_4Al_2Fe_2O_{10}$).

Table 2

Chemical composition of the synthetic seawater prepared according to ASTM D1141

Salt	Concentration (g/L)
NaCl	24.53
$MgCl_2 \cdot 6H_2O$	11.09
$CaCl_2 \cdot 2H_2O$	1.32
KCl	0.70
Na_2SO_4 anhydrous	4.09
$NaHCO_3$	0.20
KBr	0.10

Table 3

Rheology (measured at 95 °C) and API fluid loss (150 °C / 70 bar) of Class G cement/silica slurries prepared from sea water and different brines holding 0.2 % bwoc of graft copolymer and 0.5 % bwoc each of AMPS®-*co*-itaconic acid and HR®-25 retarders

Brines	API fluid loss (mL)	Shear stress (lbs/100 ft^2) at shear rate (rpm)					
		300	200	100	6	3	600
Sea water	1,423	151	116	90	60	41	269
w/o NaCl	1,207	161	117	82	58	50	285
w/o $CaCl_2$	1,250	224	161	110	66	49	>300
w/o Na_2SO_4	1,449	281	198	128	65	55	>300
w/o $MgCl_2$	32	55	31	14	2	1	112
20 % NaCl with $MgCl_2$*	1,120	>300	252	136	23	16	>300

* $MgCl_2$ concentration as present in sea water composition (see Table 2); w/o = without

Table 4

Ion concentrations found in the pore solutions of the cement slurry prepared from sea water (SW), fresh water (FW) and 20 % NaCl

Fluid system	Ca^{2+} (mg/L)	K^{+} (mg/L)	Na^{+} (mg/L)	Mg^{2+} (mg/L)	SO_4^{2-} (mg/L)
Ion contents in mixing fluid					
FW	1	0	2	0	0
SW	894	7,213	11,316	1,302	3,446
NaCl	476	6,810	79,048	2	646
Ion contents found in cement pore solution					
FW slurry	476	6,810	416	2	646
SW slurry	1,016	7,620	10,460	28	643
NaCl slurry	830	6,050	61,400	2	958

Table 5

Influence of delayed addition on API fluid loss (150 °C / 70 bar) and rheology (95 °C) of API Class G cement/silica slurries prepared from sea water holding 0.2 %bwoc graft copolymer and 0.5 % bwoc each of AMPS®-*co*-itaconic acid and HR®-25 retarders

API fluid loss	Shear stress (lbs/100 ft^2) at shear rate (rpm)					
(mL)	300	200	100	6	3	600
			Early addition*			
1423	151	116	90	60	41	269
			Delayed addition**			
50	50	30	13	2	1	95

* Addition of graft copolymer into mixing water ** Addition of graft copolymer after mixing of cement slurry

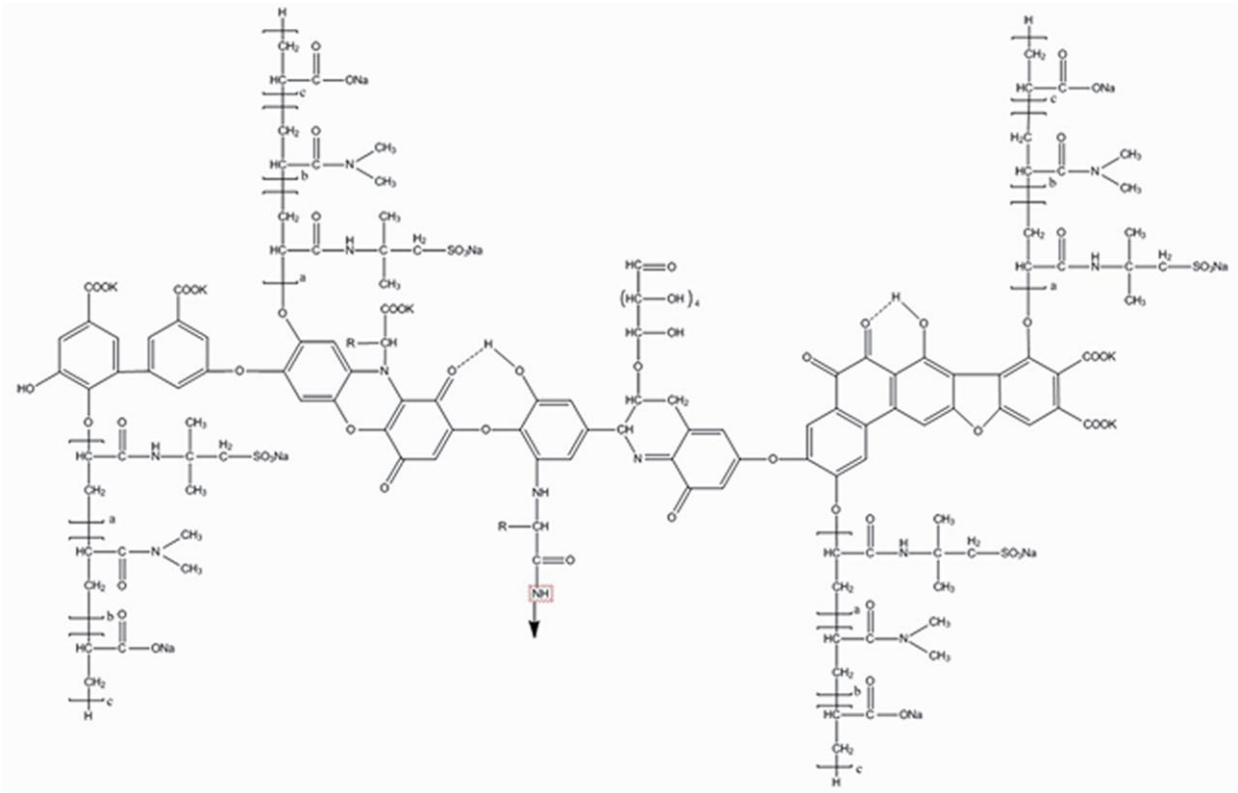

Figure 1: Proposed chemical structure of the humic acid graft copolymer

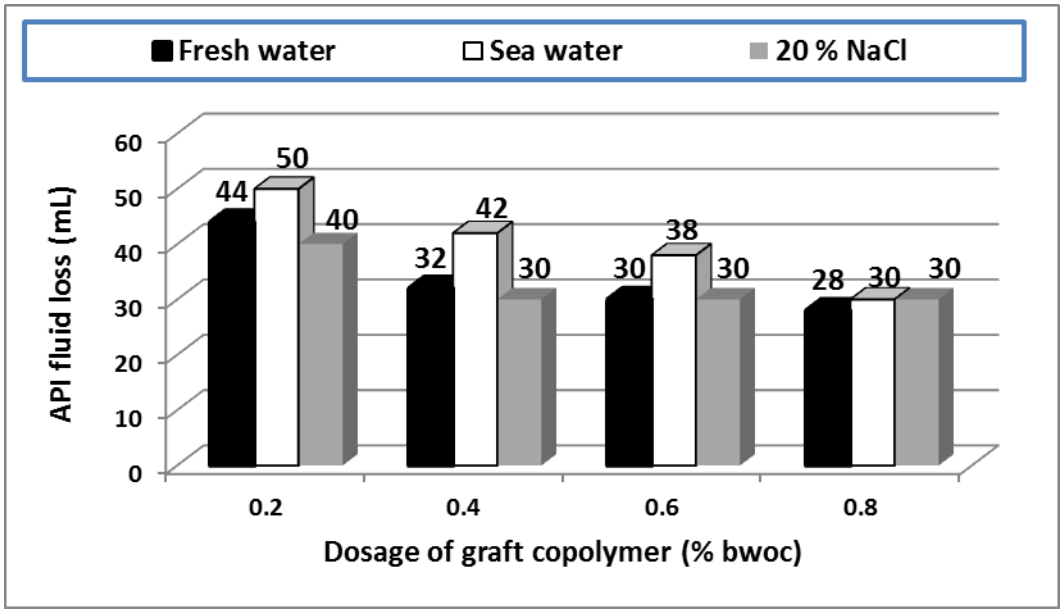

Figure 2: API fluid loss of Class G cement/silica (65:35 % wt./wt.) slurries prepared from fresh water, 20 wt.% NaCl and sea water containing increased dosages of graft copolymer and 0.5 % bwoc each of AMPS®-*co*-itaconic acid and HR®-25 retarders, measured at 27 °C

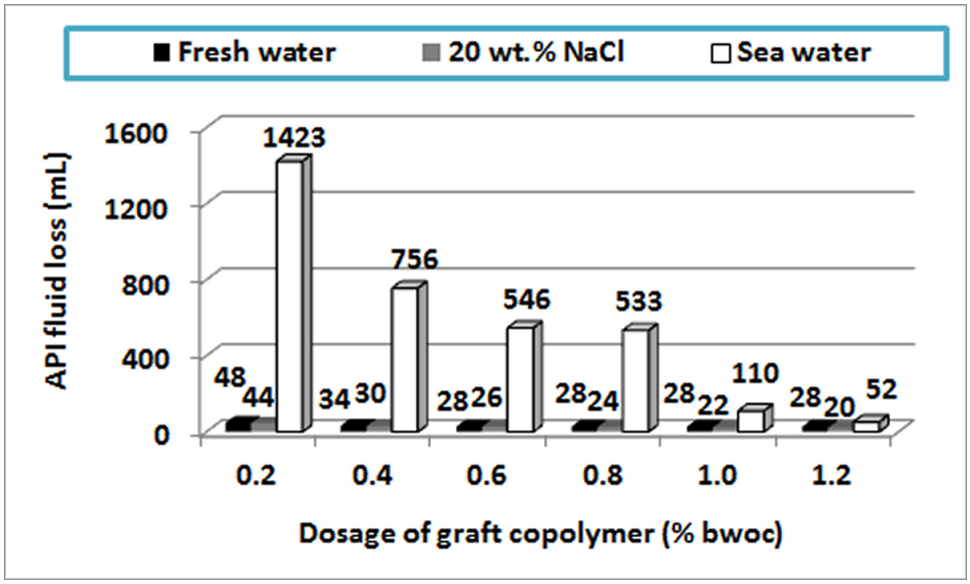

Figure 3: API fluid loss of Class G cement/silica (65:35 % wt./wt.) slurries prepared from fresh water, 20 wt.% NaCl and sea water containing increased dosages of graft copolymer and 0.5 % bwoc each of AMPS®-*co*-itaconic acid and HR®-25 retarders, measured at 150 °C

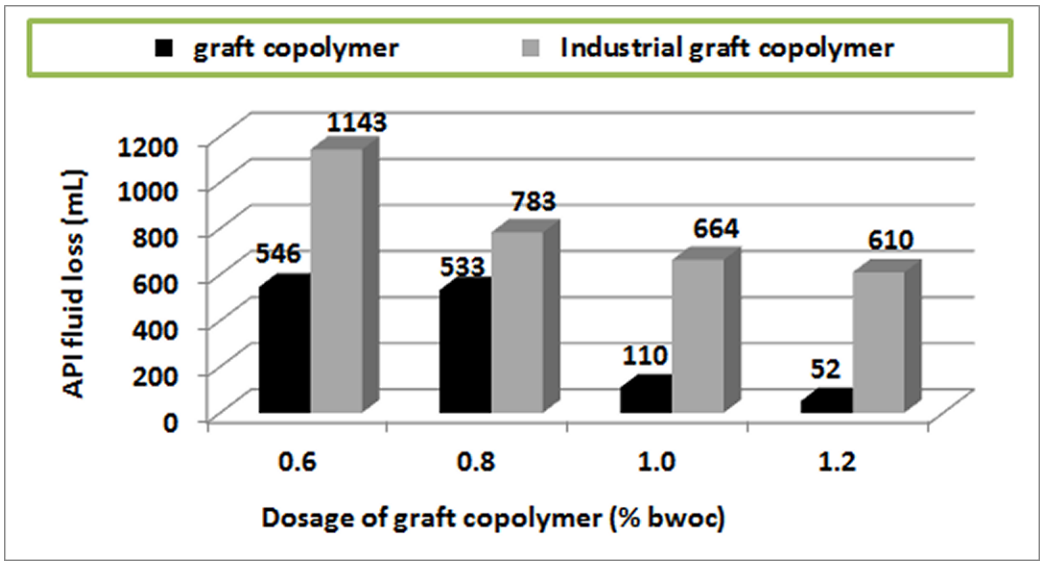

Figure 4: API fluid loss of Class G cement/silica (65:35 % wt./wt.) slurries prepared from sea water containing increased dosages of graft copolymer or of an industrial lignite-based graft copolymer in presence of 0.5 % bwoc each of AMPS®-*co*-itaconic acid and HR®-25 retarders, measured at 150 °C

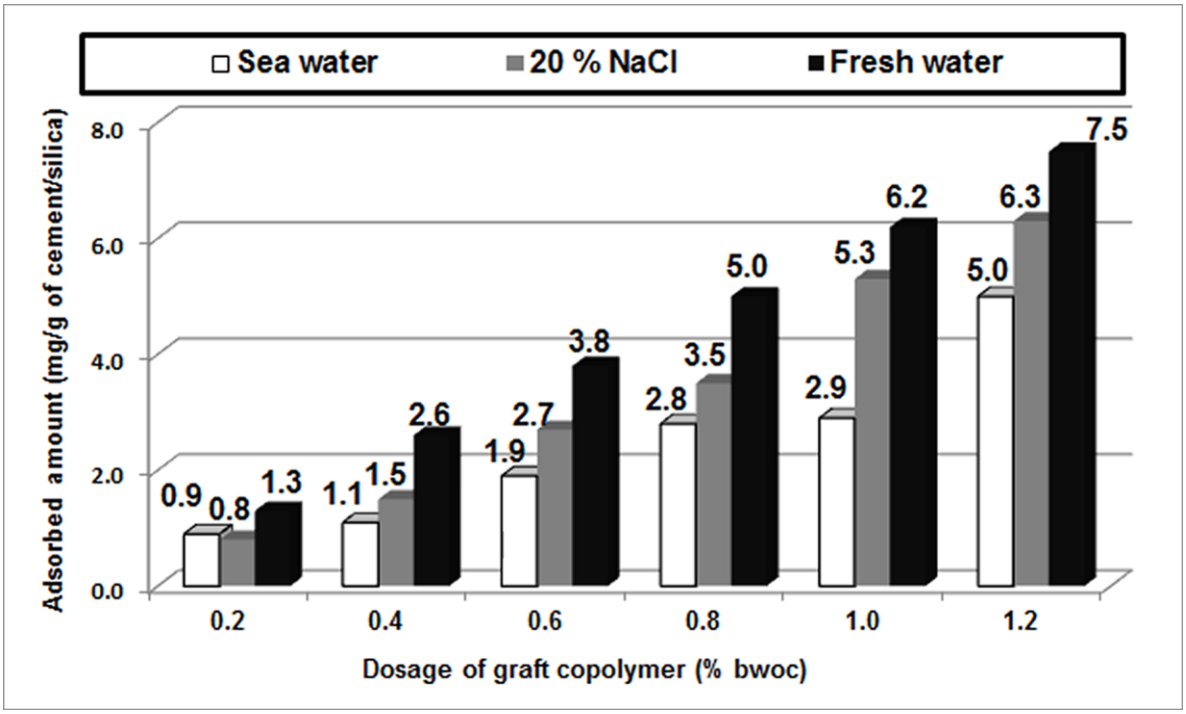

Figure 5: Adsorbed amounts of the graft copolymer on cement/silica in slurries prepared from fresh water, 20 % NaCl and sea water at increased polymer dosages, measured at 150 °C

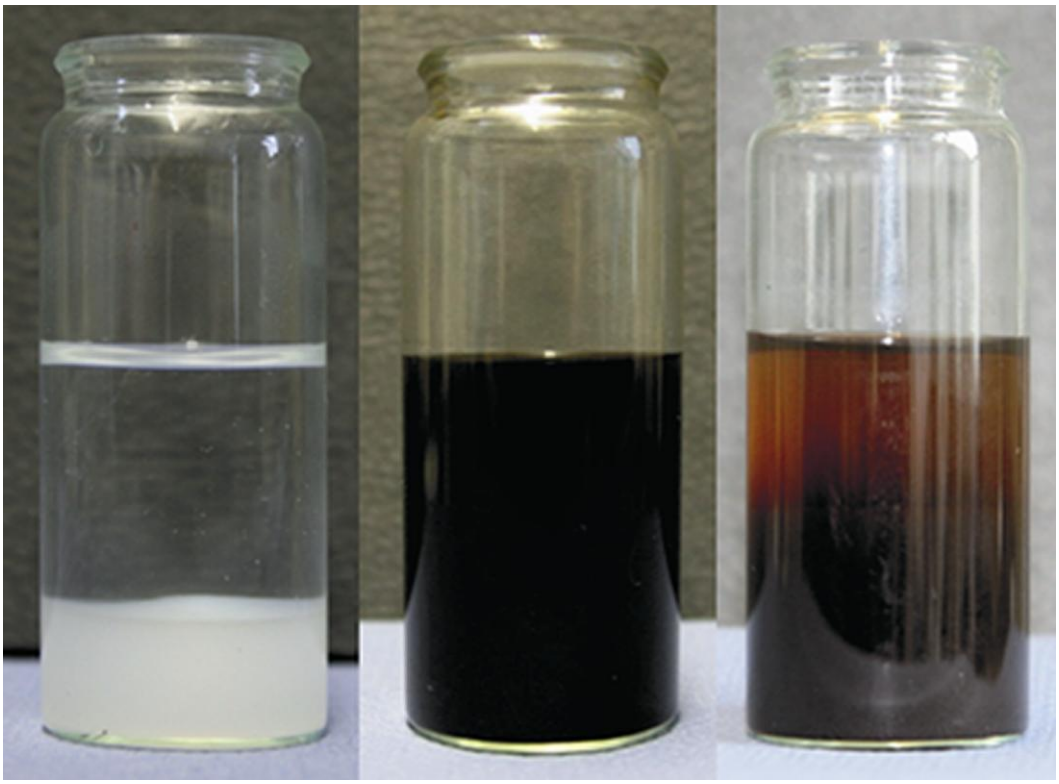

Figure 6: Left: $Mg(OH)_2$ precipitate from $MgCl_2$ solution at pH 12.5; middle: graft copolymer dissolved in $MgCl_2$ solution at pH = 6; right: graft copolymer solved in $MgCl_2$ solution, pH adjusted to 12.5 and subsequent co-precipitation with $Mg(OH)_2$

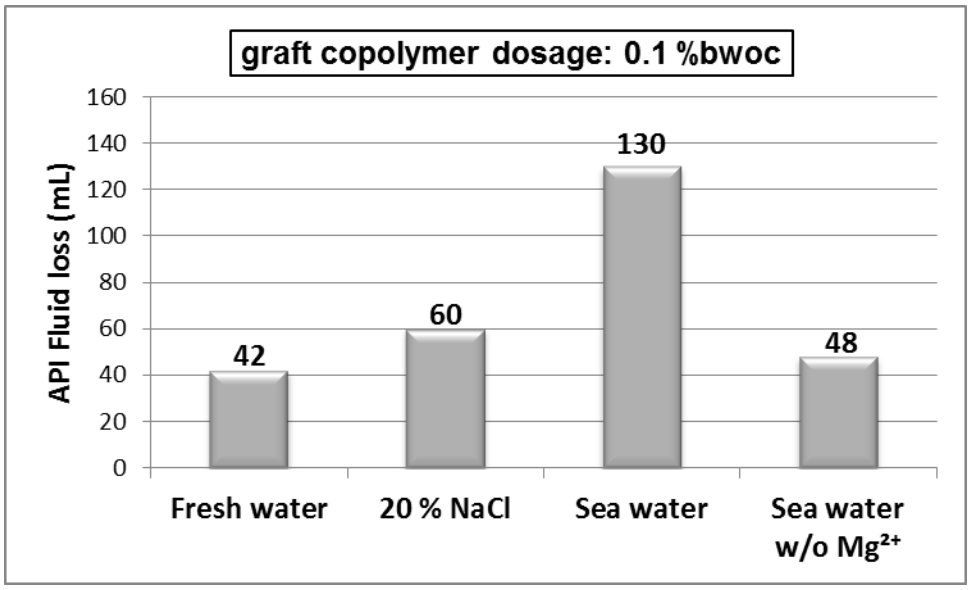

Figure 7: API fluid loss of Class G cement/silica (65:35 % wt./wt.) slurries prepared from fresh water, 20 % NaCl, sea water and sea water without $MgCl_2$, containing 0.1 % bwoc of graft copolymer and 0.5 % bwoc each of AMPS®-*co*-itaconic acid and HR®-25 retarders, measured at 27 °C

HIGHLIGHTS

- Most cement additives are negatively affected by electrolytes
- A graft copolymer was tested in cementing systems based on fresh water, 20 % NaCl and sea water
- Poor performance of polymer in sea water system noticed
- Reason is entrapment of polymers in voluminous $Mg(OH)_2$ precipitate

Graphical Abstract (for review)

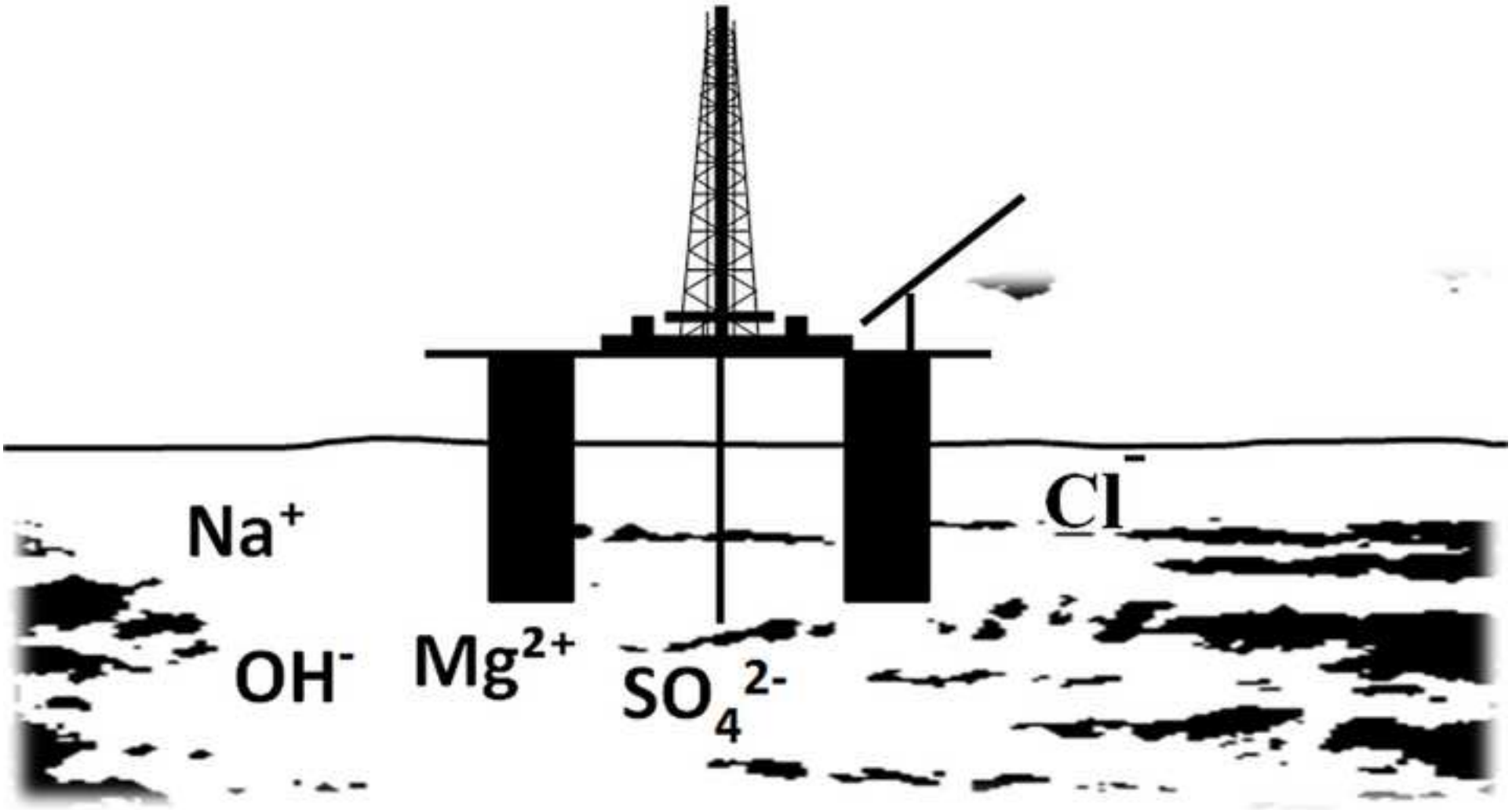

Figure 1

Click here to download high resolution image

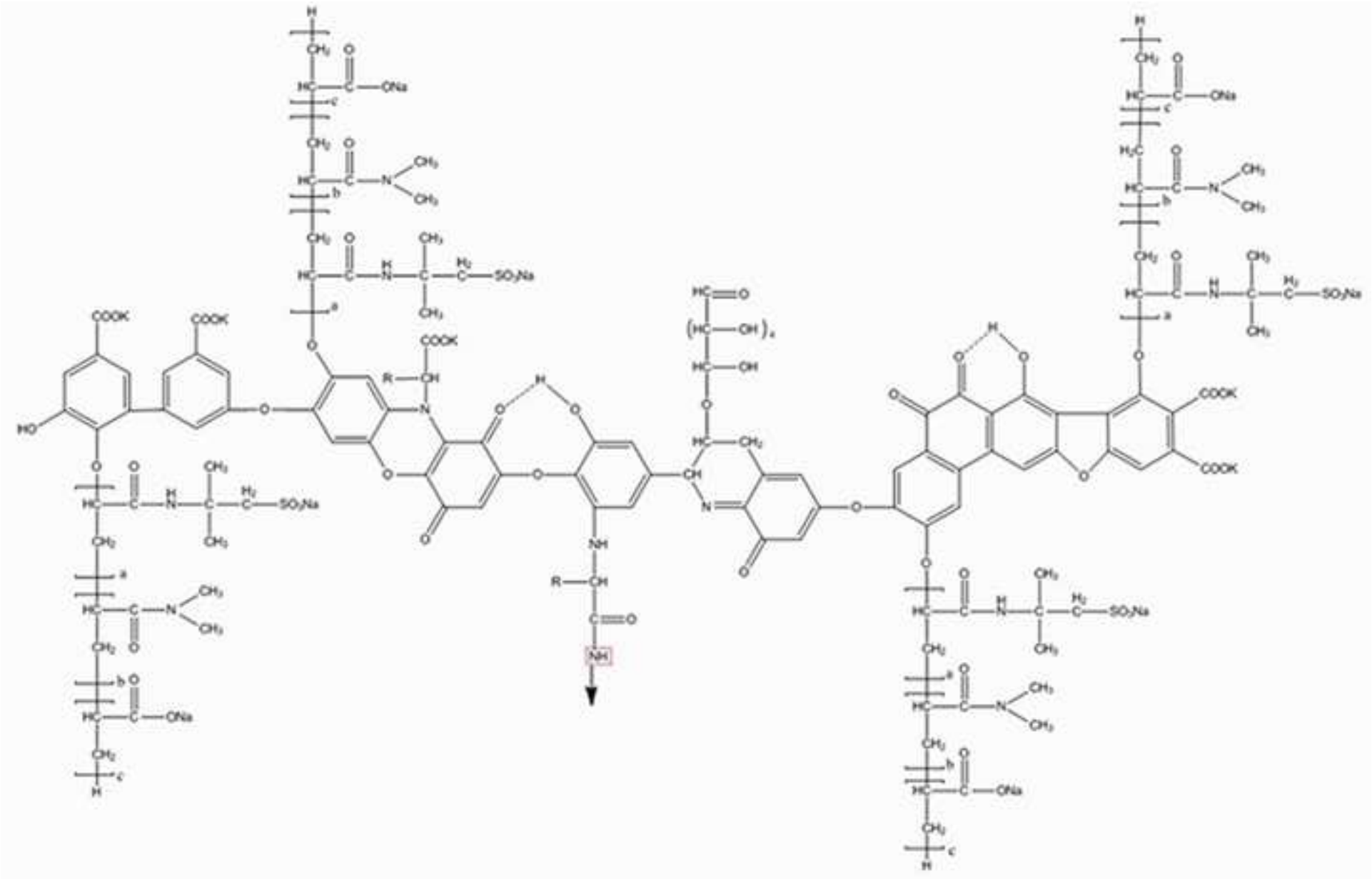

Figure 2

Click here to download high resolution image

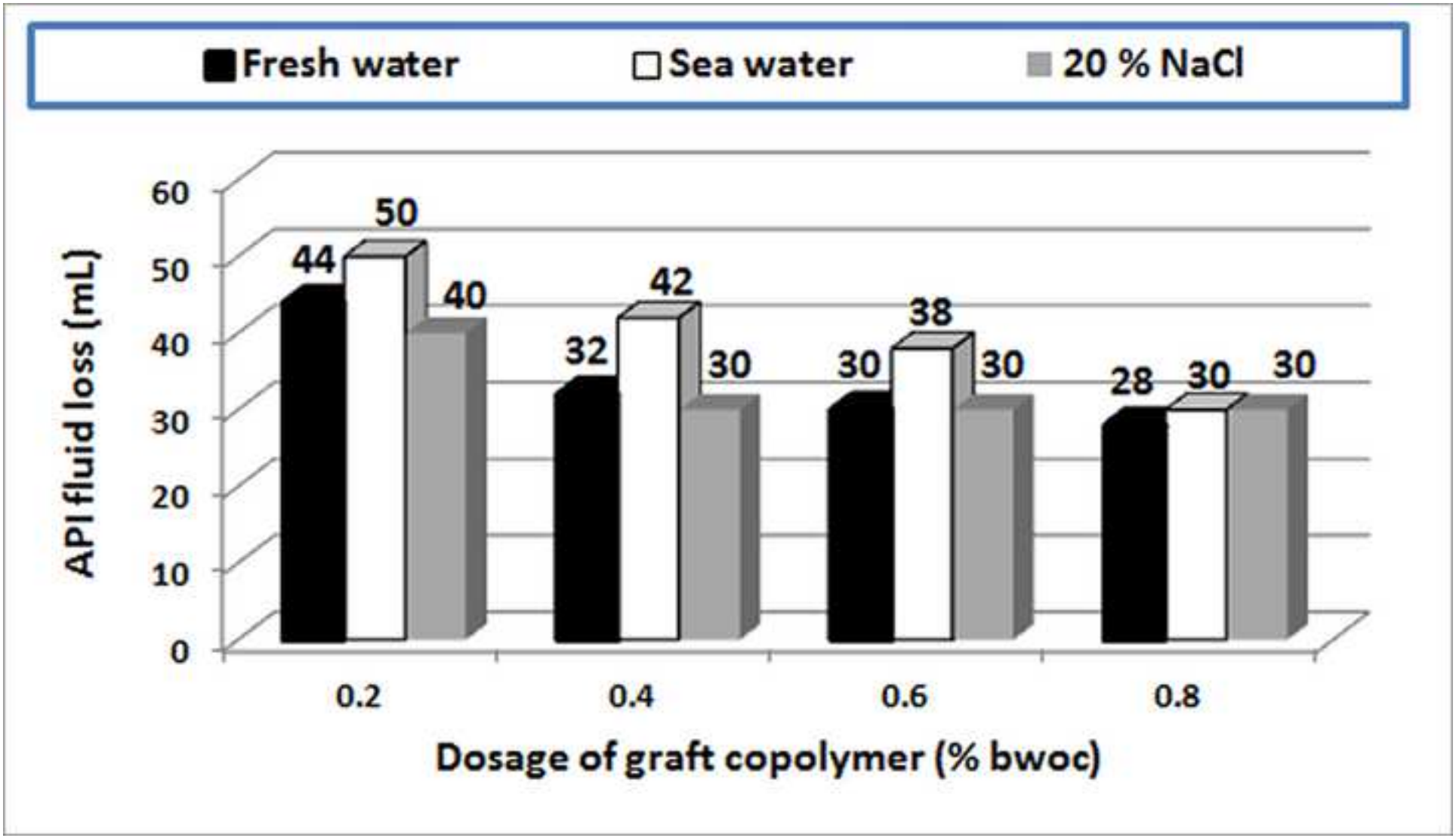

Figure 3

Click here to download high resolution image

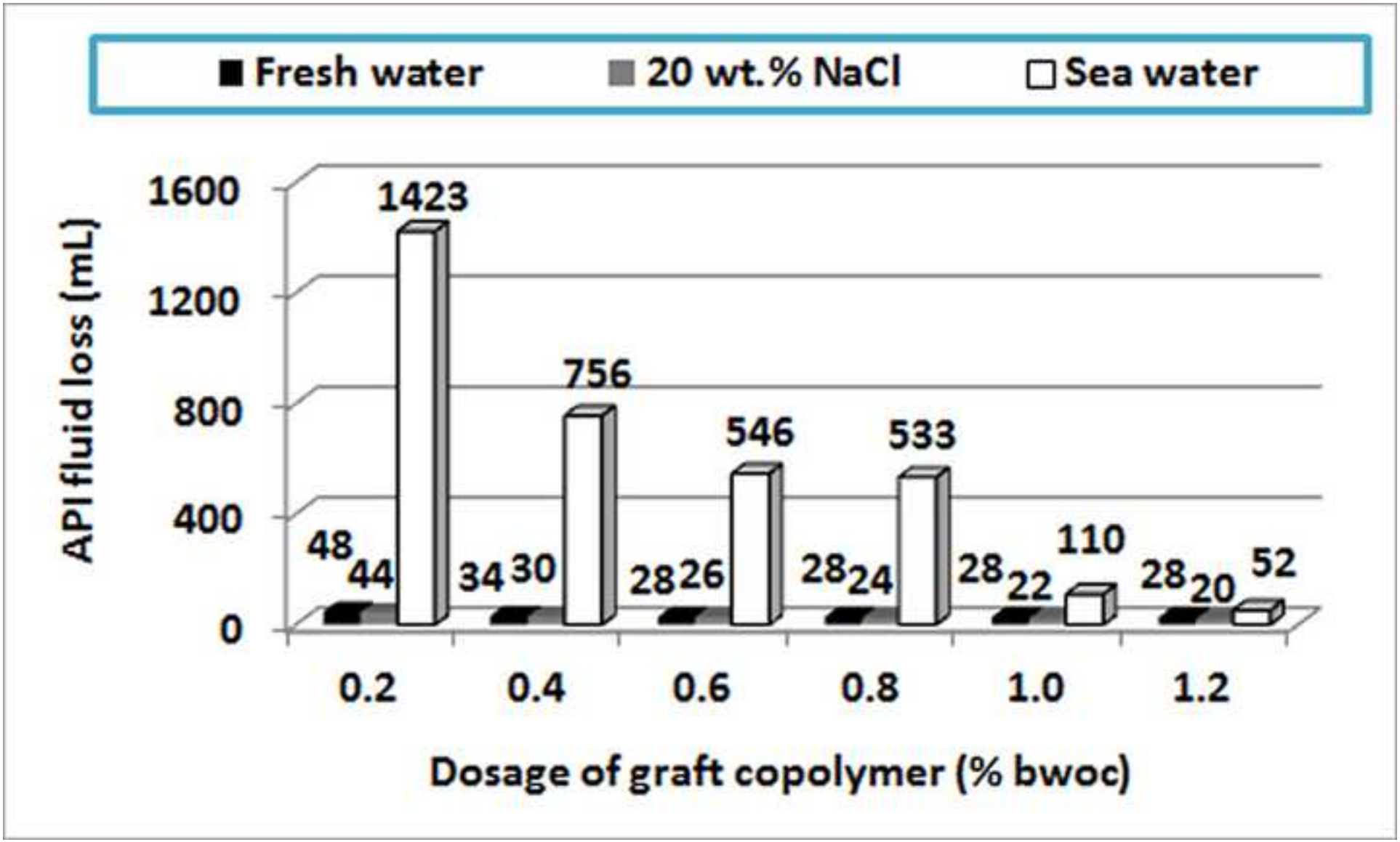

Figure 4

Click here to download high resolution image

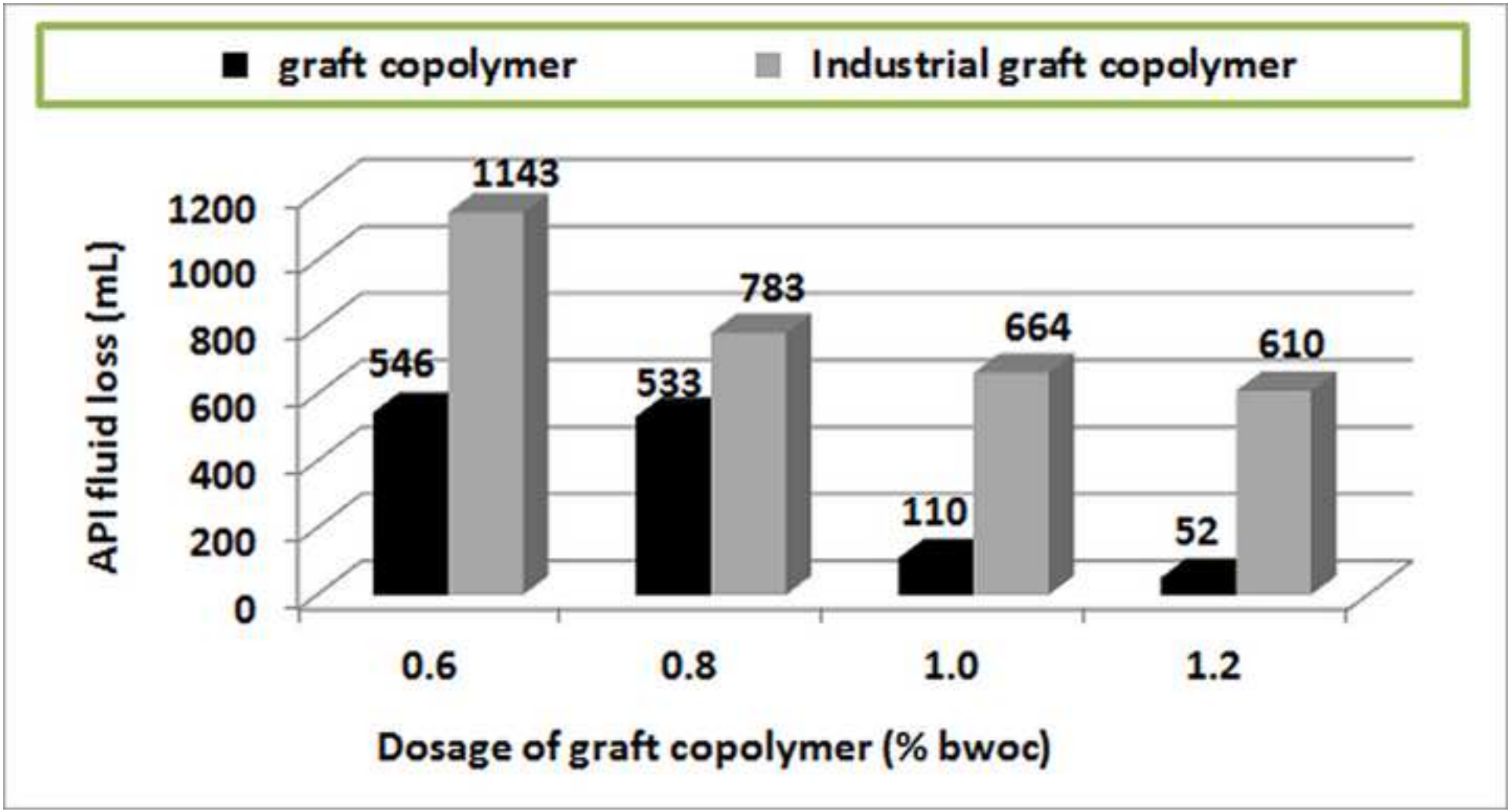

Figure 5

Click here to download high resolution image

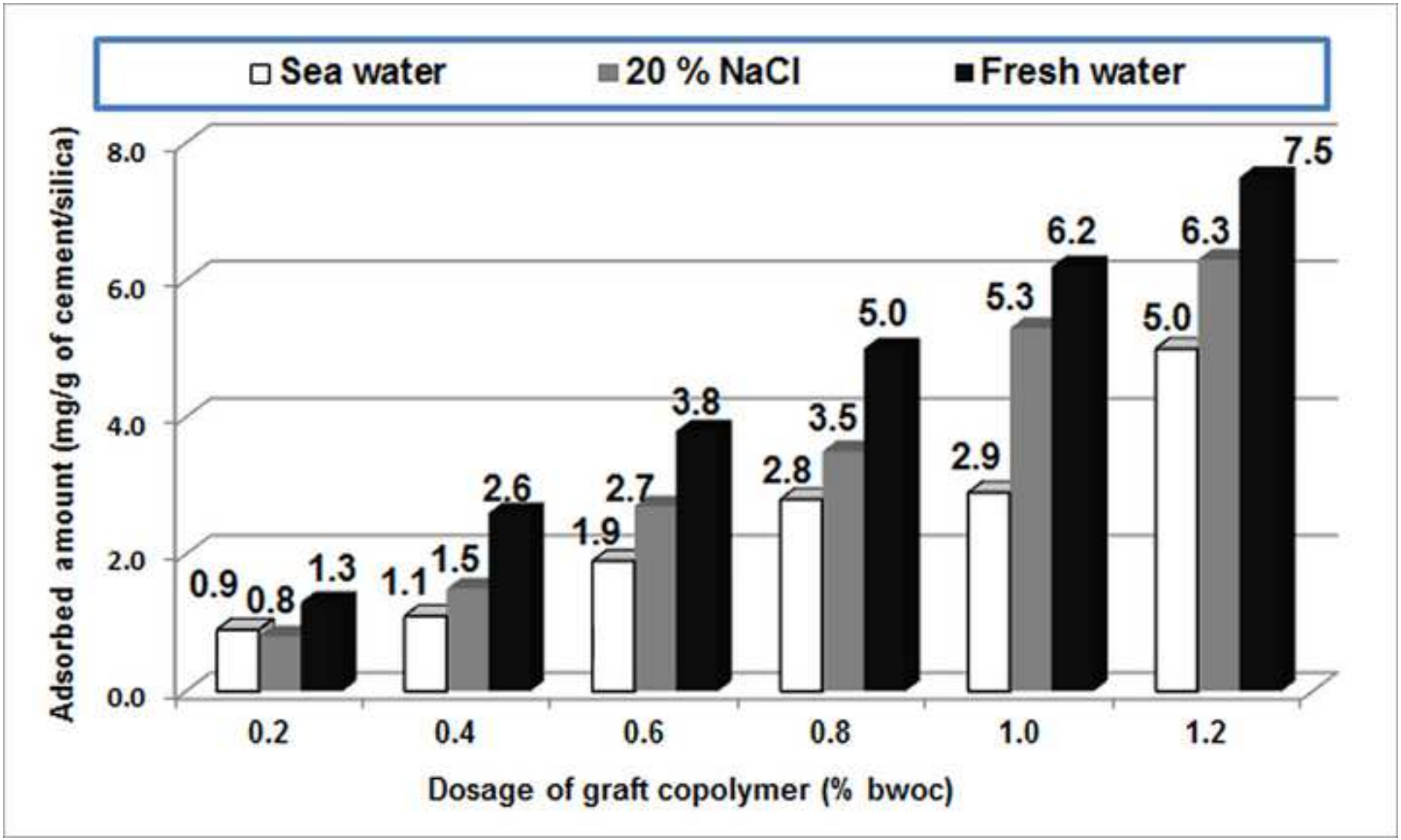

Figure 6

Click here to download high resolution image

Figure 7

Click here to download high resolution image

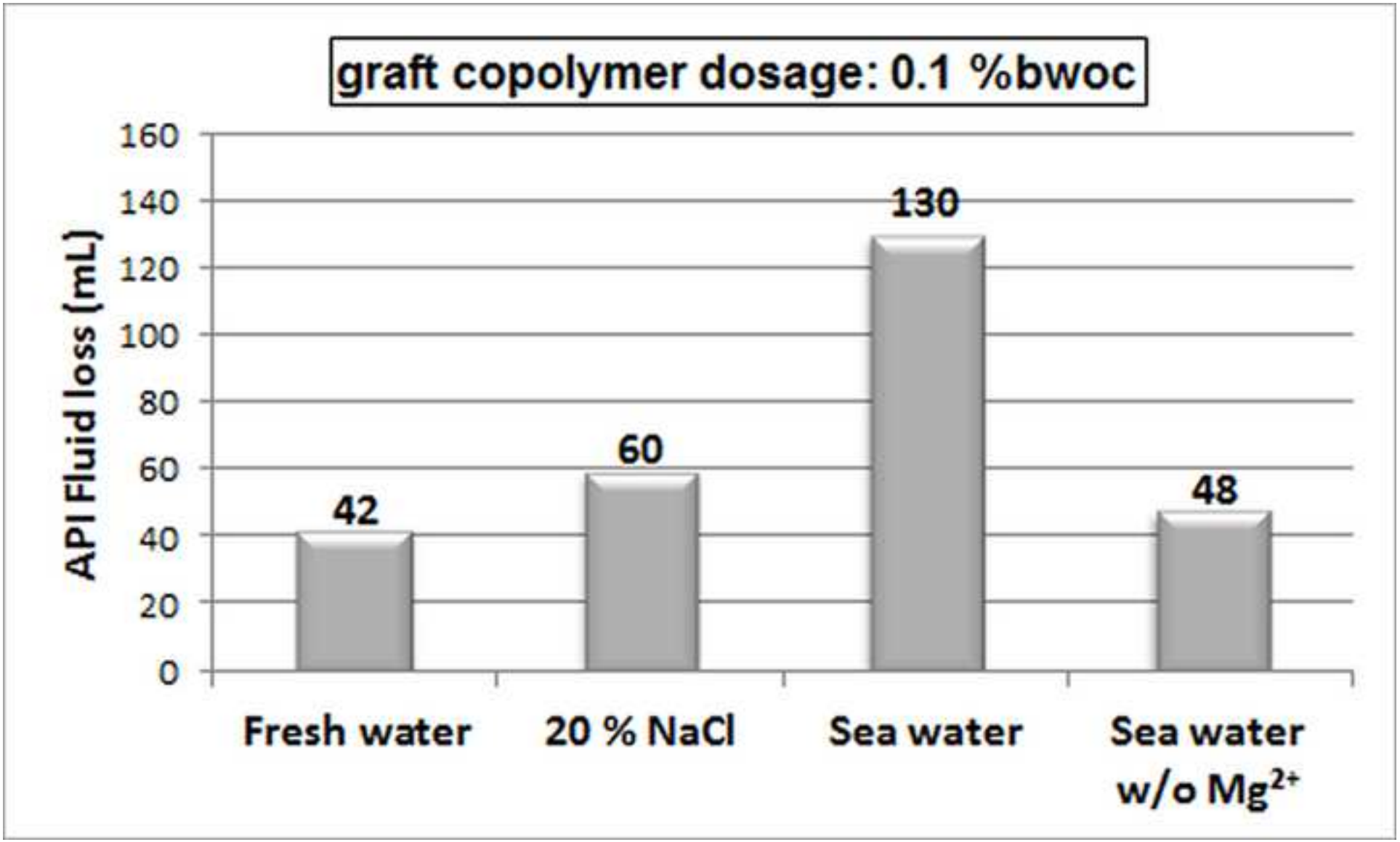

4 APPENDIX

APPENDIX A

The following presents results which were not published in the aforementioned papers. All these Figures and Tables are related to Publication #1.

Performance of viscosifying graft copolymer at 200 °C

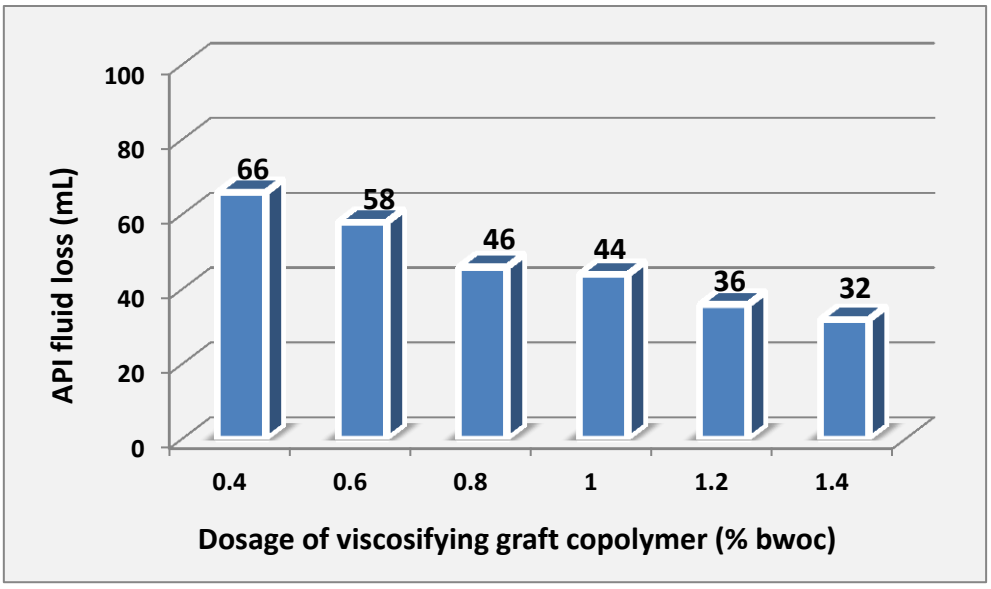

Figure 1: API fluid loss of Class G cement/silica (65: 35 % wt./wt) slurries containing increased dosages of graft copolymer and of 1.8 % bwoc of AMPS®-itaconic acid retarder, measured at 200 °C and 70 bar differential pressure under stirred condition

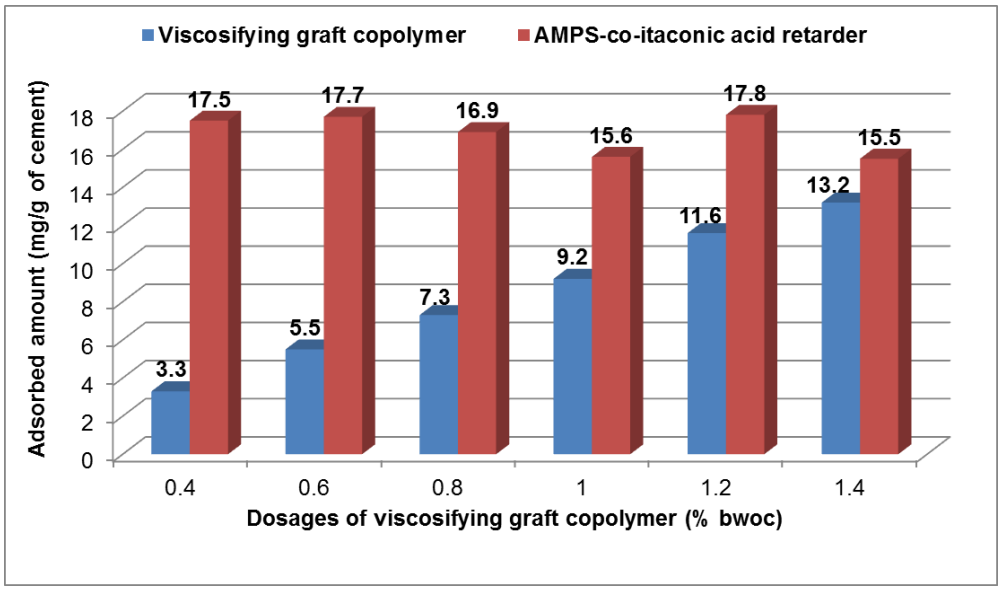

Figure 2: Adsorption of viscosifying graft copolymer and AMPS®-co-itaconic acid retarder (dosage: 1.8 % bwoc), measured from cement filtrate collected at 200 °C

Table 1: Rheology (shear stress) of API Class G cement/silica slurries containing 0.4 –1.4 % bwoc of **viscosifying graft copolymer** and 1.8 % bwoc of AMPS®-itaconic acid retarder, measured at 92 °C and at different shear rates, w/c 0.48 (**density** :1,940 kg/ m^3)

Polymer dosage (% bwoc)	Shear stress (lbs/100 ft^2) at shear rate (rpm) @ 95°C					
	300	200	100	6	3	600
0.4	145	96	52	3	2	270
0.6	179	124	64	5	3	>300
0.8	207	145	75	6	4	>300
1.0	>300	222	124	17	12	>300
1.2	>300	>300	188	38	28	>300
1.4	>300	>300	210	49	38	>300

Table 2: Rheology and API fluid loss performance of **viscosifying graft copolymer** with AMPS®-co-Itaconic acid and HR®-12 retarders at **150 °C** and **230 °C**

Retarder	Shear stress (lbs/100 ft^2) at shear rate (rpm)						API Fluid loss (mL)
	300	200	100	6	3	600	
0.8 % bwoc FLA & 1.0 % bwoc retarder @ **150 °C**							
AMPS®-itaconic acid	101	50	31	4	2	160	59
HR®-12	71	48	25	2	1	143	34
0.9 % bwoc FLA & 2.0 % bwoc retarder @ **230 °C**							
AMPS®-itaconic acid	121	66	33	3	2	162	20
HR®-12	68	45	22	5	3	98	95

APPENDIX B: LIST OF PUBLICATIONS

Peered-Reviewed Scientific Publications

1. **Salami, O. T** and J. Plank, "Synthesis, Effectiveness and Working Mechanism of Humic acid-{*sodium 2- acrylamido- 2-methylpropane sulfonate-co- N,N- dimethyl acrylamide-co-acrylic acid*} Graft Copolymer as High Temperature Fluid Loss Additive in Oil Well Cementing" J. Appl. Polym. Sci. 126:1449-1460, **2012**

2. **Salami, O. T** and J. Plank, "Preparation and Properties of a Dispersing Fluid Loss Additive based on Humic Acid Graft Copolymer Suitable For Cementing High Temperature (200 °C) Oil Wells", J. Appl. Polym. Sci.129:2544-2553, **2013**

3. **Salami, O. T** and J. Plank, "Influence of Electrolytes on the Performance of a Graft Copolymer Used as Fluid Loss Additive in Oil Well Cement", *submitted to* Journal of Petroleum Science and Engineering, **January 3, 2014**

4. Plank, J., Dugonjić-Bilić, F., Lummer, N. R. and **Taye, S**., "Working Mechanism of Poly (vinyl alcohol) as Cement Fluid Loss Additive", J. Appl. Polym. Sci., 117, 2290 – 2298, **2010**

Conference papers and posters

1. **O. T. Salami**, T. Echt, C. Tiemeyer, J. Plank: "Effect of Salts (NaCl and Sea water) on the Performance of High Temperature Cement Slurries", Oral presentation at Global WellCem Conference and Exhibition on well cement production and performance, Dubai, UAE, Jan 13-14, **2014**

2. C. Tiemeyer, B. Yang, T. Echt, **O. T. Salami,** J. Plank: "Pore Solution Chemistry and Hydration Behavior of API Class G Oil Well Cement under High Temperature (27 - 150 °C) and Pressure", Oral presentation at Global WellCem Conference and Exhibition on well cement production and performance, Dubai, UAE, Jan 13-14, **2014**

3. **O. T. Salami** and J. Plank: "Effect of Sea Water and Salt (NaCl) on a Humic acid based Graft Copolymer Fluid loss Polymer for High Temperature High Pressure (150 °C/ 1000 psi) Oil well Cementing", Poster presentation at GDCh conference, Berlin, October 7-10, **2013**

4. **O. T. Salami** and J. Plank.: "Behavior of Humic Acid Graft Copolymer Cement Fluid Loss Additive in Fresh water, 20 % NaCl and Sea Water", Poster presentation at Student Technical Conference (STC 2013) of German Section of Society of Petroleum Engineers (GSSPE), October 24-25, **2013**

5. M. IIg**, O. T. Salami,** J. Plank**: "**Synthesis, Properties and Dispersing Performance of a Low-Cost Superplasticizer with Comb Structure Prepared From Brown Coal and Acrylic Acid", paper submitted to 13th International Conference on Recent Advances in Concrete Technology and Sustainability Issues, Ottawa, Canada, July 15-20, **2015**.

6. J. Plank. and **O. T. Salami**: "Salt Cementing Systems: The Effect of Specific Ions on the Performance of High Temperature Cement Fluid Loss Polymers", SPE Paper Control/ tracking Number: 14APDT-P-407-SPE, submitted to IADC/SPE Asia Pacific Drilling Technology Conference, Bangkok, Thailand, 25-27 August **2014.**

Awards

Prize for 2nd best dissertation topic group presentation at TUM Graduate School Kick-Off Seminar in "Science Slam Competition", Herrsching, Germany, Nov 27 – 29, **2013**

Prize for 3rd best paper presentation at 1st Global WellCem Conference and Exhibition, Dubai, UAE, Jan 13 – 14, **2014**